UREA BASED HOSTS FOR OXYANIONS PREPARED BY MOLECULAR IMPRINTING. APPLICATIONS IN PHOSPHO- AND SULFO-PROTEOMICS.

A thesis presented to
the Faculty of Chemistry
at the Technical University of Dortmund

for the degree of
Doctor of Philosophy in Chemistry
(Ph.D. – Dr. rer. nat.)

by
Sudhirkumar A Shinde
born on the 9th May of 1980 in Padali, India

Supervisors:
Priv. Doz. Dr. Börje Sellergren
Prof. Dr. Frank Schulz

March 2013

Declaration

The work presented in this thesis was carried out in the Institute of Environmental Research of the Faculty of Chemistry, at Technical University of Dortmund (Germany) and is a result of the original work of the author, except where acknowledged in the text. The thesis was composed by the author and was not submitted to any other degree or professional qualification.

Sudhirkumar A Shinde
Institute of Environmental Research of the
Faculty of Chemistry,
Technical University of Dortmund
Germany

UREA BASED HOSTS FOR OXYANIONS PREPARED BY MOLECULAR IMPRINTING. APPLICATIONS IN PHOSPHO- AND SULFO-PROTEOMICS.

Dissertation

zur Erlangung des akademischen Grades

Doktor der Naturwissenschaften

(Dr. rer. nat.)

der Technischen Universität Dortmund

vorgelegt von

M.Sc. **Sudhirkumar A. Shinde**

geboren am 09.05.1980

aus Padali, Indien

März 2013

Die vorliegende Doktorarbeit wurde am Institut für Umweltforschung angefertigt und eingereicht an der Fakultät für Chemie der Technischen Universität Dortmund.

Gutachter der Dissertation:

1. Gutachter: Priv. Doz. Dr. Börje Sellergren
2. Gutachter: Prof. Dr. Frank Schulz

Tag des öffentlichen Promotionskolloquiums:

Erklärung

Hiermit erkläre ich, dass ich die vorliegende Dissertation selbständig und nur mit den angegebenen Hilfsmitteln angefertigt habe. Die Arbeit wurde bisher in gleicher oder ähnlicher Form keiner anderen Prüfungskommission vorgelegt und auch nicht veröffentlicht.

Dortmund, den

_____

Sudhirkumar Arjun Shinde

DEDICATED

TO

MY LOVELY MOTHER

&

VEENA GAVANKAR (AUTHOR OF EK HOTA CARVER)

Acknowledgments

I would like to thanks PD Dr. Börje Sellergren from Technische Universität, Dortmund for his constant support and guidance during the course of my PhD. I will always be indebted to him for immense help, advice and encouragement. The time I spend in Dortmund, is the best part of life as a learning experience.

I would like to thank Prof. Dr. Frank Schulz from Max Planck Institute of Molecular Physiology (MPI) Dortmund; for so kindly agreeing to be the second evaluator for my PhD defense. I would like to thank to Prof. Dr. Dr. h.c. Michael Spiteller for welcoming in the INFU and for providing all professional resources. I am thankful to all supporting characterization facilities of the Technical University, Dortmund. Thanks to Dr. Marc Lamshöft for mass measurements.

I feel extremely fortunate to have worked with best colleagues during my PhD studies: Jennifer Hesse, Patrick Lindemann, Deppak Chandrasekaran, Celina Wirzbicka, Melanie Berghaus, Reza Mohammadi, Dr. Cristiana Borrelli, Dr. Eric Schillinger, Dr. Javier Urraca, Dr. Wei Sun, Abed Abdel Qader, Dr. Sobhi Daniel, Annabell Tenboll, Dr. Carla Aureliano, Emelie Fritz, Dr. Mahadeo Halhalli, Ricarda Wagner, Porkodi Kadhirvel, Dr. Issam Lazraq, Dr. Ali Nematollahzadeh, Prof. Dr. Jorge Fernando Fernández Sánchez, Dr. Cem Esen, Dr. Serena Ambrosini, Georg Dropalla, Jonathan Cox, Ashok Reddy, Rüstem Kecili, Gyoergy Szekely. Dr. Deng, Dr. Farid Ramezany . Thanks to my former member of AK-Sellergren group: Dr. Andrew Hall, Dr. Marco Emgembroich, Dr. Magada Titirici, Dr. Ravindra Deshmukh, Dr. Panagiotis Manesiotis. I learned a lot from their experiences in the MIP field.

I also would like to thanks for the successful collaboration with Jing. Chen, Dr. Stefan Helling and Prof. Dr. Katrin Marcus from Functional Proteomic group, Ruhr-Universitat, Bochum and thanks for allowing to spend my time in their research laboratory. I am very thankful to Dr. Ecevit Yilmaz, MIP Technologies (part of Biotage AB), Sweden; Dr. Goetzinger. Wolfgang, Amgen, USA for the collaborations.

Dr. A. Bunschoten, Dr. Jhon Kruijtzer and Prof. Dr. Rob M. J. Liskamp from Utrecht University, in the Netherlands for valuable collaboration in the area of sulfoproteomics. It was a great learning experience in their research group in the area of synthesis. The best gift from the

visit to the Netherlands is I had great time with Yogesh. Many nice trips in the Europe with Kirtikumar, Yogesh, Sachin, Nagesh, Gajanan. Thanks Guys.

In the early stage of my research career, I would like to acknowledge Prof. Dr. Uday Desai from Shivaji University, Kolhapur India and Dr. P. G. Shukla form NCL, Pune for giving training in the organic and polymer chemistry laboratory respectively. Throughout the duration, I strongly supported by Dr. Prakash Wadgaonkar and Dr. Rahul Shingte. Thanks to God that I always blessed by their guidance, help and support. I am thankful to Kishor Jadhav and Anil Patil for their great help and support.

Thanks to Porkodiaaka, Mahadeo, Deepak, Kirtikumar and Eric. Time in Dortmund without you guys, I can not imagine. We have our own empire in Dortmund.

I have great contribution of many friends and family members. Thanks to my friends who were studying with me during master study Pinak, Prakash, Shivaji, Mandar, Aditya, Jagdish, Nana and lifetime friends **Chaitanya, Rahul, Yogesh** ….and to the members of my family, my brother Ajit, Anil, Sunil, Sushas, Sachin, Satish, Manoj, Mahesh and sisters. Chaitanya and his family have tremendous support to whole the journey. True witness of my Life!!! I am missing (Chaitanya's father) Bapu, great support and guidance from childhood. I am receiving his ashirwad!!!!!!!!!!!!!

Also thankful to Veena Gavankar who wrote such beautiful marathi book on the life story of Dr. George Washington Carver. She is Marathi mother of Carver. Thanks to Trupti ($_{VIMP}$ person).

(Million….∞) thanks to my mother (aaie), who teach me 'How to fight through adversity without becoming bitter'. This degree is for you. I love you….

Contents

Abbreviations list

AAm	acrylamide
ABDV	2,2'-azobis(2,4-dimethylvaleronitrile)
AIBN	2,2'-azobis(isobutyronitrile)
Ang	angiotensin
BA	benzoic acid
BET	Brunauer-Emmet-Teller
$[Bu_4N]$ F	tetrabutylammonium fluoride
C18	Carbon 18
C5aR	Complement 5a receptor
CCR5	Chemokine receptor 5
CD	circular dichrosim
CD_3CN	detuerated acetonitrile
$CDCl_3$	detuerated chloroform
CH_3COO^-	acetate
CIS	complexation induced shift
DCM:	dichloromethane
DMF:SO_3	sulfurtrioxide:dimethylformamide complex
DMSO-d_6	detuerated dimethylsulfoxide
DVB	divinylbenzene
EGDMA	ethylene glycol dimethacrylate
f_M	mole fraction
FM	functional monomer
Fmoc	9-fluorenylmethoxycarbonyl
Fmoc-OSu	N- (9-fluorenylmethoxycarbonyloxy)succinimide
Fmoc-pTyr-OEt	N-(9-fluorenylmethoxycarbonyl)-O'-phosphonotyrosine-ethyl ester
FT-ICR	fourier transform-ion cyclotron resonance
FTIR	fourier transform infrared spectroscopy
GPCR	G protein-coupled receptor
HILIC	hydrophilic interaction chromatography

HIV	human immunodeficiency virus
HPLC	High performance liquid chromatography
i.d.	internal diameter
IMAC	immobilized metal ion affinity chromatography
lPR	ion pairing reagent
ISEC	inverse size exclusion chromatography
ITC	isothermal titration calorimetry
K	association constant
KBr	potassium bromide
LC	liquid chromatography
M	monomer
m	multiplet
MAA	methacrylic acids
MAAm	methacrylamide
MALDI	matrix assisted laser desorption/ionisation
MDPSE	methyldiphenylsilylethyl
MeCN	acetonitrile
MeOH	methanol
MHz	megahertz
MIP	molecularly imprinted polymer
mM	milli molar
MS	mass spectroscopic
M-T	monomer-template
NH_4CO_3	ammonium carbonate
NIP	non-imprinted polymer
NMR	nuclear magnetic resonance
NOESY	nuclear overhauser effect spectroscopy
PAC	phosphoramidate chemistry
PAP	phosphoadenosine 5‘-phosphoate
PAPS	3`-phosphoadenosine 5‘-phosphosulfate
PAPS	adenosine 3'-phosphate-5'-phosphosulafte

PETA	pentaerythritol triacrylate
PMP	pentamethylpipridine
PP acid	phenyl phosphoric acid
PPA	phenyl phosphonic acid
ppm	part per milion
pS	phosphoserine
PSA	phenyl sulfonic acid
Poser	phosphoserine
pThr	phosphothreonine
PTM	post-translational modifications
Their	phosphotyrosine
pY	phosphtyrosine
s	singlet
SAX	strong anion resin
SCX	strong cation resin
SPE	solid phase extraction
T	template
TBA	tetrabutyl ammonium
TEA	triethylamine
TFA	trifluoroacetic acid
THF	tetrahydrofuan
TOF	time of flight
TPSTs	tyrosylprotein sulfotransferase
TRIM	trimethylolpropane trimethacrylate
UV	ultraviolet
V_p	pore volume
µm	micrometer

The following three-letter code and one-letter code abbreviations were used for amino acids

Ala	A	Alanine	Met	M	Methionine
Cys	C	Cysteine	Asn	N	Asparagine
Asp	D	Aspartic acid	Pro	P	Proline
Glu	E	Glutamic acid	Gln	Q	Glutamine
Phe	F	Phenylalanine	Arg	R	Arginine
Gly	G	Glycine	Ser	S	Serine
His	H	Histidine	Thr	T	Threonine
Ile	I	Isoleucine	Val	V	Valine
Lys	K	Lysine	Trp	W	Tryptophan
Leu	L	Leucine	Tyr	Y	Tyrosine

List of Figures

List of Tables

List of Schemes

1 Summary and Zusammenfassung

1.1 Summary

One of the most important challenges in protein science is the comprehensive mapping of posttranslational modifications (PTMs) in qualitative, quantitative as well as dynamic terms. These efforts are driven by the immense importance of PTMs in the regulation of cellular processes and the strong alternation in their expression in response to pathogenic conditions. At present, there is a strong need for methods sensitive enough to detect and quantify the minute amounts of different phosphorylated and sulfated peptides present in biological samples. An extensive analysis of the locations and degree of these modifications requires a combination of affinity based enrichments and mass spectrometry based identification.

As an alternative enrichment method, this thesis describes an approach, combining host-guest chemistry with the imprinting of a low molecular weight template, which is simple and generic. The resulting receptors have shown their abilities as affinity reagents in (Phospho-/Sulfo-) proteomics (proof of concept).

The performance of molecularly imprinted polymers (MIPs) is mainly dictated by the interaction of the template with the functional monomer pre- and post-polymerization on a molecular level. In the initial part of the thesis, an in depth study has been performed examining the effect of functional monomers on the morphology and performance of oxyanion imprinted polymers.

The hydrogen-bond acceptor sites in these molecules have been targeted using a 1,3-diarylurea as functional monomer and phenyl phosphonic acid (PPA) and phenyl sulfonic acid (PSA) have been used as model templates. The association parameters for the monomeric host were studied by ^{1}H NMR and ITC titrations, whereas the interaction mode between the functional monomer and the mono-TBA salts was elucidated by NOESY spectroscopy; collectively confirming the formation of the expected complex stoichiometries. The effect of the functional monomer on imprinted polymers was also found to correlate with physical characteristics like morphology (surface area and pore size distributions) and binding parameters (total number of binding sites and polymer-template association energy, capacity). These MIPs selectively recognize their anion template over other similar oxyanions but show a pronounced sensitivity to the presence of acidic and basic mobile phase additives.

With this knowledge of model oxyanion impriniting, receptors have been developed based on epitope imprinting strategy leading to a synthetic pTyr/sTyr and pSer selective imprinted polymer receptor.

For this purpose, the diarylurea host monomer (two equivalents with respect to template) was used to prepare MIPs against a model template, the bis-PMP salt of N-Fmoc-pTyr-OEt, using ethyleneglycol dimethacrylate (EGDMA) as a crosslinking monomer (pTyr-MIP). The binding site incorporates two monourea ligands placed by preorganization around a phosphotyrosine. The tight binding site displayed a good binding affinity and selectivity for amino acid and peptides containing these modifications. EGDMA based polymers shown good selectivity in organic mobile phases but showed poor selectivity in aqueous environment.

The hydrophilic pentaerythritol triacrylate (PETA) corsslinking monomer was chosen aiming the development of materials operating in aqueous environment. The polymer produced with PETA exhibited not only dramatically increased binding characteristics and selectivity, but also capability of operating in the water based mobile phases.

The phosphorylated and sulfated species in biological samples are isobaric and thus differentiation between them in routinely used mass spectrometer is problematic. Sulfated protein fragments have so far proven elusive targets, difficult to analyse by mass spectrometry and with only few effective receptors capable of recognizing such fragments. In the investigation, it was found that the pTyr-MIP crossreacts with sulfated tyrosine containing amino acids in an acidic mobile phases and is capable of capturing sulfated peptides from a mixture of peptides, whereas mass spectroscopy could not discriminate sulfated peptide over non-sulafted peptide. To the best of my knowledge, this thesis presents the first artificial receptor that has successfully demonstrated to be capable of binding tyrosine sulfated peptides. This MIPs were capable of selectively capturing both, phosphorylated and a sulfated peptides, from a complex mixture and could release the peptides separately based on elution conditions.

Further pSer-MIPs were synthesized against the model template N-Fmoc-pSer-OEt using a diarylurea host monomer complementary to pSer and PETA as crosslinking monomer. The pTyr-MIP and pSer-MIP has been analyzed using them as stationary phases in chromatopraphic column and a good specific selectivity factor was found for these amino acids. These materials packed in pipette tip SPE columns are capable of selective extraction of these modified peptides from a mixture of peptides when spiked in the complex sample.

The applications of MIPs prepared via the above substructured approaches may lead to a new concept for addressing labile biomolecules and open new ways to a wide range of tailored materials for affinity based enrichment of peptides and proteins.
Selectivity of pTyr-MIP materials was tested in collaboration with a proteomic research group using protein digests spiked with low levels of the pTyr peptide phosphor-angiotensin. Benchmarking with an established TiO_2 method, the pTyr MIP could selectively enrich the p-Tyr peptides down to the lower femtomolar level. In the pipette tip SPE study, pTyr- and pSer-MIPs are capable of selectively capturing these modified peptides from real samples in spiking experiments.

1.2 Zusammenfassung

Einer der wichtigsten Herausforderungen in der Protein-Forschung ist die umfassende Kartierung von posttranslationalen Modifikationen (PTM) in qualitativer, quantitativer sowie dynamischer Hinsicht. Diese Bemühungen werden durch die immense Bedeutung der PTMs in der Regulation zellulärer Prozesse und die starke Veränderung ihrer Expression als Reaktion auf pathogene Bedingungen voran getrieben. Derzeit besteht ein großer Bedarf an Verfahren zum Nachweis und zur Quantifizierung kleinster Mengen verschiedener phosphorylierter und sulfatisierten Peptide in biologischen Proben. Eine umfassende Analyse der Lokalisierung und des Grades dieser Veränderungen erfordert eine Kombination von affinitätsbasierten Anreicherungsmethoden und Massenspektrometrie-basierter Identifikation.
Als alternative Anreicherungsmethoden beschreibt diese Arbeit einen Ansatz, welcher Wirt-Gast-Chemie mit der Prägung eines niedermolekularen Templats kombiniert. Diese Methode ist einfach und allgemein anwendbar. Die daraus resultierenden Rezeptoren konnten ihre Tauglichkeit als Affinitätsreagenzien in der (Phospho-/ Sulfo-) Proteomik unter Beweis stellen (proof of concept).
Die Leistung von molekular geprägten Polymeren (MIP) wird auf molekularer Ebene hauptsächlich durch die Wechselwirkung des Templates mit funktionalen Monomeren vor und nach der Polymerisation bestimmt. Zu Beginn der Arbeit wurde eine eingehende Untersuchung des Einflusses funktionaler Monomeren auf die Morphologie und die Leistung von mit Oxyanionen geprägten Polymeren durchgeführt.

Die Wasserstoff-Akzeptor-Stellen in diesen Molekülen wurden über ein funktionales 1,3-Diarylharnstoff-Monomer adressiert und als Modell-Template wurden Phenylphosphonsäure (PPA) und Phenylsulfonsäure (PSA) verwendet. Die Bindungsparameter zu dem Wirt-Monomer wurden über ^{1}H-NMR und ITC Titrationen untersucht, während die Art der Wechselwirkungen zwischen den funktionalen Monomeren und dem TBA-Mono-Salz durch NOESY-Spektroskopie aufgeklärt wurde; beides bestätigte die Bildung der Komplexe in der erwarteten Stöchiometrie. Es wurde auch der Einfluss der funktionalen Monomere auf die physikalischen Merkmale der geprägten Polymere wie Morphologie (spezifische Oberfläche und Porengrößenverteilung) und Bindungseigenschaften (Anzahl der Bindungsstellen, Bindungsenergien zwischen Polymer und Template sowie Bindungskapazitäten) analysiert. Diese MIPs erkennen selektiv ihre anionischen Template in Gegenward anderer, ähnlicher Oxyanionen, zeigen aber eine ausgesprochene Empfindlichkeit gegenüber der Anwesenheit von sauren und basischen Zusatzstoffen in mobilen Phasen.

Mithilfe des so erworbenen Verständnisses über die Prägung mit Modell-Oxyanion wurden Rezeptoren auf der Grundlage der Epitop-Prägungs-Strategie entwickelt. Dadurch wurde ein künstlicher, pTyr / Styr und pSer selektiver, geprägter Polymer-Rezeptor erhalten. Dabei wurde ein Diarylharnstoff-Wirt-Monomer verwendet (zwei Äquivalenten bezogen auf das Templat), um MIPs für ein Modell-Templat, das Bis-PMP-Salz von N-Fmoc-pTyr-OEt, herzustellen (pTyr-MIP). Ethylenglykoldimethacrylat (EGDMA) fungierte dabei als vernetzendes Monomer. Die Bindungsstelle enthält zwei Monoharnstoff-Liganden, die sich durch Präorganisation um das Phosphotyrosin anordnen. Die erhaltenen Bindungsstellen zeigten eine gute Affinität und Selektivität für die Aminosäure und Peptide mit dieser Modifikation. Obwohl EGDMA basierte Polymere eine gute Selektivität in organischen mobilen Phasen haben, ist letztere in wässriger Umgebung eher schlecht.

Das hydrophile Pentaerythrittriacrylat (PETA) wurde als Crosslinker-Monomer gewählt, um Materialien herzustellen, die auch in wässriger Umgebung funktionieren. Die mit PETA produzierten Polymere zeigten nicht nur stark erhöhte Bindungseigenschaften und Selektivität, sondern waren auch für Wasser-basierte mobile Phasen geeignet.

Phosphorylierte und sulfatisierte Spezies in biologischen Proben sind Isobaren, somit sind sie durch routinemäßig verwendete massenspektrometrische Methoden schwer zu unterscheiden. Sulfatisierte Proteinfragmente haben sich als schwer erfassbare Analyten herausgestellt, für die

sich ernsthafte Schwierigkeiten bei massenspektrometrischer Untersuchung ergeben und für die bisher nur wenige effektive Rezeptoren existieren, die in der Lage sind solche Fragmente zu erkennen . In der Untersuchung wurde festgestellt, dass die pTyr-MIPs mit Aminosäuren, die ein sulfatisiertes Tyrosin enthalten, in sauren mobilen Phasen kreuzreagiert und so sulfatisierte Peptide aus einer Mischung von Peptiden gezielt anreichern können, wohingegen mit der Massenspektroskopie keine Unterscheidung von sulfatisierten Peptide und nicht sulaftisierten Peptiden möglich ist. In dieser Arbeit wurden meines Wissens nach das erste Mal künstliche Rezeptoren, die Tyrosin-sulfatisierte Peptide binden können, erfolgreich nachgewiesen. Diese MIPs waren in der Lage, sowohl phosphorylierte als auch sulfatisierte Peptide in einer Mischung selektiv zu erfassen und je nach Elutionsbedingungen getrennt wieder freizugeben.

Desweiteren wurde ein pSer-MIP mit dem Modell-Templat N-Fmoc-pSer-OEt unter Verwendung des Diarylharnstoff-Wirt-Monomers und PETA als Vernetzungsmonomer komplementär zu pSer synthetisiert. Das pTyr-MIP und das pSer-MIP wurden als stationäre Phasen in chromatopraphischen Säulen getestet und es wurden eine guter spezifischer Selektivitäts-Faktor für diese Aminosäuren gefunden. Diese Materialien wurden als Festphasen-Extraktions-Säule in Pipettenspitzen gepackt und sind in der Lage, selektiv diese modifizierten Peptide aus einer komplexen Probe (Mischung verschiedener Peptide) zu extrahieren.

Die Anwendungen von MIPs, die mit Hilfe der zuvor genannten Ansätze hergestellt wurden, könnte ein neues Konzept für die Erfassung labiler Biomoleküle sein und neue Wege für eine breite Palette von maßgeschneiderten Materialien für die affinitätsbasierten Anreicherung von Peptiden und Proteinen ebnen. Die Selektivität der p-Tyr-MIPs Materialien wurde in Zusammenarbeit mit einer Proteom-Forschungsgruppe anhand von Proben aus Proteinverdaus getestet, die mit kleinen Mengen des pTyr-Peptids Phosphor-Angiotensin versetzt waren. Im Leistungsvergleich mit einem etablierten TiO_2-basierten Verfahren konnten pTyr-MIPs die pTyr-Peptide bis zum unteren femtomol Bereich selektiv anreichern. In der Festphasenextraktions-Studie mit Pipettenspitze waren pTyr- und pSer-MIPs in der Lage, selektiv modifizierten Peptide aus Realproben im Spiking-Versuche zu erfassen.

2 Background of the work and introduction

2.1 Oxyanions and their biological relevance

The study of binding interaction is of great importance their involvement in most of the chemical and biochemical processes[1]. Anions are present in roughly 70% of all enzymatic sites, hence playing essential structural roles in many proteins, and are critical for the manipulation and storage of genetic information (DNA and RNA are polyanions). A well known example is caboxypeptidase A [2] an enzyme that coordinates to the C-terminal carboxylate group of polypeptides by the formation of an arginine-aspartate salt bridge, and catalyzes the hydrolysis of the residue. Anions are also involved in regulating osmotic pressure, activating signal transduction pathways, maintaining cell volume, and in the production of electrical signals. adenosine diphosphate (ADP), adenosine triphosphate (ATP), phosphate, citrate, maleate, oxaloacetate, sulfate, glutamate, fumarate, and halide are involved in the transport of anions through cell [3, 4].

The consequences of binding interactions as a fundamental events in molecular recognition are as disparate as cellular self-assembly, enzyme/substrate affinity, host/guest association, crystallization, and the formation of new materials [5, 6]. It is widely recognized that carboxylate, phosphate, sulfate and nitro groups are often involved in binding interaction. The design of synthetic anion receptors is particularly challenging when compared to the design of receptors for cations. “There are a number of reasons for this. 1) Anions are larger than the equivalent isoelectronic cations [7] and hence have a lower charge to radius ratio. 2) Anions can be pH sensitive (becoming protonated at low pH and so losing their negative charge). 3) Anionic species have a wide range of geometries and therefore generally a higher degree of design and complementarity is required to make receptors that are selective for a particular anionic guest than for most simple cations”. In particular, the extraction of phosphate and sulfate is highly challenging because of their high solvation energy, large size, and tetrahedral shape as shown in Table 2.1.

Table 2.1 The properties of sulfate and phosphate

Anion	SO_4^{2-}	PO_4^{3-}
Volume $(A^o)^3$	51	56.5
R (X-O) (A^o) from X-ray Data	1.45	1.52
pKa (Conjugate Acid)	-3, 1.9	2.12, 7.20, 10.9
Z_{ave}	-2.0	-1.4
ΔH Hydration (KJ/mol)	-1130	-498

Z_{aver} is at pH=6.5

2.2 Oxyanion Receptors

The phosphate-binding protein (PBP) and sulfate-binding protein (SBP) are the most common examples of natural receptors involved in phosphate and sulfate transport.

In recent years, numbers of reviews have appeared on synthetic receptors, which are generally considered as well-defined anion receptor motifs[5, 6, 8], but also on the number of recognition subunits. Included among these are amides, guanidiniums[9], steroids [10], pyrroles[11, 12] and metal-based systems [13]. Few of the successful receptors and their binding properties are shown in Figure 2.1 and Table 2.2 respectively.The guanidinium-based anion receptor has been studied extensively in the context of oxyanion recognition [4, 9, 14-16]. The capacity of the guanidinium group to bind oxyanions is due to its geometrical Y-shaped, planar orientation. This group directs the hydrogen bonding, and to its high pKa value (around 12–13), ensures protonation over a wide pH range. More recently, urea and its N,N -substituted derivatives assumed a leading role in the emerging field of anion coordination chemistry. Since the pioneering work of Wilcox [17] and Hamilton[18] showed that urea moieties can act as appropriate binding sites for anions, in particular oxoanions such as phosphonates, sulfates and carboxylates. A variety of receptors containing a urea and (thio)urea subunit have been developed and applied for anion complexation and sensing over the past years [19-21].

Selective binding, extraction and separation of anions are frequently invoked as potential solution for a number of fundamental problems. Oxyanion receptors have been used as scavenger for many species namely radioactive contaminants (e.g. pertechanetate), toxic (e.g. sulfate, chromate, arsenate and phosphate) or matrix elements that can interfere with proposed waste treatment processes (e.g. sulfate in the US Department of energy (DOE) complex)[22]. Recently,

synthetic receptors has been developed as anion antiporter and been applied as anion transporter across the lipid bilayer [23] and transmembranes [24]. The sensors [25, 26] have been reported using oxyanion receptor in combination with a signaling unit namely photochemical sensing, electrochemical sensing, or an externally measureable change (e.g. in colour or pH). Despite of usefulness of synthetic hosts (Figure 2.1), one major drawback is their strength of hydrogen bond interaction with anion decreases rapidly as polarity of solvent increases (table 2.2). Simple, efficient, highly selective and economical anion receptors are still a challenging task.

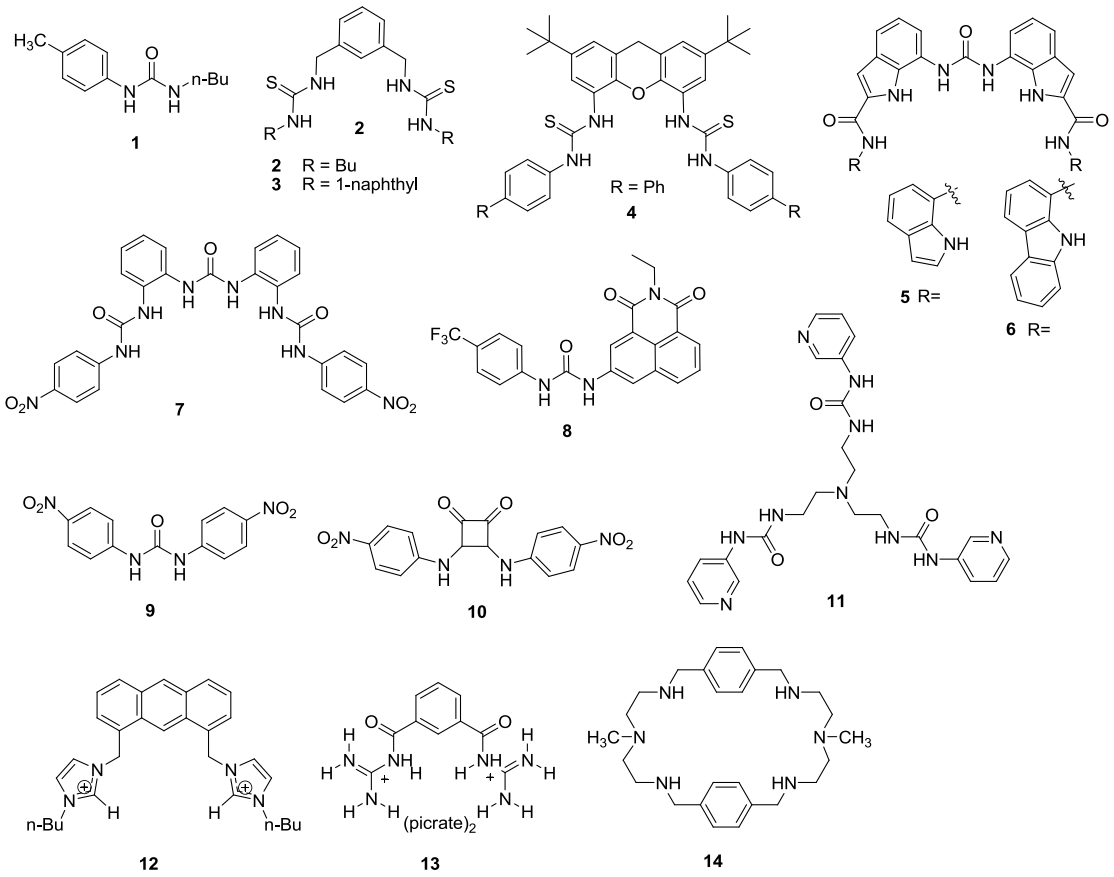

Figure 2.1 Examples of synthetic anion receptors.

Table 2.2 Stability constants of synthetic receptors listed in the figure 2.1

Host	Guest	K (M^{-1})	Solvent	Host: Guest	Method	Ref
1	$PhPO_3^{2-}$	2.5×10^3	DMSO (d_6)	1:2	^{1}H NMR	[27]
2	$H_2PO_4^-$	8.2×10^2	DMSO (d_6)	1:1	^{1}H NMR	[28]
3	$H_2PO_4^-$	1.0×10^3	DMSO (d_6)	1:1	^{1}H NMR	[28]
4	$H_2PO_4^-$	1.95×10^5	DMSO (d_6)	1:1	^{1}H NMR	[28]
5	$H_2PO_4^-$	1.2×10^2	DMSO(d_6):D_2O/ 90:10	1:1	^{1}H NMR	[29]
6	$H_2PO_4^-$	3.2×10^2	DMSO (d_6):D_2O/90:10	1:1	^{1}H NMR	[29]
	HSO_4^-	$\geq 10^4$				
7	$H_2PO_4^-$	1.0×10^5	DMSO (d_6):D_2O/75:25	1:1	UV-vis	[30]
	SO_4^{2-}	5.37×10^4				
8	$H_2PO_4^-$	2.13×10^2	DMSO (d_6)	1:1	^{1}H NMR	[31]
		3×10^3	DMSO (d_6)	1:1	UV-vis	[31]
9	$H_2PO_4^-$	2.34×10^5	MeCN	1:1	UV-vis	[32]
	HSO_4^-	1.82×10^4	MeCN	1:1	UV-vis	[32]
10	$H_2PO_4^-$	2.63×10^5	MeCN	1:1	UV-vis	[33]
	HSO_4^-	1.04×10^4	MeCN	1:1	UV-vis	[33]
11	$MgSO_4$		MeOH:D_2O/1:1	1:1	Crystallization	[34]
12	$H_2PO_4^-$	1.3×10^6	MeCN	1:1	Fluorescent	[35]
13	$Ph_2PO_3^-$	4.6×10^4	MeCN	1:1	UV-vis	[36]
14	Na_2SO_4	3.6×10^3	D_2O (pH = 2.1)	1:1	^{1}H NMR	[37]

Tetrabutylammonium (n-Bu_4^+) salt of guest was used otherwise mentioned.

2.3 Proteomics and post-translational modifications: Phosphorylation and sulfation

Proteomics is the quantitative analysis of proteins present in an organism, tissue or cell at a certain time and under certain conditions. This includes the set of all protein isoforms and modifications, the interactions between them, as well as structural description of proteins and their complexes [38, 39]. Proteomics faces the challenge of having to separate some 10,000

different protein species present in a single cell with relative abundances differing by five to ten orders of magnitude [40]. A highly important area of proteomics is the analysis of post-translationally modified proteins. Phosphorylation and sulfation are the most important post-translational modifications (PTM) affecting the biological properties of carbohydrates, proteins and glycoproteins. A single methyl or hydroxyl group can have a considerable effect on the biological properties of a steroids hormone. Similarly, protein phosphorylation and sulfation, which are relatively simple PTM in chemical terms, can dramatically affect signal transduction. The study of PTMs can improve our understanding of essential cellular processes, and provide insights at the molecular level on the causes of various diseases. Sensitive and selective detection of these PTMs is therefore an urgent goal in drug discovery, proteomics and diagnostics [39, 41-45].

2.3.1 Phosphoproteomics

Protein phosphorylation (the reversible, covalent attachment of a phosphate group to one or more amino acids) is the most common post-translational modification and occurs on more than one-third of all cellular proteins [46] (Figure 2.2). These PTMs are involved in almost all functions: metabolism, osmoregulations, transduction pathways, intercellular communication during the development and functioning of nervous system. Phosphorylation changes regions on a protein from hydrophobic to hydrophilic and this can result in a conformational change of the whole protein. Kinases and phosphatases (Figure 2.2) are the enzymes that phosphorylate and dephosphorylate proteins, respectively, on a timescale of seconds to minutes [47].

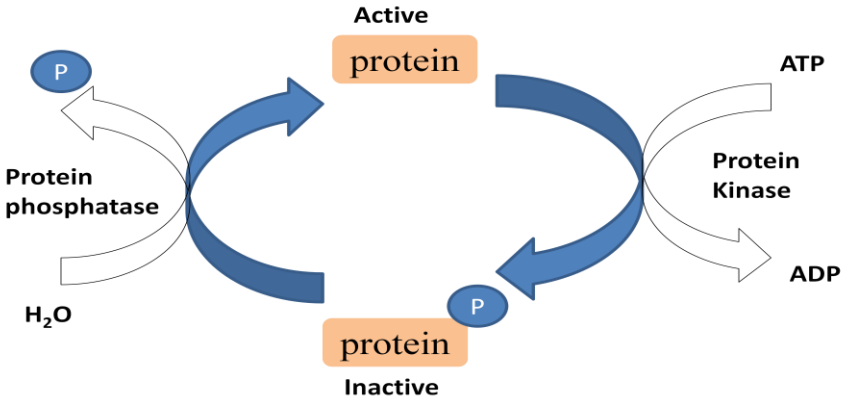

Figure 2.2 Reversible protein phosphorylation. Activation/inactivation of proteins via phosphorylation/dephosphorylation by protein kinase/protein phosphatase.

In the human genome there are 518 protein kinases [48] and about 150 protein phosphatases[49] that regulate the phosphorylation networks and control biological processes such as proliferation, differentiation and apoptosis [50]. Misregulation of the phosphorylation processes can cause severe damage to the cells, leading to diseases like cancer, diabetics or neurodegeneration. Phosphorylation takes place mainly on serine residues (86.4%), followed by threonine residues (11.8%) and tyrosine residues (1.8%)[51],[52] (Figure 2.3).

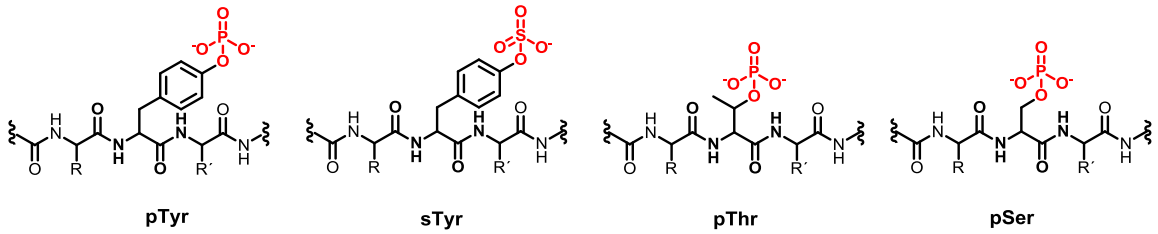

Figure 2.3 The main motifs formed by post-translational phosphorylation/sulfation of proteins.

2.3.2 Synthetic receptors for phosphopeptides

In literature, some efforts have been reported for the synthesis of small synthetic receptors capturing phosphorylated peptides (Figure 2.4). Himachi et al. showed that anthracene-labelled Zn (II)-dicyclolylamine (DPA) **15** and Zn $(II)_2$-bisdipioclylamine (BDPA) chemosensors **16**, were able to selectively bind polyanionic phosphopeptides relative to non-phosphorylated peptides under physiological conditions.[53, 54] Andreas grauer *et al*. also reported the binding of carboxylate side-chain-containing phosphorylated peptide using synthetic receptors based on bis (Zn (II)- cyclen)-triazine **17** [55] and these receptors have found affinity to phosphorylated peptide with nanomolar range in buffered aqueous solution. The guanidiniocarbonyl pyrrole based synthetic receptors **18** have reported by Schmuck *et al*. [56]. They have showed guanidiniocarbonyl pyrrole based receptors **18** have much higher affinity towards carboxylate and phosphate compared with simple guanidinium ion based receptor [56]. Hamachi and co-workers also investigated the utility of bipyridine bis(ZnDpa) receptors **19** as cross-linkers in solutions of hyperphosphorylated peptide sequences[54]. These interactions were attributed to the stabilization of helix formation as a result of the simultaneous binding of multiple phosphate residues enforced by the complexes. Himachi and coworkers developed a sequence selective fluorescent chemosensor **20** for bis-phosphorylated peptides. In this case, a rigid stilbene-based scaffold **20** orients two Zn $(II)_2$-DPA binding moieties in a confirmation suitable for

recognization adjacent phosphorylated amino acid residues [57]. Importantly author demonstrated that receptor was able to distinguish bis-phosphorylated peptides on the basis of relative proximity of two phosphate groups. Zhang *et al.* have synthesized receptor **21** by combining Zn-dipicolylamine at one end and guanidiniocarbonyl pyrrole at the other end, and these receptors have found affinity to bis-phosphorylated peptides [58]. König *et al* have prepared high affinity luminescent chemosensor using small phosphorylated serine peptides as a template and polymerizable bis-zinc cyclen receptor **22** by surface imprinting. The receptor sites created on the surface of vesicles and the resultant imprinted diacetylene patches was selectively bound the template peptide [59]. However, these receptors are difficult to engineer in useful formats for the recognition of guests of higher complexity or larger size [60].

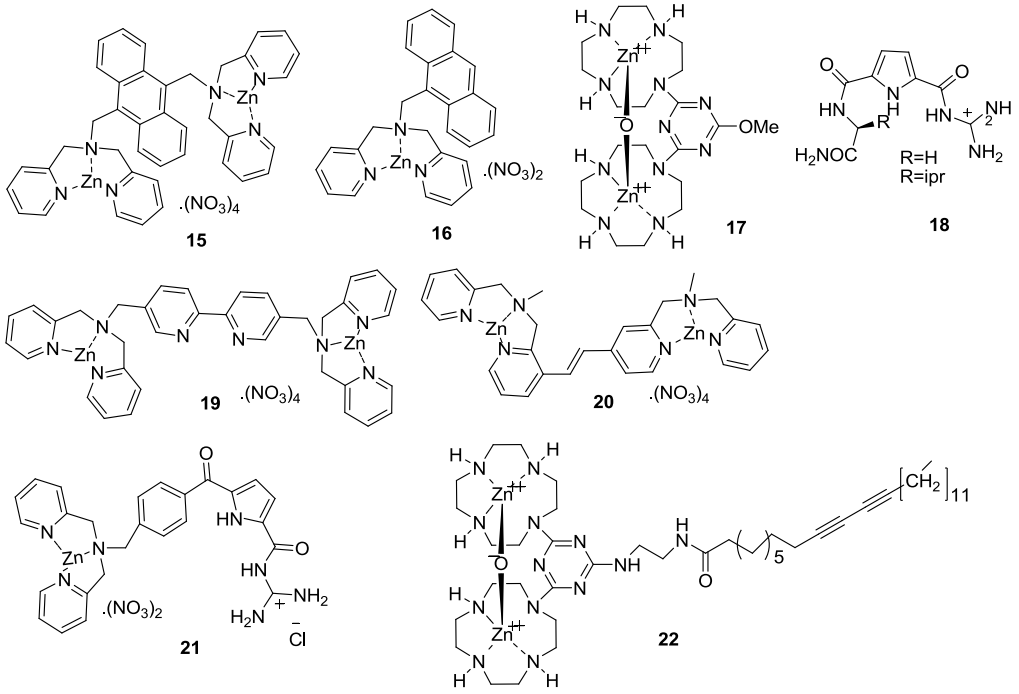

Figure 2.4 Synthetic receptors for phosphopeptides.

2.3.3 **Sulfoproteomics**

The sulfation of tyrosine is mediated by tyrosylprotein sulfotransferase (TPSTs) and occurs in approximately 30% of all secretory and membrane proteins [61]. Tyrosylprotein sulfotransferases (TPSTs) catalyze the transfer of SO_3 from the universal sulfate donor adenosine 3'-phosphate-5'-phosphosulafte (PAPS) to the phenolic hydroxyl group of an enzymatically

accessible Tyr residue within a protein or peptide to form a Tyr O^4-sulfate ester and PAP (3', 5'-ADP) (Figure 2.5).

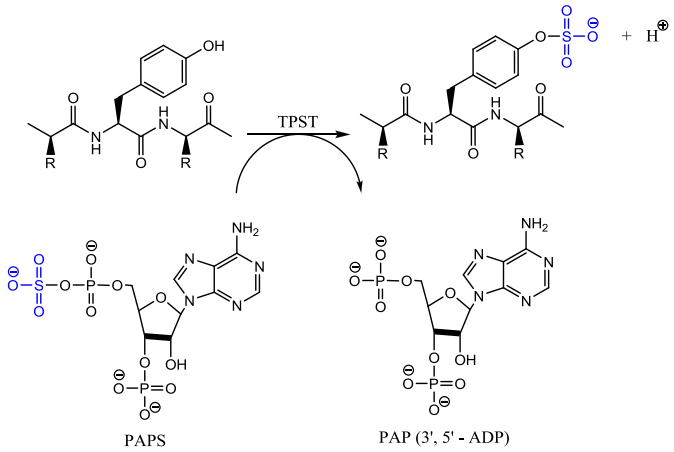

Figure 2.5 Tyrosylprotein sulfotransferases (TPST)-catalyzed Tyr Sulfation reaction.

Many classes of proteins contain sulfotyrosine including G protein-coupled receptors, adhesion molecules, coagulations factors, hormones and extracellular matrix proteins, which are implied in a variety of pathophysiological processes [62]. These act on secreted and integral membrane proteins and are playing an important role in blood coagulation, leukocyte adhesion and trafficking, hormone regulation, retroviral and parasitic infection, and the humoral immune responses [63, 64]. Thereforethe development of methods for site determination of sulfation in proteins and peptide is an important task in the area of sulfoproteomics [65].

2.4 Enrichment and Characterization of phospho and sulfopeptides

A comprehensive analysis of protein phosphorylation (phosphoproteomics) involves identification of phsophoproteins and phosphopeptides, localization of the exact amino acid residues that are phosphorylated and quantification of phosphorylation. Phosphoproteins are mostly characterized by using mass spectroscopic (MS) methods after proteolytic processing. However phosphopetides are notoriously difficult to analyze by MS [66], especially in presence of non-modified analogous peptides. This is mainly ascribed to the following factors:

1. Phosphate groups attached to serine and threonine are labile because of β-elimination [67] and have low ionization efficiency due to suppression by more abundant non-phosphorylated species during mass spectrometry analysis (ion suppression phenomenon).

2. Phosphorylated species are less abundant due to dynamic kinase and phosphatase activity.
3. Phospho-groups make peptides more hydrophilic, hence making reverse phase HPLC separation and purification difficult, and as a result affecting subsequent MS or other detection methods.
4. Phospho-groups have affinity to metals like aluminum and iron causing sample loss.
5. Phospho-groups are negatively charged and hence are electrostatically unfavorable to detection using negative charged nanoparticles (silver and gold) typically used in surface-enhanced Raman spectroscopy (SERS) measurements.
6. Isolation methods such as anti-phosphotyrosine antibodies do not distinguish between different tyrosine-phosphorylated proteins. Moreover, there is only a limited number of phospho-site specific antibodies available for enrichment *via* affinity chromatography [68].

Due to their high hydrophilicity, phosphopeptides do not bind well to the analytical columns that are routinely used for purification of peptides before analysis. Therefore, robust methods for the purification and enrichment of these peptides before MS are required.

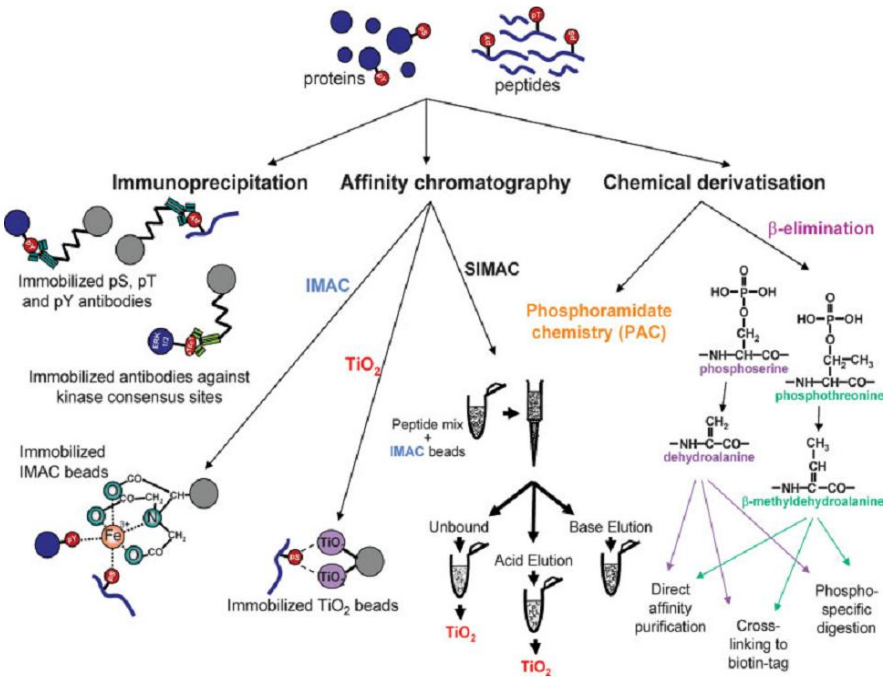

Figure 2.6 Most commonly used strategies for phospho-specific enrichment adapted from [45].

Some of the current techniques addressing these difficulties (Figure 2.6) make use of phospho-specific antibodies to visualize or enrich proteins containing phosphorylated amino acid residues. Alternatively, proteins or peptides containing such residues can be enriched by metal chelate or metal oxide based chromatography [39, 41-43, 45] (Figure 2.6). The different methods for phosphoprotein or phosphopeptide enrichment however provide different results. Some methods selectively target specific phosphorylated species, such as antibodies against pTyr in immunoprecipitation techniques, or a combination of β-elimination and Michael addition reactions for the study pSer and/or pThr peptides. Other enrichment methods, such as calcium phosphate precipitation, strong cation resin (SCX), strong anion resin (SAX), and hydrophilic interaction chromatography (HILIC), are used as pre-separation techniques to reduce sample complexity prior to more specific phosphopeptide enrichment methods including immobilized metal ion affinity chromatography (IMAC) [43], titanium dioxide (TiO_2) [44] chromatography, sequential elution from IMAC (SIMAC) and phosphoramidate chemistry (PAC) [45]. The enrichment techniques themselves have specific advantages and disadvantages, including different specificities. TiO_2 chromatography enriches mono-phosphorylated peptides more efficiently than multiply phosphorylated peptides as the latter binds too strongly for sufficient elution, whereas IMAC has a preference for multiply phosphorylated peptides, but is limited by a low capacity and selectivity when used for highly complex samples. SIMAC seems to provide a significant improvement by allowing the identification of more multiply phosphorylated peptides than any other enrichment method currently available. However, this technique also needs to be combined with a prefractionation technique in order to identify large number of phosphopeptides from complex samples.

Localization of tyrosine sulfation, has remained a daunting challenge for mass spectrometry analysis because sulfotyrosine is labile in both, positive and negative ion MS/MS experiments, yielding unmodified tyrosine [69, 70]. Sulfotyrosine decomposes under high temperature and low pH conditions, which precludes it from being analyzed by chemical sequencing experiments. Moreover, phospho- and sulfotyrosine have isobaric masses. This creates a need for highly selective enrichment techniques, which could provide a crucial aid for the sulfotyrosine site determination.

2.5 Molecularly Imprinted Polymers (MIPs)

Despite the success of biological and clinical applications of proteomics, there is still a high need for cheaper and faster enrichment techniques that can be implemented in mainstream labs and even in clinics [47]. In this area, molecularly imprinted polymers (MIPs) could play an important role, complementing currently used immunological and chemical methods.

Molecularly imprinted polymers (MIPs) are a class of solid-phase synthetic receptors. They are able to mimic the recognition processes found in nature. MIPs are based on a complex formation between functional monomer and template (step 1, Figure 2.7). The three dimensional network created around the template molecule is crosslinked (step 2, Figure 2.7). By removing the template molecule after polymerization specific recognition sites complementary in shape, size and chemical functionality of the template molecule are created in the polymer (step 3, Figure 2.7). Thus, the resultant polymer recognizes and binds selectively the template molecule (step 4, Figure 2.7). In this way, molecular memory is introduced into the polymer [71]. Three main approaches have been used routinely to create imprinted sites. They are distinguished by the nature of the monomer-template interaction during synthesis and during rebinding such as 1) covalent imprinting; 2) semi-covalent imprinting and 3) non-covalent imprinting.

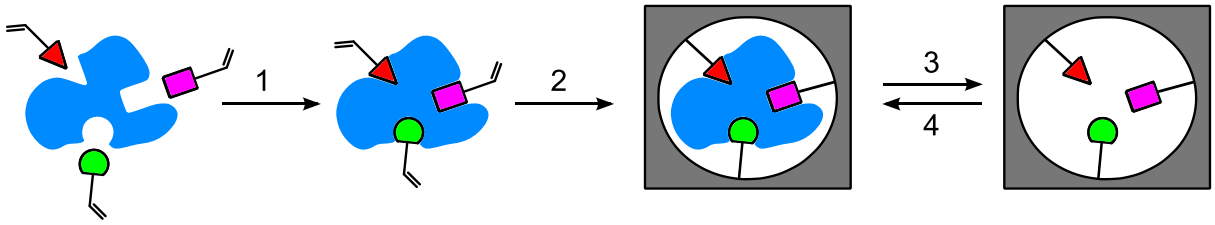

Figure 2.7 General principle for non-covalent imprinting of polymers starting from templates and monomers: (1) arrangement of monomers around the template(s), (2) crosslinking of monomers (3) removal of template; (4) rebinding of template.

All imprinting strategies have been reported in many books [60, 72-75]. Each method has its own advantages and disadvantages. Out of all strategies, the non-covalent imprinting approach is simple and widely applied. In these cases, one or several monomers are mixed with template before polymerization. A monomer-template complex is created by self assembly and is stabilized exclusively by non-covalent interactions. After the polymerization, the template can be removed by solvent extraction without requiring additional reactions to break a covalent bond. In

some cases, the template can even be recycled. The resultant imprinted material can be used for selective separation of the template from a complex mixture [76].

2.6 Reagents for MIP synthesis

The factors influencing the process of molecular imprinting are the template, the selection of functional monomers, the crosslinker and the level of crosslinking, the initiator and the solvent used as porogen. The role of each reagent will be described in the following subsection.

2.6.1 Template

The template is the key reagent in the preparation of molecularly imprinted polymers. A wide variety of templates have been successfully used for imprinting, among these are biological and chemical molecules including amino acids proteins [[77], nucleotide derivatives, pollutants, pesticides [78] and drugs [79]. However, there are certain criteria a template should fulfill in order to make it suitable for imprinting. Apart from the ability to interact with the monomer via functional groups [80] it is important that the target molecule is resistant to the polymerization conditions such as temperature and UV-irradiation. Problems can occur if the template is too toxic and dangerous to be used in laboratories. It should be easily available as well. Another prerequisite for creation of ideal binding sites is stability (in term of degradation and conformation) and solubility of the template in organic solvents. Otherwise, the imprinted material is unable to recognize the template. The latter is especially a problem when it comes to the imprinting of proteins. Moreover, these macromolecules experience a limited diffusion in the polymer network due to their size.

2.6.2 Monomers

The choice of functional monomers is very important in order to create highly specific binding sites designed for the template molecule. Figure 1.4 shows the chemical structures of some of the widely used commercially available functional monomers employed in the non-covalent approach. Monomers are categorized according to acidic, basic or neutral functional groups (for example carboxylic acids, aromatic or aliphatic bases, amines, and amides etc). Because of

hydrogen bonding donor and acceptor ability, methacrylic acids (MAA) has been extensively used as a functional monomer in most of imprinting processes in the literature [81, 82].

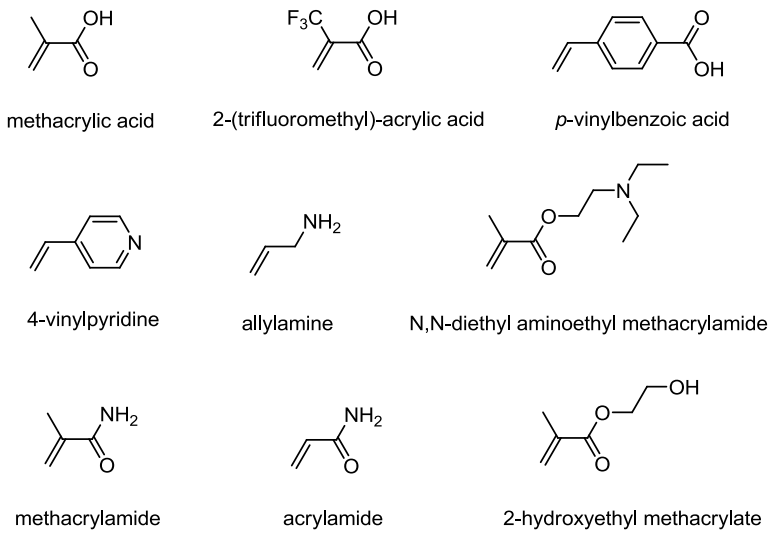

Figure 2.8 Commercially available monomers for molecular imprinting.

2.6.3 Crosslinkers

Different crosslinkers have been used in the synthesis of imprinted polymers (Figure 2.9). Crosslinkers have numerous functions in the synthesis of imprinted polymers. They control the morphology; they stabilize the imprinted binding site and introduce mechanical stability to the polymer matrix in order to retain its molecular recognition capability [83]. Crosslinking-levels higher then 80% of the total monomer composition are generally used in order to access robust materials. Crosslinker and monomers are chosen in a way to have similar reactivity order to have an equal distribution of co-monomers in the polymer matrix. A cross-linker has only a low effect on the specific interactions between the template and functional monomers but it has an impact on the physical properties of polymer [[84-86]]. Ethylene glycol dimethacrylate (EDMA), divinylbenzene (DVB), trimethylolpropane trimethacrylate (TRIM), pentaerythritol (PETA) are the most commonly employed crosslinkers (Figure 2.9). The amount of crosslinker should be adjusted carefully in order to have an optimal distance between binding sites in the imprinted polymer to achieve the highest possible imprinting efficiency.

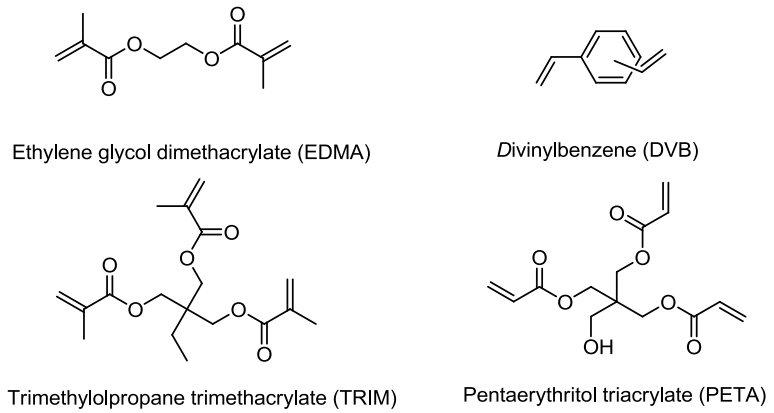

Figure 2.9 Structure of the most common cross-linkers used for molecular imprinting.

2.6.4 Porogenic solvents

The role of solvents is to bring all the reagents (i. e. template, functional monomer(s), cross-linker and initiator) into one phase in the polymerization and it is responsible for creating the pores in the macroporous polymers. Therefore, the solvent is also referred to as porogen in the case of polymerization. The choice of solvent strongly depends on the polarity and solubility of monomers,crosslinkers and templates. A suitable solvent forms well-defined pores within the network of imprinted polymer and increases its surface area [87]. Another function of the solvent is to disperse the heat of the reaction during the polymerization. This is important because high temperatures can harm the stability of the pre-polymerization complex between template and monomer. Moreover, the heat could degrade temperature sensitive templates. The nature and the volume of the porogen can be used to control the morphology and the total pore volume of the macroporous polymer. When choosing a solvent, it is very important to consider its role in promoting the formation of the monomer-template complex. It means that solvent molecules should not interfere with the interactions between monomer and template.

Aprotic solvents like toluene or chloroform, are usually preferred in MIPs synthesis to facilitate polar non-covalent interactions like hydrogen bonding. By contrast, protic solvents or water is less suitable solvents for the imprinting system because they disrupt hydrogen bonding. Protic solvents are useful in the complexation process by hydrophobic forces. The most common solvents used for MIPs synthesis are toluene, chloroform, dichlorometane or acetonitrile.

2.6.5 Initators

In the synthesis of MIPs, radical initiation methods such as heat (thermolysis), UV (photolysis), redox or chemical/electrochemical for polymerization can be used. Photochemically or thermally stability of template and monomer-template complex is a crucial criterion for the selection of an initiator. The chemical structures of two common initiators are 2,2'-azobis(isobutyronitrile) (AIBN) and 2,2'-azobis(2,4-dimethylvaleronitrile)(ABDV) (Figure 2.10).

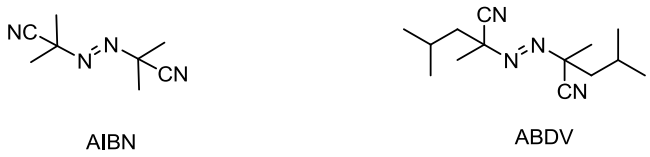

AIBN ABDV

Figure 2.10 The most common initiators used in molecular imprinting.

The pre-polymerization mixture has to be degassed with argon, nitrogen or by freeze-and-thaw cycles under reduced pressure to release trapped oxygen that might retard or inhibit the polymerization.

2.6.6 Particles

A great number of techniques for making imprinted polymer have been rapidly developed in the recent years, both in the academic community and in the industry. Consequently, significant progress has been made in developing polymerization methods that produce different MIP formats with enhanced binding properties or in order to suit the desirable final application, such as beads, films or nanoparticles.

In this thesis, imprinted polymers have been synthesized based on the bulk polymerization method. The reason, I have chosen the monolith format is to study performance of imprinted polymers using novel monomer. This method is the most widely used because of its simplicity and universality.

Monomer-template complex, crosslinker, solvent and initiator are mixed in polymer tube and then polymerized. The result is a polymeric block, which is manually crushed to give smaller particles (Figure 2.11). These particles are irregular in shape and size and thus fractionated by sieving. In the work reported herein, particle of size range 25-36 μm-sized particles were packed

in LC column for chromatographic application or in cartridge for solid phase extraction (SPE) applications.

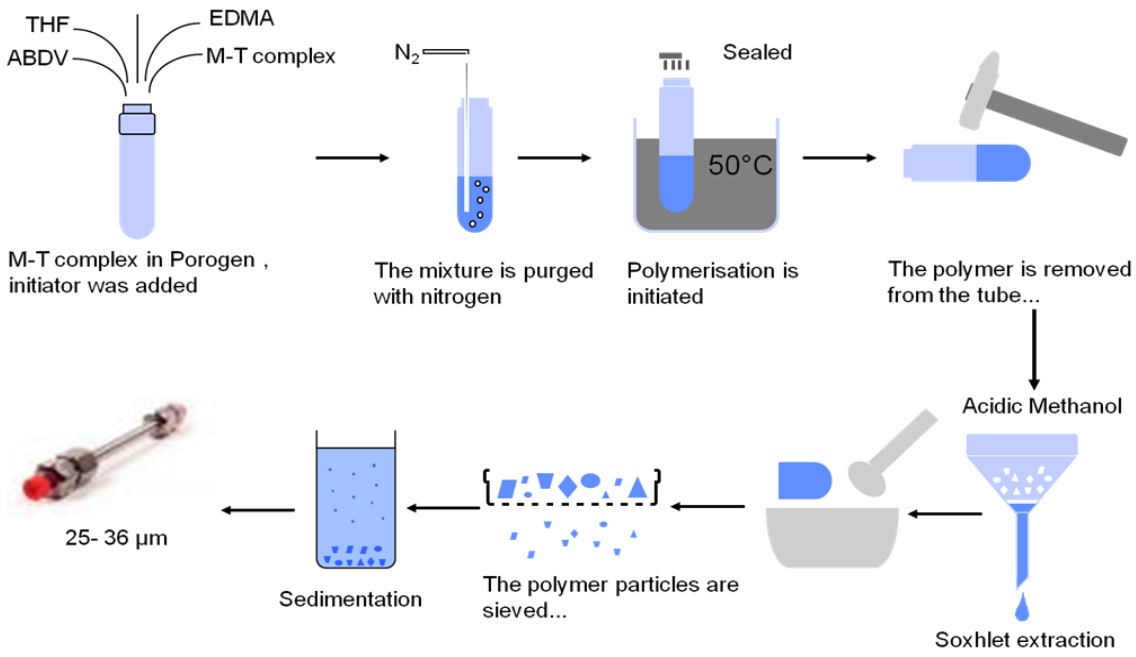

Figure 2.11 The crushed monoliths (bulk polymerization) approach to MIP particles.

2.6.7 Bio-molecule imprinting

Although molecularly imprinted polymers (MIPs) have proven their value for the enrichment of low molecular weight analytes (up to 1.5 kD), they have until now had little success in enriching biological macromolecules [88]. The absence of robust approaches to imprint such targets and the limited performance of conventional MIPs in water are the main factors that have hindered the imprinting technology in the protein science area [89].

Despite advantages in the development of MIPs, there have been intrinsic limitations inhibiting the step from conventional imprinting of small molecule to the imprinting of large bio-molecules like peptides or proteins. The limitations in imprinting large bio-molecules are due to molecular size, complexity, conformational flexibility and solubility [89]. The conventional polymerization medium (mostly non-polar solvent) is unsuited for bio-molecule imprinting.

The steric accessibility of the pore structure of the material within the template removal and rebinding is a major difficulty when a native protein is imprinted. Both, diffusion out of and into

the highly cross-linked polymer network to the imprinted binding sites are limited. In protein imprinting, multiple weak interactions are likely to favor nonspecific binding [73]. Different regions of proteins exhibit distinct physiochemical properties and hence problems can arise with recognition and cross reactivity. The non-physiological conditions often employed during polymerization may denature proteins or force them into conformations or aggregates that are not suitable for imprinting.

2.6.8 Epitope Imprinting

One alternative method has been developed by Rachkov to overcome the number of key inherent problems like permanent entrapment, poor mass transfer, denaturation, and heterogeneity in binding pocket affinity in protein imprinting [90-92]. This method is referred to as 'epitope imprinting'.

A short peptide representing only a small fragment of a protein is used as a template, the resulting molecularly imprinted polymer should also be able to retain the whole protein molecule (Figure 2.12). The term "epitope approach" was derived from the fact that small fragments of antigens responsible for the specificity of antibody-antigen interaction are called epitopes.

It has been proven that the MIPs prepared by the epitope approach recognize not only the template, but also some larger peptides possessing the same structural fragment as that of the template. The materials with such properties could be used for detection and separation of important peptides and proteins.

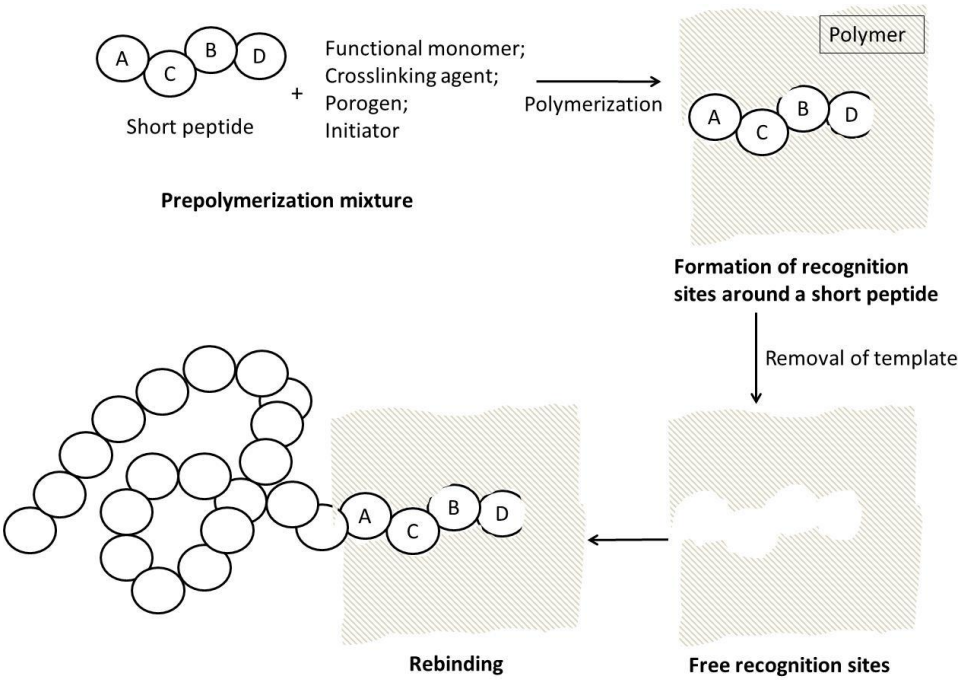

Figure 2.12 Schematic representation of the epitope approach.

Selective recognition of oxytocin, a nonapeptide, was demonstrated by a polymer imprinted with a tetrapeptide, YPLG. Both peptides possessed the same amino acid sequence at the C-terminal. This technique allows specific, strong interactions with parts of the protein to be formed, rather than relying on numerous weak interactions all over the biomolecule.

B. Sellergren *et al*. have reported sub-structure imprinting approach [93-95], which is similar to epitope imprinting , where a fragment of complex molecule has been used as a template and the resultant MIP can be used to capture whole molecule poeesessing this fragement. The concept of interfacial epitope imprinting was also demonstrated by Sellergren *et al.* [96, 97] in which, peptide epitope was immobilized on porous silica support and the resulting hierarchically imprinted material has surface-confined sites for larger peptides of the epitope template.

In the recent years, Shea *et al.* [98-101] have applied the epitope imprinting concept to many proteins, e.g. Cytochrome C, alcohol dehydrogenate and bovine serum albumin. The epitope imprinting technique allows the usage of organic solvents for polymerization, where small peptides are not subject to the major conformational and degradation problems faced by whole proteins.

2.6.9 Challenges in the imprinting of PTM peptides and proteins

The process of epitope imprinting is challenging for PTM proteins for the following reasons. 1) It is difficult to produce a high amount of PTM-proteins by overexpression; 2) phosphorylation and sulfation processes occurs only in eukaryotic cells; 3) along with this, they are expensive and/or difficult to produce chemically or biochemically in large scale.

The majority of molecular imprinting takes place in apolar, organic solvents in an attempt to maximize electrostatic interactions, such as hydrogen bonding. However, the poor stability and solubility of PTM- peptides (highly polar phospho- or sulfo groups) in apolar solvents limits their use in conventional imprinting methods. This also limits the choice of monomers available for selection, as many monomers are insoluble or only partially soluble in water.

The complexity, inconsistency, expenses and synthetic difficulty are the major limiting factors hindering the development of MIPs for phosphorylated/sulfated peptides and proteins. To overcome this issue, N- and C-terminal protected phosphorylated amino acid as templates for imprinting will be discussed in this thesis.

2.6.10 Stoichiometric imprinting of anions

With few exceptions, imprinted polymers for anion recognition have been made using commercially available functional monomers (e.g. vinylpyrdine, N,N-di-ethyl-2-aminoethyl methacrylate, methacrylamide (Figure 2.8), which are able to provide only weak interactions with the template molecule in solvents with low polarity. Generally, this means that a large excess of functional monomer is used in order to ensure a high degree of complexation of the template. Such conditions are not compatible with the vast majority of biomolecules, which instead require polar or aqueous environments for imprinting.

Figure 2.13 Stoichiometric Imprinting: strong interactions between Monomer (M) and template (T) lead to MIPs with increased capacity and affinity for the template.

One approach to improve this situation involves the preparation of functional monomers -that provide strong and stoichiometric interactions with a given template (Figure 2.13). If the

monomer-template interactions are sufficiently strong, stoichiometric use of the monomer should lead to a high percentage of complexation in the pre-polymerization solution. Consequently, this could form a high yield of imprinted sites in the polymer. This may lead to a drastic reduction in the degree of non-specific binding in the obtained imprinted polymer.

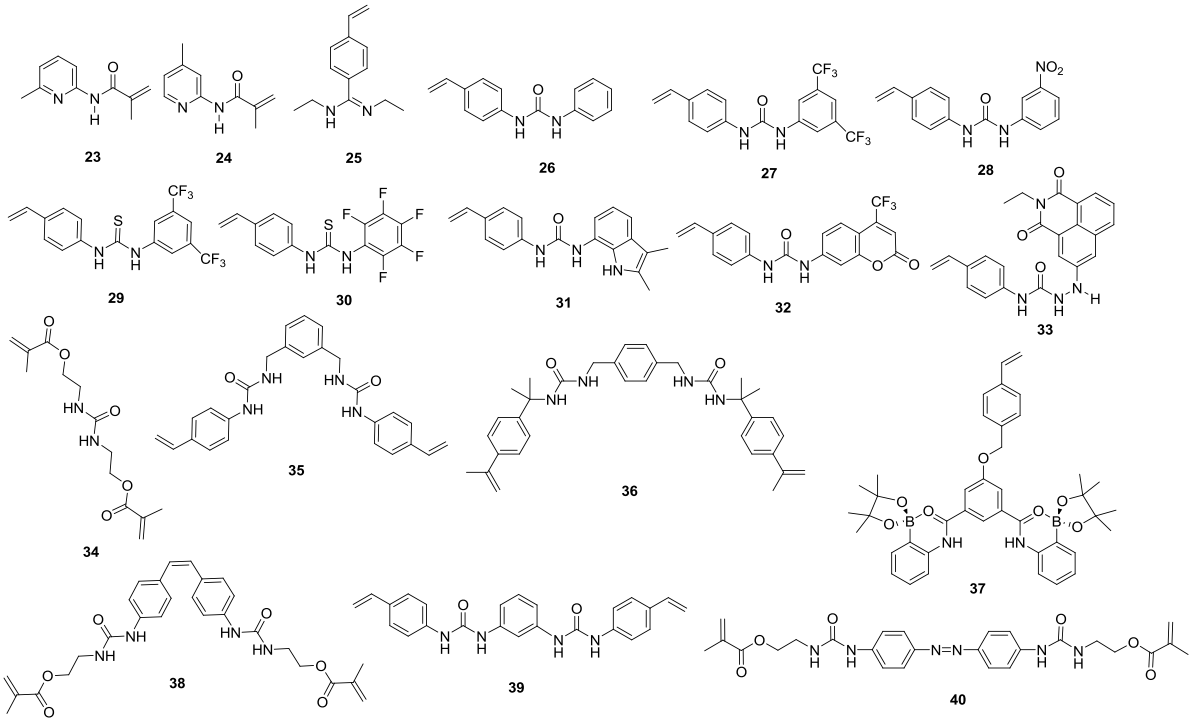

Figure 2.14 Some monomers designed to bind oxyanions for stoichiometric imprinting.

The most successful functional monomer for the imprinting of neutral acids is the amidine-based monomer **25** reported by the group of Wulff [102]. This monomer is capable of engaging in electrostatic and cyclic hydrogen bonding interactions with carbonic and phosphorous acids. In $CDCl_3$, the interactions ($K_a > 10^6\ M^{-1}$) are strong enough to allow beaded MIP preparation *via* traditional, aqueous-based suspension polymerization techniques [103]. The association is also strong in CD_3CN ($K_a \approx 10^4\ M^{-1}$). The stoichiometric use of **25** in such solvents leads to >95% complexation prior to the polymerization, which has been shown to translate into a near-quantitative yield of imprinted sites in the final polymer. A limitation of **25** is that the association strength decreases dramatically on moving to solvents of yet higher polarity, e.g. DMSO-d_6 ($K_a < 10M^{-1}$), due to the adoption of an unfavorable conformation for binding.

A series of new monomers have been reported (Figure 2.14), exhibiting improved affinity properties in polar media (Table 2.3). Some materials based on these monomers have failed to recognize in aqueous media.

Table 2.3 Binding properties of monomer (listed in Figure 2.14) with guest molecules

Monomer	**Guest**	**Ka (M^{-1}) ca.**	**Solvent**	**Technique**	**Reference**
23	Proponic acid	650	$CDCl_3$	^{1}H NMR	Sellergren *et al.*[95, 104]
24	Proponic acid	777	$CDCl_3$	^{1}H NMR	Sellergren et al.[95, 104]
25	Phosphorous acid	$\geq 10^6$	$CDCl_3$	^{1}H NMR	Wulff *et al.*[102, 103, 105]
		$\geq 10^4$	CD_3CN	^{1}H NMR	
		≤ 10	DMSO (d_6)	^{1}H NMR	
26	Benzoate [a]	1300	DMSO (d_6)	^{1}H NMR	Sellergren *et al.*[106]
27	Benzoate [a]	9000	DMSO (d_6)	^{1}H NMR	
	4-nitro benzyl bromide	1370	DMSO (d_6)	Fluroscence	Athikomarattanakul *et al.*[107]
	Napthyl phosphate [b]	≥ 10000	DMSO (d_6)	^{1}H NMR	Sellergren *et al.*[108]
28	Benzoate [a]	8000	DMSO (d_6)	^{1}H NMR	Sellergren *et al.*[106]
29	4-nitro benzyl bromide	440	DMSO (d_6)	Fluroscence	Athikomarattanakul *et al.*[107]
	Napthyl phosphate [b]	1000	DMSO (d_6)	^{1}H NMR	Sellergren *et al.*[108]
30	4-nitro benzyl bromide	280	DMSO (d_6)	Fluroscence	Athikomarattanakul *et al.*[107]
31	Benzoate [a]	15084	DMSO (d_6)	Fluroscence	Lazraq *et al.*[109]
32	Benzoate [a]	15084	DMSO (d_6)	UV-Vis	Lazraq *et al.*[109]
33	Benzoate [a]	10000	DMSO (d_6)	UV-Vis	Sellergren *et al.*[110]
34	Diphenyl phosphate [a]	176	$CDCl_3$	^{1}H NMR	Shimizu *et al.*[111]
35	Glutarate [b]	1500	DMSO (d_6)	^{1}H NMR	Sellergren *et al.*[106]
36	Glutrate [b]	790	DMSO (d_6)	^{1}H NMR	Sellergren *et al.*[94]
		1300	DMSO (d_6)	ITC	
37	Carboxylate	280	DMSO (d_6)	^{1}H NMR	Whitcombe *et al.*[112]
38	N-Z-L-Glutamate [b]	3370	DMSO (d_6)	^{1}H NMR	Schmitzer *et al.*[113]
		22000		ITC	
39	N-Z-L-Glutamate [b]	4000	DMSO (d_6)	^{1}H NMR	
		27000		ITC	
40 (Cis)	N-Z-L-Glutamate [b]	2800	DMSO (d_6)	^{1}H NMR	Schmitzer *et al.*[114]
40 (Trans)	N-Z-L-Glutamate [b]	2200	DMSO (d_6)	^{1}H NMR	Schmitzer *et al.*[114]

[a] nono-tetrabutyl ammonium and [b] bis-tetrabutylammonium salt

Sellergren *et al*. have introduced a new type of monomers, containing 1,3-disubstituted urea moieties, for targeting oxyanions [115],[18]. This moiety has shown extremely strong binding to and recognition of oxyanions, [116] also in polar environments, e.g. DMSO. The bis-urea monomer **36** used stoichiometrically against the tetrabutylammonium (TBA) salt of N-*Z*-L-glutamic acid to prepare MIPs is able to recognzse the anti-cancer drug methotrexate, which contains a glutamic acid residue [94].Polymerisable 1,3-diaryl *mono*-ureas (**26-28**) [117] have been synthesized. The acidity of ureas can be tuned by choosing appropriate substituents on the phenyl groups. These resultant monomers provide strong interactions in the polar media. Sellergren *et al*. have used monomer **28** (K_a with benzoate *ca.* 8000 M^{-1}) to create another MIP against N-*Z*-L-glutamic acid. However, This polymer have observed better recognition properties in organic solvent but decreased retention properties in water containing mobile phases[117]. A stoichiometrically imprinted polymeric receptors for the class-selective recognition of β-lactam antibiotic has been prepared using urea monomers **27** targeting the carboxylate functionality of procaine-penicillin-G [118]. The resulting MIPs have shown to effectively retain similar compounds from aqueous environmental samples (for example river and tap water) [119].

The combination of urea host monomer **27** from this MIP also enables the capture of phosphorylated peptides. The neutral hydrogen bond receptors provide sufficient binding energy to capture these peptides in aqueous environment and in even more complex samples.

Apart from the synthesis and characterization of the MIP based materials, this thesis will present results confirming the versatility of the urea host monomers for imparting highly discriminative strong binding sites for these PTMs.

3 Preparation and characterization of urea-based MIPs for model oxyanions

3.1 Objectives

The performance of molecular imprinted polymers (MIP) is mainly dictated on the interaction between the functional monomers and templates in pre- and post-polymerization mixtures at the molecular level [106, 118]. In this chapter, the effects of functional monomer on the performance and morphology of oxyanion imprinted polymer have been investigated in depth. The hydrogen-bond acceptor sites in these molecules have been targeted using a 1,3-diarylurea based functional monomer **27**. The model templates phenyl phosphonic acid (PPA) and phenyl sulfonic acid (PSA) have been used in this study of crudely mimic phosphate and sulfate functionalities. Imprinted polymers are crosslinked materials, which are insoluble in almost all solvents. Therefore, it is important to study the interaction of monomer with oxyanion before the polymerization in solution. Further recognition behaviors of the imprinted materials have extensively tested using closely similar anions and different mobile phase. The preparation and application of imprinted polymers have been extensively reviewed in many publications in recent year. However, only few studies [120] have been reported about fundamental understanding for oxyanion recognition by imprinted polymer. The following points have to be taken consideration in order to understand the principle concepts of the oxyanion recognition by imprinted polymer: 1) The association behavior of monomer with oxyanion in solution and in imprinted polymers, 2) the influence of the functional monomer on the performance of MIPs, 3) the fundamentals of stoichiometric imprinting, 3) the effect of the functional monomer on the physical characteristics like morphology (surface area and pore size distributions) as well as on the binding parameters (total number of binding sites and polymer-template association energy, capacity), 4) cross-selectivities of resultant MIPs with different oxyanions, 5) the effect of different mobile phases and modifiers on the rebinding of oxyanions.

3.2 Synthesis of functional urea monomer

In order to find suitable host monomers for oxyanions, urea-derivatives have been selected, since they establish appropriate binding sites for anions, in particular oxoanions such as phosphonates, sulfates and carboxylates[17] [18]. Unsymmetrically substituted aromatic urea derivatives 1-(4-vinylphenyl)-3-(3,5-bis(trifluromethyl) phenyl)-urea monomers **27** have been synthesized by

condensation of 1,3-bis(trifluoromethyl) phenyl isocyanate and 4-amino styrene [106] (Figure 3.1). 3,5-bis (trifluromethyl) phenyl substituents was appended to the urea moiety since it was expected that the presence of of the electro-withdrawing substituent $-CF_3$ enhance the acidity of the urea function and as a consequence increases the H-bond donor properties of the receptor. The presence of vinyl substituent makes the derivative polymerizable.

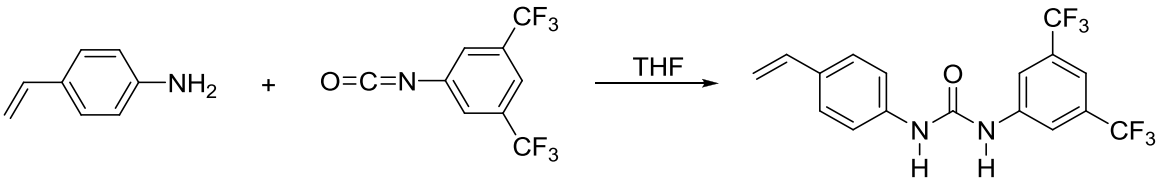

Figure 3.1 Synthesis of a polymerizable, functional urea monomer (FM).

In this context, the association parameter and interaction mode of the urea host monomer (FM) have been investigated with model anions (Table 3.1) using ^{1}H NMR, NOESY spectrosopy and ITC titrations.

3.3 Monomer/model anion complex formation

As a first step in the evaluation of hosts for complex formation, the interaction between the synthesized host monomer and with three model anions of phenylphosphonic acid (PPA), benzoic acid (BA) and phenylsulfonic acid (PSA) in the form of TBA salts were investigated with respect to the complex stability.

Table 3.1 Model anions. phenlyphosphonic acid (PPA), phenylsulphonic acid (PSA), benzoic acid (BA) and phenyl phosphoric acid (PP Acid)

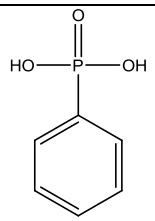	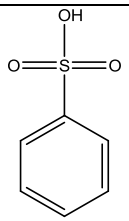	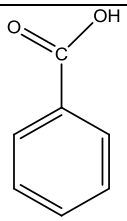	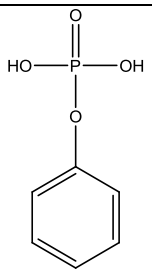
phenylphosphonic acid (PPA)	phenylsulfonic Acid (PSA)	benzoic acid (BA)	Phenyl phosphoric acid (PP acid)
pKa1:1.83; pKa2:7.47	pKa:2.7	pKa: 4.19	pKa1: 0.9; pKa2: 6.28

pKa values adapted from [121]

Table 3.2 Complex stoichiometry and association constants of functional urea monomer (FM) and anions obtained from NMR (X) and ITC titration experiments (Y)

Guest	**Ka (M^{-1}) [X]**	**CIS**	**Ka (M^{-1}) [Y]**	**ΔH (cal/mol)**
Mono-TBA BA	8820±1600	3.39	8150	-3872±508
Mono-TBA PPA	1926.8 ±105	2.914	-	-
Mono-TBA PSA	-	-	Weak	weak

[X)] Ka refers to the average of the individual values CIS of both urea protons.

[Y)] Ka measured by Isothermal Titration Calorimeter (ITC) performed in DMSO against solution of functional urea monomer at 25^0C.

The receptor monomer solutions (1mM in d_6-DMSO) was titrated with a standard solution of the anion guest up to a ten-fold molar excess. Table 3.2 shows the complexation induced ^{1}H-NMR shifts (CIS) of the protons which were used to calculate the given binding constants (K). The complex stoichiometries were determined by Jobs method of continuous variation.[122, 123] and binding parameters were determined by Isothermal Titration Calorimetry (ITC). After having confirmed the 1:1 stoichiometry from the Job's plots from NMR-titration, the 1:1 binding model was used in order to determine the respective association constants. In agreement with the predictions, the oxourea monomer formed a more stable complexes with benzoate anion (K=8820 M^{-1}) compared to the phosphomonoanion (K=1926 M^{-1}) whereas the complex with the sulfonate was too weak to be detected.

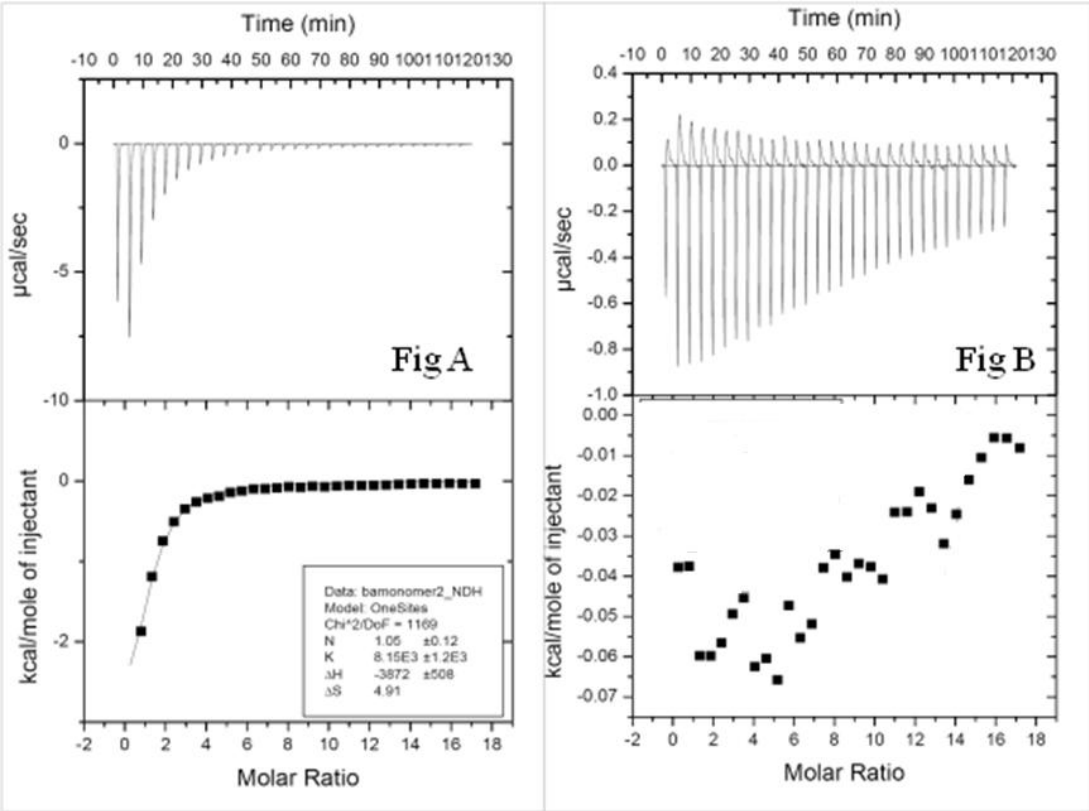

Figure 3.2 Isothermal Titration Calorimetry of urea monomer 27 with (A) mono TBA benzoic acid (BA) and (B) mono TBA phenyl sulphonic acid (PSA) in DMSO.

The association constant estimated by ITC for functional monomer and tetrabutylammonium benzoate was Ka=8150 M^{-1} in DMSO (Figure 3.2). Ka estimated by ITC are in good agreement with previously reported values from NMR titration studies.[106]. However, tetrabutylmmonium phenylsulphonate showed very weak binding to the functional monomer under the same conditions as TBA benzoate. The association constants obtained from the monomer with the tetrabutylammonium hydrogen phenyl phosphonic acid 1926 M^{-1} is similar to the association constant reported with tetrabutylammonium hydrogen napthylphosphate (TBA NP) [108].

3.4 Physical evidence of monomer/template complexation

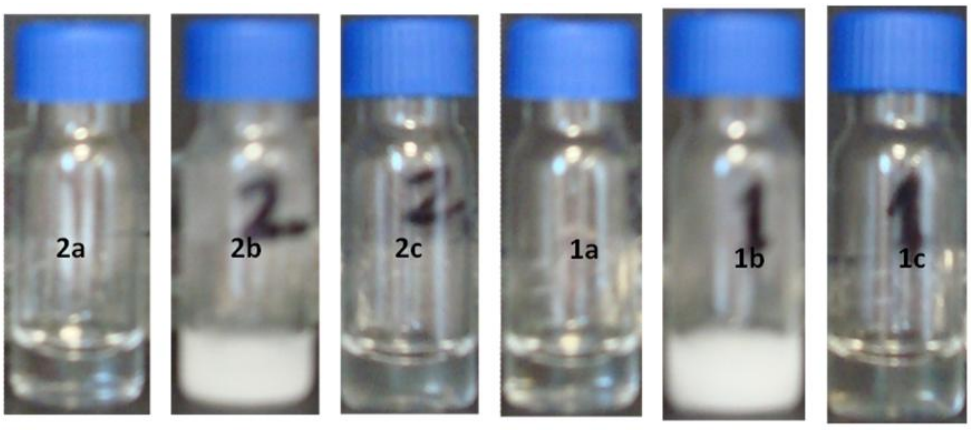

Figure 3.3 Solubilization of mono and bis pentamethylpiperidine (PMP) salt of PPA by functional urea monomer in stoichiometric amount in polymerization solvent THF. 1a, 2a: PPA in THF; 1b, 2b: bis-PMP and mono-PMP of PPA in THF; 1C, 2C: PPA/Monomer: 1:2and 1:1 in THF respectively.

The visual evidence of complexation was observed during polymerization (Figure 3.3). During the synthesis of the MIP, phenylphosphonic acid (PPA) template was taken up in tetrahydrofuan (THF) as a solvent, in which it was completely soluble (Figure 3.3- 1a, 2a). Pentamethylpiperidine (PMP) salts were generated by addition of PMP to PPA in THF and it was found that these PMP salts precipitate and insoluble in the THF (1b, 2b). After the addition of the functional monomer (FM) in stoichiometric ratio to these PMP salts of PPA, they dissolved completely in THF (Figure 3.3- 1c, 2c). This visual observation has supported the strong complexation of monomer and template previously investigated by NMR and ITC. Such experimental evidences were not observed in case of PSA template, which is consistent with observations in NMR and ITC studies (Table 3.2).

3.5 ^{1}H NMR titration study

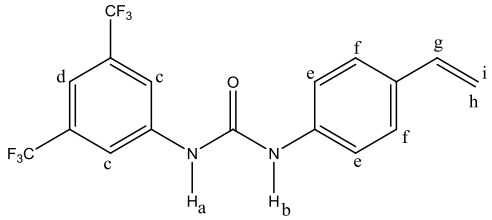

Figure 3.4 Functional urea monomer alphabetically numbered for NMR titration studies.

The interaction of the functional urea monomer with phenyl phosphonic acid (PPA) (used as mono tetrabutylammonium salt) was investigated at molecular level in more details by ^{1}H NMR spectroscopy. First it was observed that both N-H protons undergo a downfield shift, which reflects the establishment of an H-bond interaction with PPA as shown in the Figure 3.5.

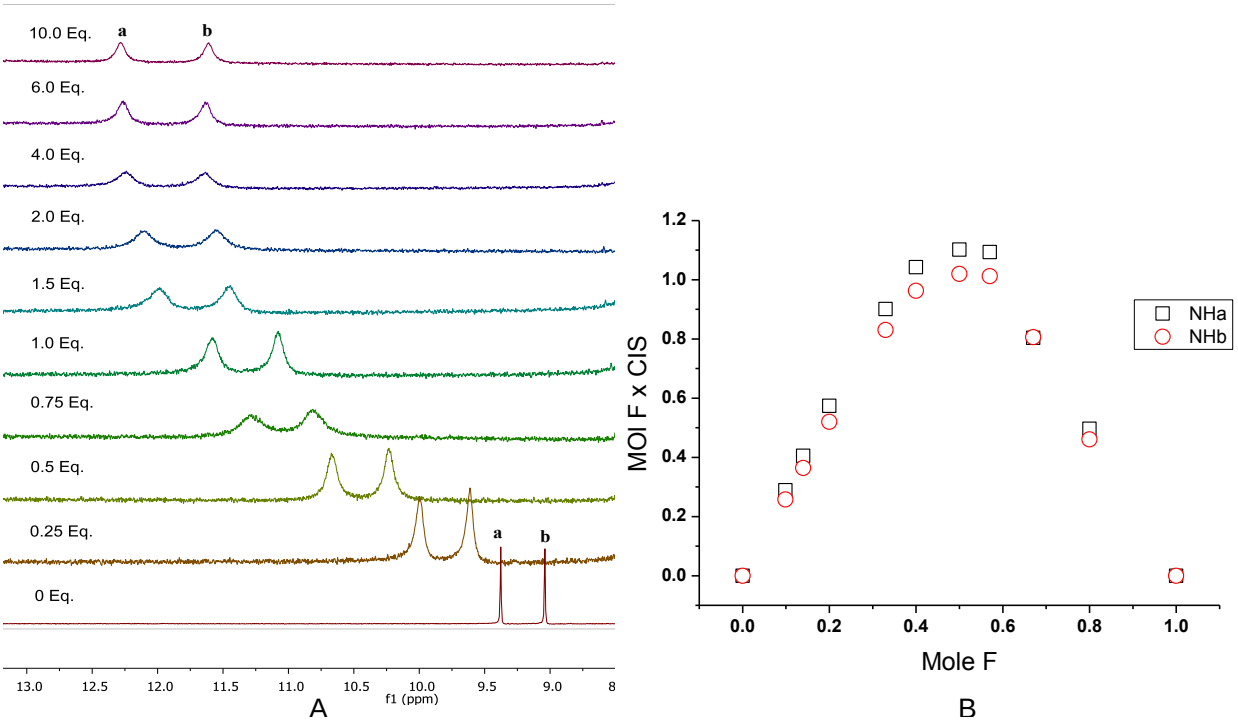

Figure 3.5 ^{1}H NMR Spectra (zoomed portion 8-13 ppm) recorded over the course of titration of DMSO solution (5 x 10^{-3} M) of the functional urea monomer with a standard solution of mono-TBA salt of phenyl phosphonic acid.

The complexation induced shift (CIS) of protons of functional monomer was calculated as a function of total concentration of mono- tetrabutylammonium (TBA) hydrogen phenyl phosphonic acid in d_6-DMSO. The complex stoichiometry between the functional urea monomer and the mono-tetrabutylammonium hydrogen phenyl phosphonic acid was determined by using the Job plot method. Therefore, the product of mole fraction (f_M) and the complexation induced shift (CIS) of either urea or aromatic protons was plotted against the mole fraction (f_M).

In particular, $\Delta\delta$ values of both protons show a saturation profile, which confirms a 1:1 stoichiometry. In addition, the complexation induced shifts (CISs) of the host urea was followed and a 1:1 binding isotherm was fitted to the the raw titration data by nonlinear regression.

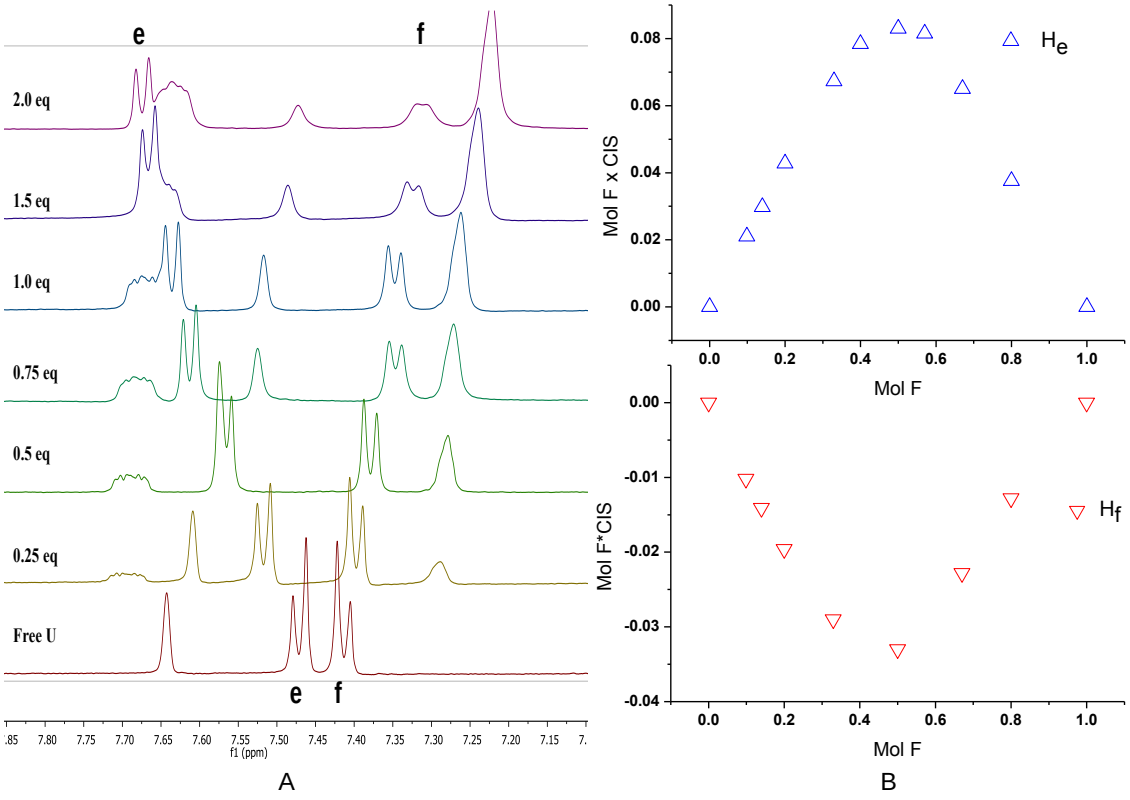

Figure 3.6 ^{1}H NMR Spectra (zoomed portion 7.0-7.85 p.m.) taken over the course of titration of DMSO solution (5 x 10^{-3} M) of functional urea monomer with a standard solution of mono-TBA salt of phenyl phosphonic acid (A) and Job plot for determining the complex stoichiometry between functional urea monomer and mono- TBA PPA (B). The product of mole fraction (f_M) and CIS of aromatic proton 'H_e and H_f' were plotted versus f_M.

During the course of titration of urea functional monomer (FM) with TBA-PPA was found that shift of the aromatic protons close to the urea subunit of FM is shown in Figure 3.6. The hydrogen bond formation between urea subunit and the anion have induced two distinct effects on the aromatic substituent. This effect is in electrostatic in nature, drastically decreases upon increasing distance between envisaged C-H proton and the site of H-bond interaction. It is seen that the electrostatic effect predominate for the proton Hc (Figure 3.8) and He (Figure 3.6), as indicated by the pronounced downfield shift which stops after a 1 equivalent addition as shown in the Figure 3.6B. This reflects the rather strong through-space interaction with N-H protons polarized by bonding with PPA.

On the other hand, C-H_f protons feel neither the anion-induced electrostatic effect nor the C-HR polarization effect, thus being affected only by the through-bond effect, which induces a moderate upfield shift as shown in Figure 3.6A. In addition, in this case, shift stops after a 1 equivalent addition of mono-TBA salt of PPA as shown in Figure 3.6B. Similar titration behavior has been shown by Fabbrizzi *et al*.[32] in the case symmetrical non-polymerizable urea (1,3-bis(4-nitrophenyl) urea). They have observed similar patterns in ^{1}H NMR spectra, when a urea derivative was titrated with tetrabutylammonium carboxylate [Bu_4N] CH_3COO (Figure 3.7). Fabbrizzi *et al.* have explained this effect as "(i) it increased electron density on the phenyl ring with a through- bond propagation, which generate shielding effect and produced an upfield shift of C-H protons; (ii) it induced polarization of the C-H bonds via through-space effect, where the partial positive charge created onto the protons causes deshielding effects and produced downfield shift"[32].

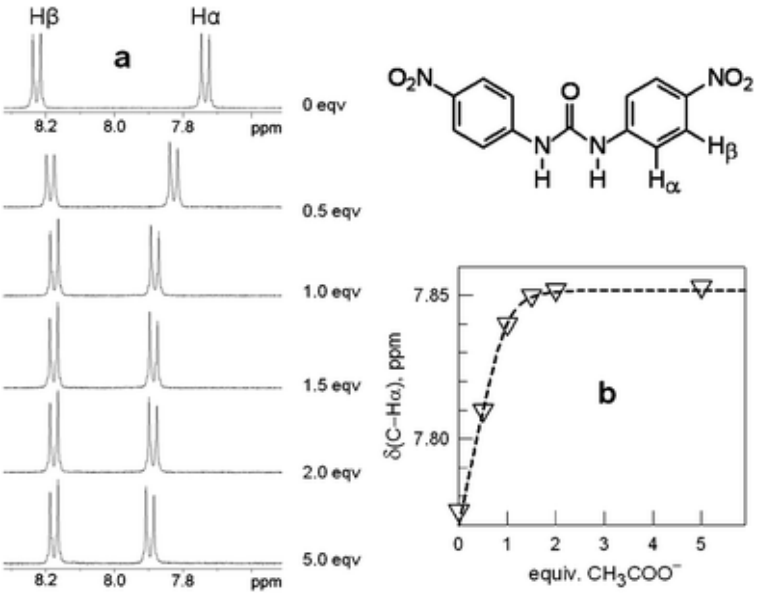

Figure 3.7 (a) ^{1}H NMR spectra recorded over the course of the titration of a 5×10^{-3} M solution of urea in DMSO-d_6 with $[Bu_4N]CH_3COO$, illustrating the spectral shifts of the aromatic protons; (b) titration profile based on the shift of the C–Hα proton (triangles). (The figure was adapted from Fabbrizzi *et al.*) [32, 124].

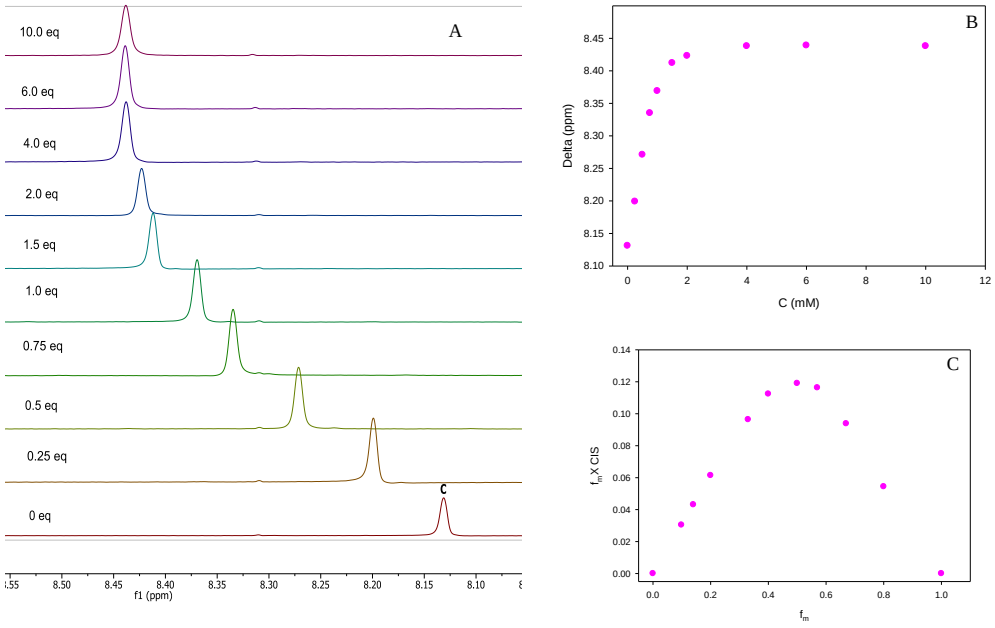

Figure 3.8 ^{1}H NMR Spectra (zoomed portion for proton Hc) taken over the course of titration of DMSO solution (5 x 10^{-3} M) of functional urea monomer with standard solution of mono-TBA PPA (A); chemical shift of aromatic proton 'c' of functional monomer as a function of total concentration of mono-TBA PPA (B); Job plot of determining the complex stoichiometry between FM and mono-TBA PPA (C).

3.6 NMR interaction in pre-polymerization conditions

So far, the functional monomer-template (FM-T) interactions was studied in dry deuterated DMSO and in dilute concentration, whereas the polymers should be prepared in tetrahydrofuran (THF). Pre-polymerization conditions are completely different in term of monomer and template concentration compared to the NMR titration study described in previous section. To get a realistic picture of interactions between monomer and template, the later was investigated in deutrated tetrahydrofuran with the concentration and stoichiometry in the range of prepolymerization. The formation of FM-T complex was done exactly under pre-polymerization conditions where functional urea monomer was added in the bis-pentamethylpiperidine salt of PPA in the ratio of 2:1 respectively for the NMR measurement. The complexation of the functional urea monomer was monitored by changes in the chemical shift of urea proton upon addition of bis PMP salt of PPA. In a NMR titration in deuterated THF, a systematic downfield shift of urea protons was found. Changes in the chemical shifts of urea N-H protons defined as $\Delta\delta_{max} = \delta_{bound} - \delta_{free}$. δ_{max} after addition (a and b assigned in the structure of urea proton) PPA were found to be 1.174 and 1.095 respectively and other chemical shifts of protons from FM as shown in Table 3.3.

Table 3.3 Δδ in ppm of urea host monomer **27** after complexation of bis-PMP salts of PPA in 2:1 ratio deuterated tetrahdydrofuran. Downfield shift reported in positive value and upfield shift reported in negative value

Protons	**a**	**b**	**c**	**d**	**e**	**f**	**g**	**h**	**i**
Δδ PPA	1.174	0.888	0.076	-0.08	0.047	-0.065	-0.026	-0.038	-0.035

3.7 NOESY Study of complex

In order to obtain further information about the complex formation, NOESY experiments fo the urea monomer were performed in the absence and presence of PMP salts of PPA in deuterated THF. The pure urea monomer showed strong NOESY contacts between urea protons H_a and H_b with water (Figure 3.10). After the addition of Bis-PMP salts of PPA, the NOESY contact of the urea NH-proton to the water ($NH.H_2O$) disappeared dramatically. The most significant change observed was the urea NH_a was showing NOE with proton NH_b (Figure 3.11) after addition of

the salts. This observation indicates that hydrogen bond formation takes place between N-$H_{a,\ b}$ of the urea moiety of functional monomer and the PPA anion as shown in the Figure 3.9. Similar experimental observation was reported for squaramide[125], urea [126] and carbazole [127] based receptors with inorganic anions.

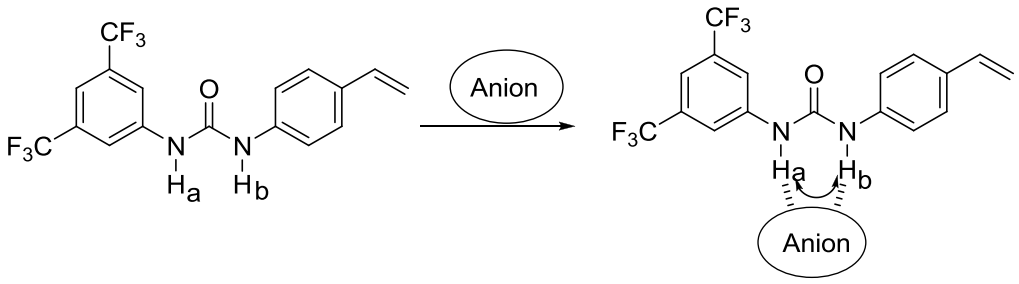

Figure 3.9 NOE detected in functional urea monomer (FM) for the urea NH protons in the presence of PMP salt of PPA anion in THF solvent.

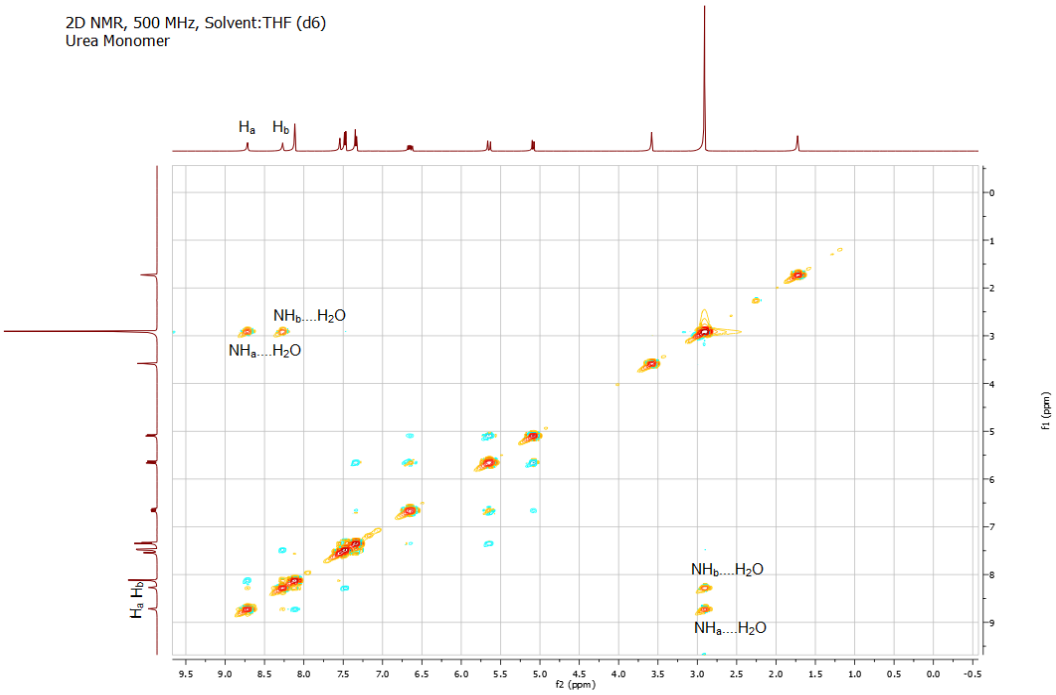

Figure 3.10 NOE NMR spectra of functional urea monomer in THF.

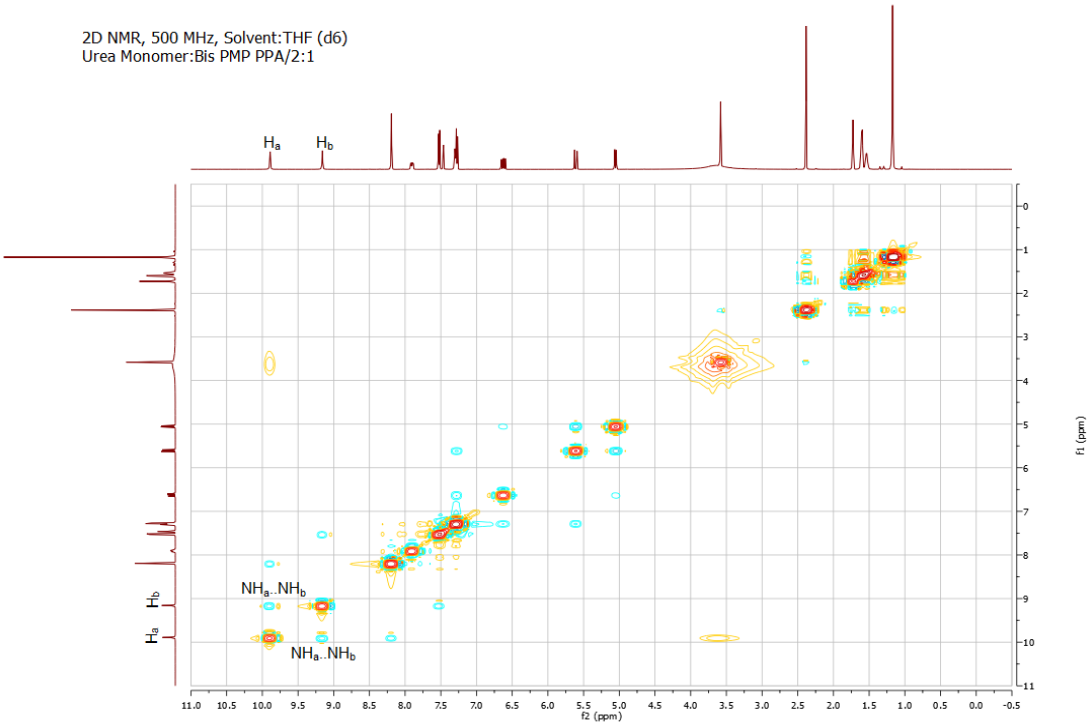

Figure 3.11 NOE NMR spectra of complex of functional urea monomer and bis PMP salt of phenyl phosphonic acid (PPA) in THF.

3.8 Conclusion for the studies of monomer-template interaction

The association parameters for the functional urea monomer with mono TBA salt was studied by ^{1}H NMR spectroscopy and confirmed the formation of the complex in 1:1 stoichiometry. The interaction mode and hydrogen bond formation between the functional monomer and the Bis-PMP salts of PPA was elucidated by NOESY spectroscopy.

3.9 Synthesis of polymers

Imprinted polymers were synthesized using model oxyanions such as PSA and PPA. The functional monomer (FM) was used in the stoichiometric ratios of 2:1 and 1:1 for both the PPA and PSA respectively in the tetrahydrofuran as a porogen. NMR study of the functional monomer with PPA suggested the formation of prepolymerization complexs as shown in the Figure 3.12.

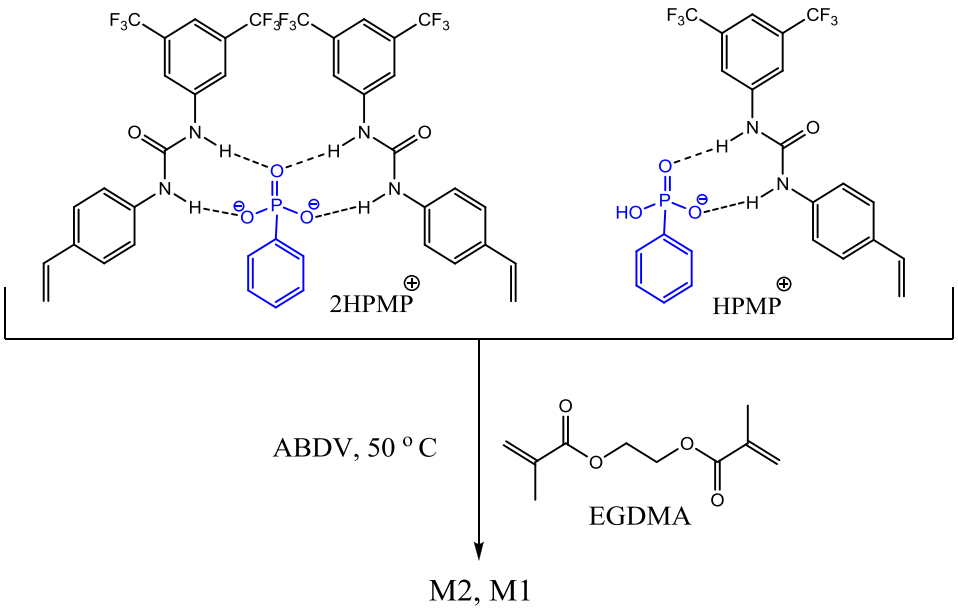

Figure 3.12 Proposed prepolymerization complexes between monourea monomer (FM) with phenyl phosphonic acid in 2:1 and 1:1 and procedure for preparation of the corresponding imprinted polymers.

The two series of polymers M1, M3 and M2, M4 were synthesized by using PPA and PSA as template in 1:1 and 1:2 stoichiometric ratio in presence of EGDMA crosslinker without any co-monomer to find out exact role of functional monomer (Table 3.4).

Table 3.4 Polymer compositions for PPA, PSA imprinting.

Polymers	**Compositions**	**Stoichiometry**	**Porogen (ml)**	**Method**
M1	FM/ PPA/PMP/EDMA	0.5/0.5/0.5/20	THF (5.6 ml)	Thermal 50°C
M3	FM/ PSA/PMP/EDMA	0.5/0.5/0.5/20	THF (5.6 ml)	Thermal 50°C
N1	FM /EDMA	0.5/20	THF (5.6 ml)	Thermal 50°C
M2	FM/ PPA/PMP/EDMA	1/0.5/1/20	THF (5.6 ml)	Thermal 50°C
M4	FM/ PSA/PMP/EDMA	1/0.5/1/20	THF (5.6 ml)	Thermal 50°C
N2	FM/ EDMA	1/20	THF (5.6 ml)	Thermal 50°C

Conventional azo-initiated thermal polymerization at 50^{o}C subsequently resulted in the imprinted and non-imprinted polymers. The non-imprinted polymer N1 and N2 were used as reference materials prepared in exactly same the way, but in absence of template. Template was removed from the polymers by soxhlet extraction using acidic methanol. Particle in the size 25-36 µm were obtained by crushing and sieving. The fine particles were removed by repeated

sedimentation in a solvent mixture of MeOH:Water/80:20. The irregular particles were evaluated with respect to their imprinting properties.

3.10 Evaluation of imprinted properties

3.10.1 Static rebinding experiments

A static rebinding experiment was performed to evaluate the imprinted polymers in terms of molecular recognition. A fixed amount of polymer was incubated with different solutions of the template in varying concentrations in HPLC vials and equilibrated for more than 24 hours. Afterwards, the amount of non-bound template was quantified by determining the concentration of the template in the supernatant. Imprinted polymers (Figure 3.13) in blue are considered as single imprinted particle having cavities for the template uptake (Figure 3.13 - red considered as template molecule). Non-imprinted polymers do not have cavities and it does not facilitate the selective template uptake by the polymers.

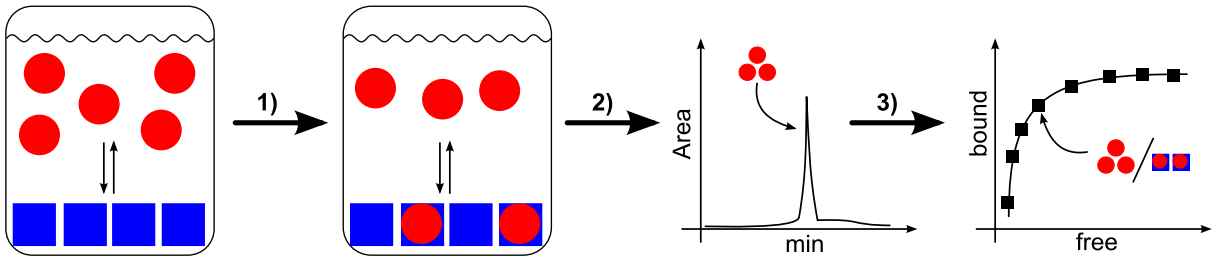

Figure 3.13 Batch rebinding experiment. 1) Incubate polymer with analyte (initial concentration C0); 2) Determine free analyte Cf in supernatant (with HPLC); 3) Calculate bound analyte Cb = C0 - Cf and insert more points with different concentrations in bound versus free concentration create binding isotherm.

The unbound (free) template was checked by HPLC-UV (step 2) and the amount of bound template was calculated per gram of polymer (either MIP/NIP separtely). If imprinting is successful, the graph of bound template (µmol/g) versus the free concentration (mM) reflect enhanced uptake of template by the MIP compared to NIP (step 3). The graph is most often in correlation with the binding strength and selectivity and commonly denoted as binding isotherm.

3.11 Evaluation of imprinting property in presence of pentamethyl piperidine (PMP)

In the first step of evaluation of imprinting properties, MIPs and NIPs (Table 3.4) were incubated in MeCN with an increasing amount of pentamethyl piperidine (0 to 1%) at single concentration of 0.6 mM of PPA. After incubation for 24 hours, the unbound template in the supernanent solution was analyzed by HPLC (Figure 3.14). Polymers M1, M2 recognize template PPA in both polymer compositions; however, non-imprinted polymers did not observe any imprinting effect (Figure 3.15). The concentartion in the supernatant from M2, M1 is small compared to N2, N1 after incubation for 24 hours. Representative graph of HPLC-UV chromatograms of supernatant solution of PPA after rebinding from M2, N2 are shown (Figure 3.14) at 0.4 mM and 0.6 mM. The bound template was calculated by comparing peak areas of standard solution of template with the peak area after incubation with MIP, NIP.

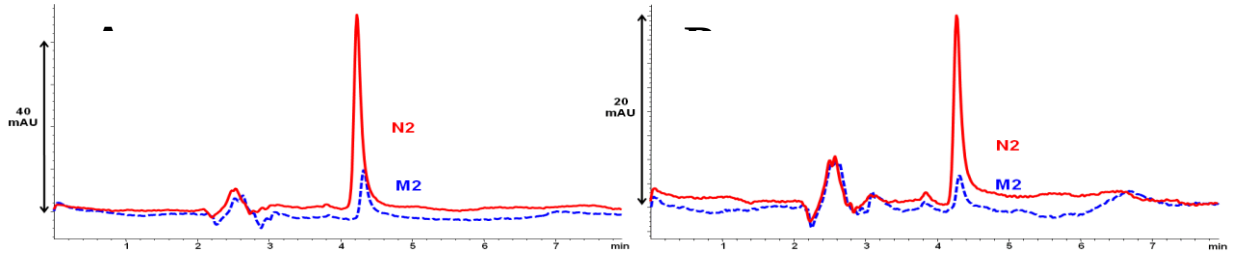

Figure 3.14 RP-HPLC chromatograms of PPA of supernatant solution after rebinding experiment of imprinted (M2) and non-imprinted polymer (N2) with various concentration (A) 0.6 mM; (B) 0.4 mM PPA respectively.

PMP has been chosen as an ion pairing reagent (IPR) in the solvent during rebinding, because it has been used during polymerization. The PMP was found to have major effect on rebinding of PPA in rebinding solution by MIP (M2, M1) and NIP (N2, N1) at concentration of 0.1%. The 0.1% v/v concentration of PMP is sufficient to deprotonate the template. The pentamethylpiperidine (PMP) is a bulky base, and the PMP salt of PPA will increase in hydrophobicity. Counter ion helps template enter into the imprinted cavites (Figure 3.15). This observations are similar to B Sellergren *et al*. [108] who have observed that the presence of a counter ion such as tetrabutylammonium during synthesis of imprinted polymer exhibit strong memory effect [108]. During analysis of these imprinted polymer, an addition of an ion pairing

reagent (IPR) in the mobile phase provided a strong retention of the template in an imprinted polymer, however there is no such effect on the retention of non-imprinted polymer, when these materials were packed in HPLC columns [108]. It means that the IPR facilitates the access to the template in the imprinted sites. The polymers (M3 and M4) were prepared using PSA as template did not show any imprinting effect and no IPR effect on the rebinding of PSA was observed (Figure 3.16). The similar results were obtained from interaction behavior of FM with PSA in solution (ITC titration, Figure 3.2).

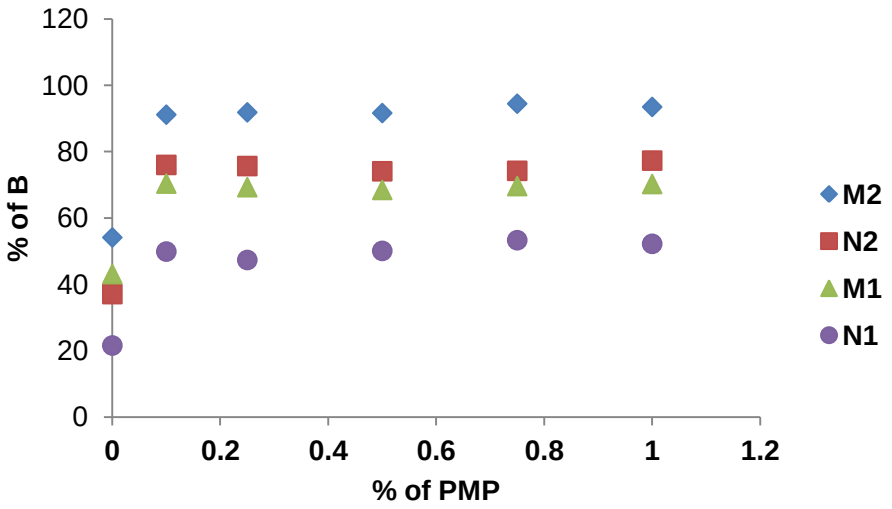

Figure 3.15: Rebinding of PPA (0.6 mM solution) with PPA imprinted and corresponding non-imprinted polymer in MeCN with increasing % of PMP. (FM:PPA/2:1 (M2) and 1:1 (M1) and corresponding non-imprinted polymers N2 and N1).

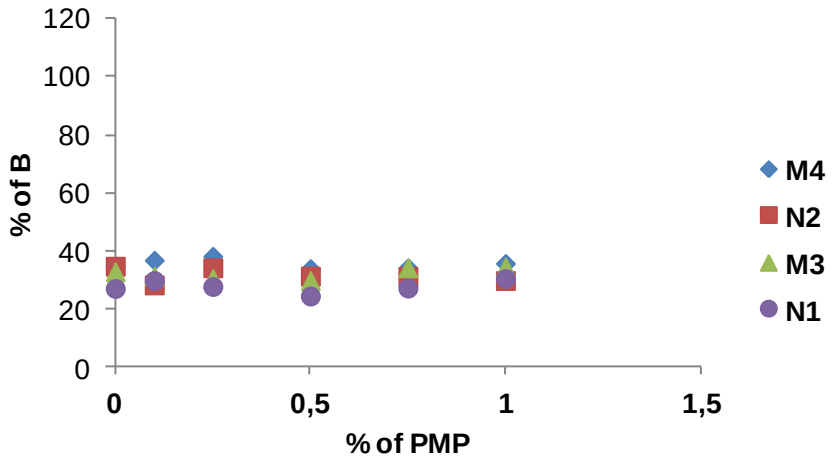

Figure 3.16: Rebinding of PSA (0.6 mM solution) with PSA imprinted and corresponding non-imprinted polymer in MeCN with increasing % of PMP. (FM:PSA/2:1 (M4) and 1:1 (M3) and corresponding non-imprinted polymers N2 and N1).

PPA imprinted polymers have shown a good imprinting effect; however PSA imprinted polymer has shown a poor imprinting effect. Further, studies described in the following section are focusing on focused on PPA imprinted polymer to understand the effect of functional monomer on pre- and post-polymerization at the molecular level. The effect of functional monomer will be examined for PPA and will be correlated with physical characteristics like morphology and binding parameters of imprinted polymers. Conventional analytical techniques such as IR, elemental analysis and solvent swelling studies will be used for characterization. Selectivities of these MIP will be tested by using benzoic acid (BA), phenyl sulphonic acid (PSA), phenyl phosphonic acid (PPA), phenyl phosphoric acid (PP acid) and different mobile phase with modifiers.

3.12 Physical properties of polymers

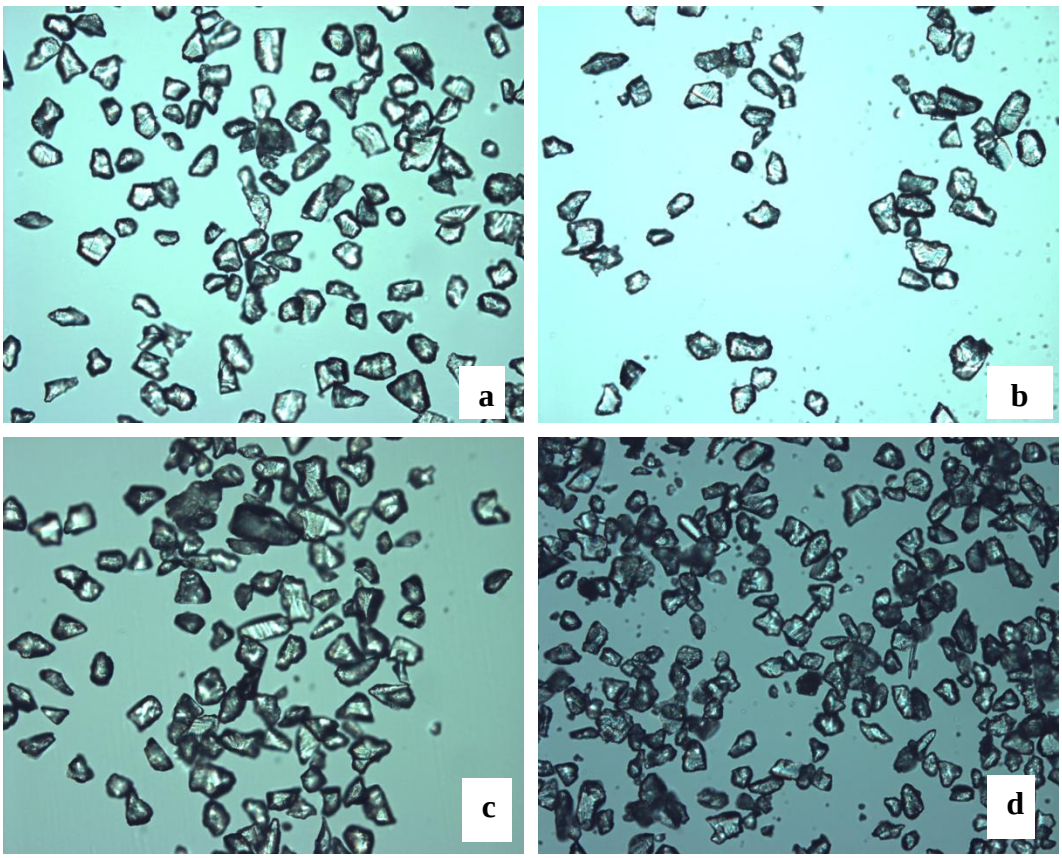

Figure 3.17: Representative optical photograph of 25-36 µm sized bulk polymers (M1. N1, M2 and N2 are a, b, c and d respectively) at 20X magnification.

The representative microscopic pictures of imprinted bulk polymers in the size of 25-36 µm are shown in Figure 3.17. Elemental analysis of imprinted and non-imprinted polymers after removal of template showed that N/C ratio of both MIP and NIP are comparable assuming conversion of all monomers into polymer (Table 3.5). This indicates that removal of template from the polymer is successful and there is no adverse template effect on the polymerization of MIP.

The FTIR spectra (Figure 3.18) showed the following characteristic bands: 3476, 3402 cm^{-1} for the free CONH group and N-H stretching respectively, 3000 cm^{-1} for the C-H stretching group , 1700 for C=O group. No difference was observed between the spectra of MIP and NIP. This is again confirmation the successful template removal from the imprinted polymers.

Table 3.5 Elemental analysis of imprinted and non-imprinted polymers were prepared in presence of EDMA crosslinker

	% C	% H	% N	N/C ratio
N2	58.36	7.13	0.65	0.0111
M2	58.89	6.92	0.68	0.0115
M4	58.74	7.04	0.72	0.0123
N1	59.08	7.66	0.45	0.0076
M1	55.65	7.15	0.46	0.0078
M3	58.6	7.44	0.39	0.0066

The elemental composition of the polymers assuming full incorporation of the monomer are C- 60.21 %, H- 6.82 %, N – 0,75 %, N/C ratio – 0.0125 and C- 60.4 %, H- 6.98 %, N- 0.45 %, N/C – 0.0075 in the ratio 1:2 and 1:1 template to monomer respectively.

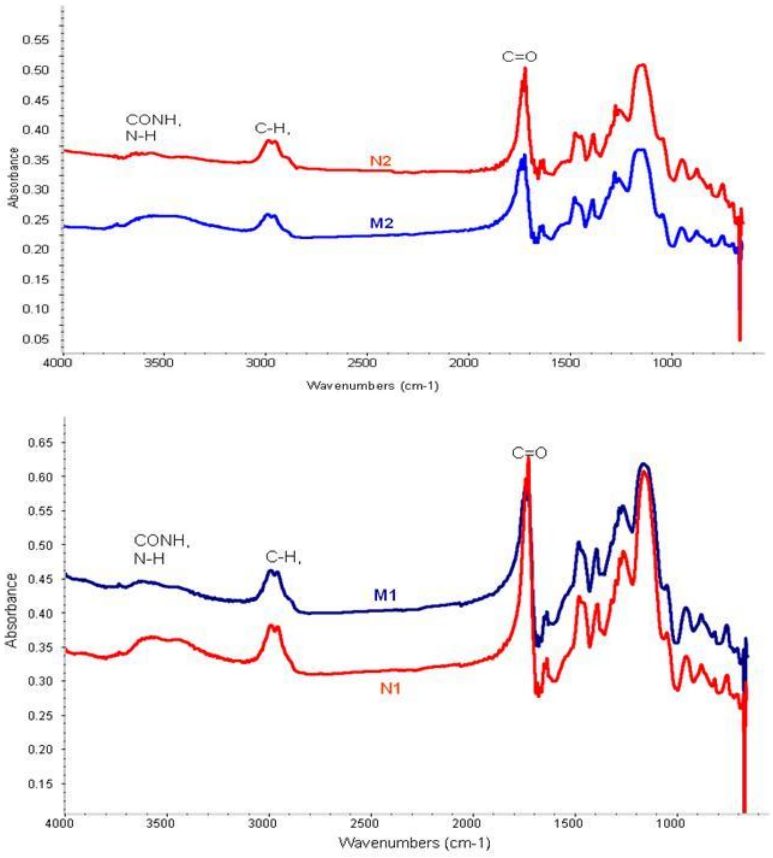

Figure 3.18: Transmission infrared spectra (KBr) of the bulk imprinted and non-imprinted polymers.

3.13 Effect of template molecular structure on polymer microstructure

Pore volume distributions was measured by the Brunauer-Emmet-Teller (BET) method from the nitrogen desorption isotherms. The resultant polymers had a pore size distributions in the mesoporous regime (2 to 50 nm diameter). The representative plots of pore volume distributions are shown in the Figure 3.19 as cumulative pore volume (CC/g) versus pore diameter (nm).

Table 3.6 BET surface area, pore volume and pore diameter of imprinted and non-imprinted polymers were prepared in presence of EGDMA crosslinker.

	Surface area	**Pore Volume**	**Pore Diameter**		**Swelling Ratio**
	m^2/g	CC/g	Dv (d) nm		v/v (ml/ml)
N2	336.27	0.161	3.699	4.36	1.4
M2	270.18	0.161	3.714		1.5
N1	474.62	0.345	3.711	10.35	1.4
M1	365.18	0.281	3.912	5.58	1.5

The molecular structure of template molecules influences the polymer microstructure[128]. The imprinted and non-imprinted polymers had surface areas in the range of 250 to 475 m^2/g. In the case of MIP and NIP polymers, there was a slight difference in surface area (Table 3.6). The pore size distribution of N2 showed two peaks consisting a narrow distribution a 3.6 nm and 4.36 nm in the mesoporous region (Figure 3.19). Imprinted polymers had produced only one distribution of pore at about 3.7 to 3.9 nm, and there was no broad peakening of larger pores. This effect that the interaction the interaction of functional monomer with the template affects the polymer microstructure and pore size distribution.

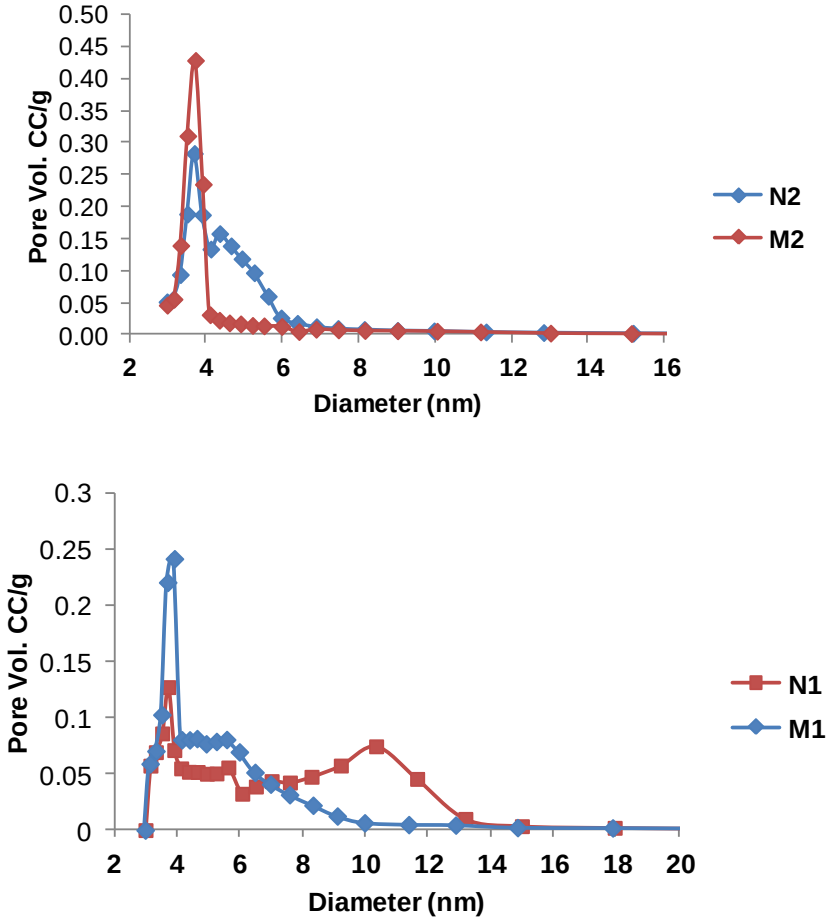

Figure 3.19 pore size distribution of PPA imprinted and non-imprinted polymers as a ratio of PPA:FM 1/1:1 and 1:2 as N1, M1 and N2, M2 respectively crosslinked in the presence of EGDMA crosslinker. The graph was plotted cumulative pore volume (CC/g) versus pore diameter (nm).

The pore size distribution of polymer N1 has two peaks consisting of narrow distribution about the 3.71 nm and a wide distribution about 10.351 nm in the mesopore region (Figure 3.19). The imprinted polymer M1 had a similar pore size distribution where pores were dominant at a region between 3.7 to 10 nm and a shoulder around 5.6 nm. The influence of polymerization conditions and the presence of a removable template molecule have been shown to enable a wide spectrum of polymers with varying pore size distributions and surface areas to be synthesized. The pore size distribution is slightly different the two polymer series and also beween MIPs and NIPs within the same series. Pore distribution of non-imprinted polymers were found to be a little broader compared to imprinted polymers (Figure 3.19).

3.14 Binding isotherms and affinity distribution of MIPs

Many natural receptors like antibodies and enzyme have monoclonal high binding affinity sites. However in case of imprinted polymers, heterogeneous binding sites are created. This means that MIPs have a variety of binding sites differing in the affinity to the template. Especically the use of the non-covalent imprinting approach results in a high degree of hetrogenity. This imprinting approach has this inherent weakness because of its weak interactions and often there is no control over the interaction of monomer and the template. To increase formation of selective binding sites with high affinities in the material, the stoichiometric non-covalent imprinting approach has been applied. This approach allows the use of high temperature and polar solvents during polymer synthesis. To analyze the degree of success in the applied method, affinity distribution study of MIP and NIP have been carried out. To gain insight into the binding energy and site density of the polymers, the equilibrium binding isotherms for both the imprinted and non-imprinted polymers have been measured in the MeCN (0.1% PMP).

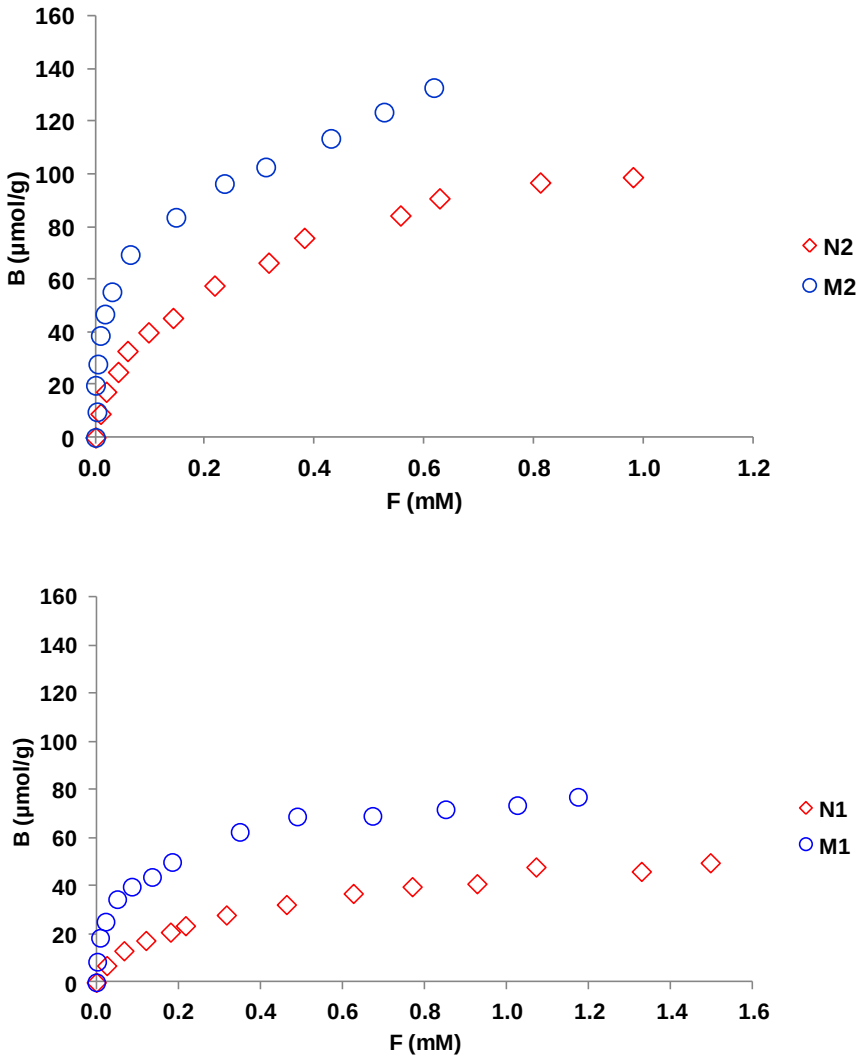

Figure 3.20 Equilibrium binding isotherm for the uptake of the PPA by MIP (blue) and NIP (red) in MeCN (0.1% PMP). MIP and corresponding NIP were prepared by FM:PPA/ 2:1 (M2) and 1:1 (M1) and corresponding NIPs (N2 and N1). F = concentration of free PPA, Bound = Specific amount of bound PPA.

For an accurate assessment of binding site affinity, the Bi-Langmuir binding model applied to the experimental data, generated through batch rebinding experiments (Figure 3.20). The isotherms for the imprinted polymer showed a good fit to a Bi-Langmuir model (Eq. 1.8), resulting in two different kinds of binding sites, high energy binding sites and low energy binding sites (Table 3.7). As the initial concentration of PPA to polymer composition remained constant for both the polymer during synthesis except a change in functional monomer

concentration, in theory they should provide equal number of binding sites in both the polymers. However, applying the Bi-Langmuir isotherm model to the polymer indicates that this is not the case. An interesting result was found that the polymer M2 has three fold more high energy binding sites (69 µM) compared to M1 (23 µM) with a binding energy in the range of 10^6 M^{-1}. This is related to the hydrogen donor ability from the binding sites in the polymer. Polymer M2 has quadruple hydrogen donor groups from two urea moieties in the binding site compared to bidentate hydrogen donor groups resulting from one urea group. As can be seen in Table 3.7 there was a five-fold increment of low energy binding sites in M2 compared to M1, whose affinity is in the range of 10^3 M^{-1}.

Table 3.7: Binding constants (Ka) and specific binding site densities (q) and binding capacity were obtained from fitting plots

Polymer		Affinity constant, k ($\times 10^6$ M^{-1})	Binding site density, q (µM)	Binding capacity, q x k	Regression Coefficient, r^2
M2	Class-I	**0.11 ± 0.05**	**69 ± 13**	7.59	0.998
	Class-II	0.0004 ± 0.0001	310 ± 698	0.124	
M1	Class-I	**0.23 ± 0.05**	**23 ± 3**	5.29	0.999
	Class-II	0.0004 ± 0.0001	63 ± 3	0.025	

In order to understand the role of the urea moieties in the material and excluding the polymer matrix, isotherms have been plotted as the (MIP-NIP) bound PPA (µmol/g) versus free PPA (in mM) (Figure 3.21). The binding isotherm have shown different slope, trends and different saturation profile. The polymer prepared from the ternary complex displayed a much steeper slope with a saturation at roughly 38 µmol/g. This is in contrast to the polymer prepared from the binary complex which showed a much shallower curve, although with a similar saturation capacity. Analyzing these curves assuming a Langmuir monosite model (Eq. 1.7)) gave Ka of 1.7 x10^5 M^{-1} and 3.1x10^4 M^{-1} rescpectively. Showing that the former exhibits a slightly higher affinity for the templated oxyanion. Referring the capacity to the nominal capacity gave a site utilization of 33 %.

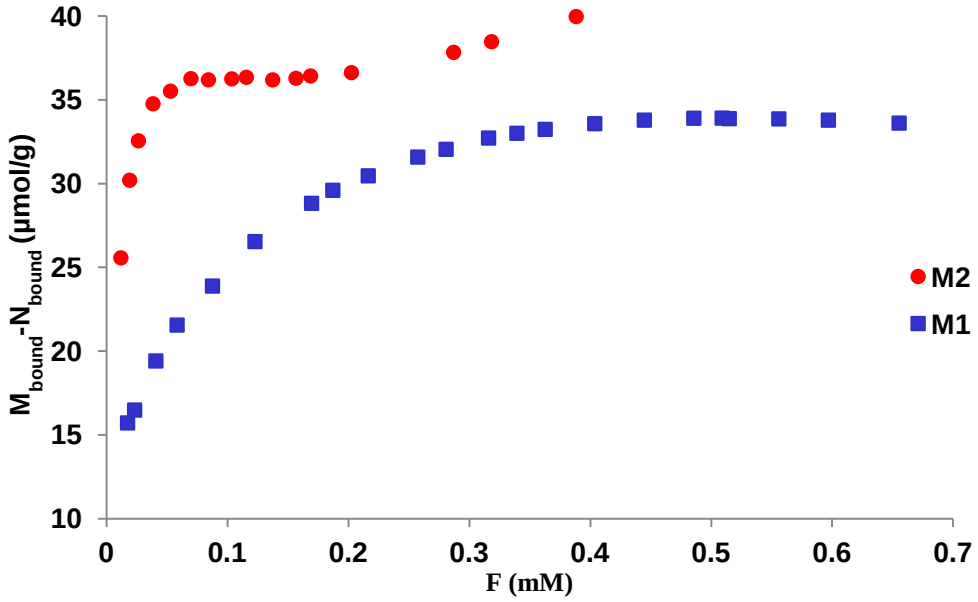

Figure 3.21 Difference of equilibrium binding isotherm for the uptake of PPA by MIP and NIP. Graph was plotted as MIP-NIP (µmol/g) bound PPA against free concentration of PPA. MIP-NIP (red color) were prepared by FM:PPA/1:2 and MIP-NIP (blue color) were prepared by FM:PPA/1:1 crosslinked in EGDMA.

The total number of high affinity binding sites and overall capacity was found to be increased with stoichiometrically imprinted polymer M2. Overall the above study suggests that the strong interactions between the template and the functional monomer results in a larger portion of the template being complexed prior to polymerization, which results in a higher yield of templated sites.

3.15 Chromatographic evaluation of imprinted polymers

One of the easiest ways to determine imprinting properties of materials is to pack then into a stainless steel HPLC column and subsequently evaluate the binding properties of analytes by injecting the later in the the column in dynamic mode. The 25-36 µm particle size fraction of the synthesized polymers obtained after crushing and sieving was repeatedly sedimented (80:20/MeOH:water) to remove fine particles and then slurry-packed into HPLC columns of size 30 mm x 4.6 (i.d.) mm using the same solvent mixture as pushing solvent. Subsequent analyses of the polymers were performed using an Agilent HP1050 system equipped with a diode array-

UV detector. Analyte detection was performed at a flow rate of 0.5 mL/min. The retention factor (k) was calculated as $k= (t-t_0)/t_0$, where t = retention time of the analyte, t_0 = retention time of the void marker (Eq.1 2) Here, acetone was used as void marker. Peak areas for reference concentrations of the analyte were obtained by injecting without column and the bound percentage of analyte was calculated by injection into the column packed with imprinted and non-imprinted polymer. The results were compared with term of percentage of bound analyte to each column. This method has been adapted because of the high affinity binding sites created in the imprinted sites; the anaylte was not eluted out of the imprinted column (Figure 3.22).

The objective was to investigate the influence of different additives in the mobile phase on the template rebinding and to study the selective memory capacity of these polymers to discriminate the template from other similar oxyanions. Thus, template PPA was injected on the columns in different mobile phases 1) 100% acetonitrile; 2) acetonitrile buffered with triethylamine (TEA) and 3) acetontrile buffered with trifluoroacetic acid (TFA).

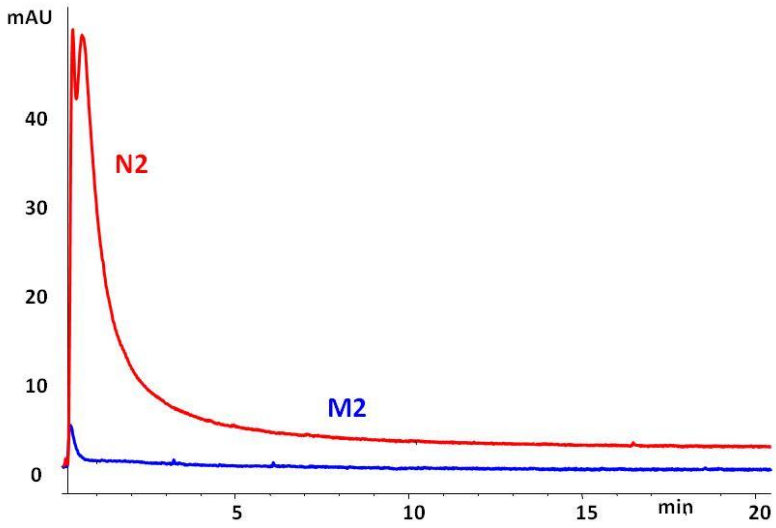

Figure 3.22 Representative chromatographs of PPA when injected in M2 and N2. LC conditions: concentartion:1 mM of PPA; flow rate: 0.5 ml/min; Injection Vol: 5 µL; mobile phase: 100% MeCN, column size: 25 x 4.6 (i.d.) mm.

When PPA was injected into the PPA imprinted column (M2), the template was completely retained in the column (Figure 3.22). This showed that the imprinted polymer has high affinity to

the template. In contrast, when injected into the column filled with non-imprinted polymer (N2), it was completely eluted out as shown in the Figure 3.22.

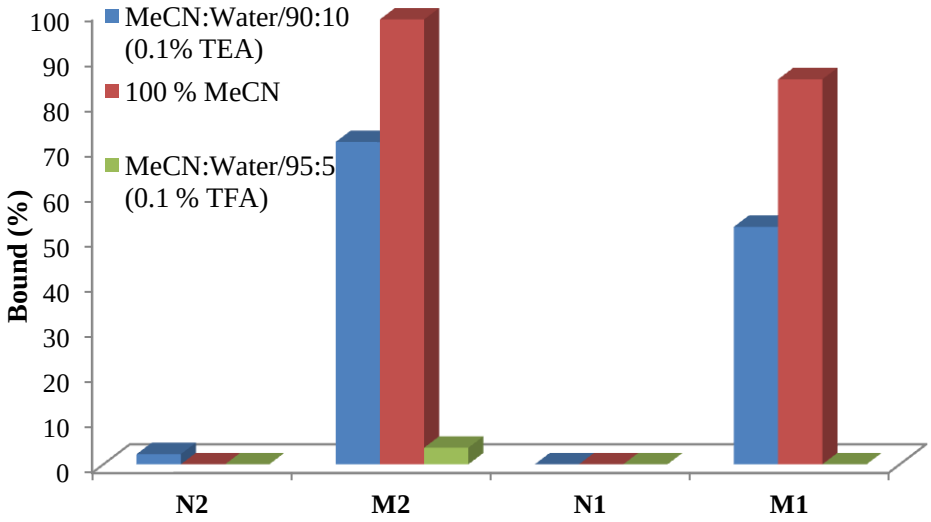

Figure 3.23 Percentage of bound PPA in the PPA imprinted column (M2, M1) and non-imprinted column (N2, N1) in different mobile phase.

The polymer M1 and M2 exhibited strong affinities for the template PPA in the mobile phase of MeCN and MeCN buffered with TEA. On the other hand, N1 and N2 exhibited no affinity for PPA under the same conditions. M2 exhibited stronger template retentivity than M1, which showed that number of binding sites was increased resulting increase of the binding capacity in M2. Basic conditions were used in order to promote deprotonation of the template and thus allowing stronger interactions. In the acidic mobile phases, both the imprinted and non-imprinted polymer did not bind the template PPA (Figure 3.23).

3.16 Cross-selectivity of anions

Selectivities of the polymers were assessed by injecting different oxyanion guests for example phenyl phosphonic acid (PPA), phenyl phosphoric acid (PP acid), phenyl sulphonic acid (PSA), benzoic acid (BA) in the imprinted (M1, M2) and non-imprinted columns (N1, N2). PPA, PSA and BA were injected using acetonitrile as mobile phases and it was found that PPA and PSA bound in the M1 and M2 column there was no binding for BA (Figure 3.24). Non-imprinted polymer N1 and N2 did not show any affinity towards all the anions. The polymer M2 which

was prepared with 0.5/1:PPA:FM ratio showed a higher capacity for the PPA and the PSA analyte compared to polymer M1, which was prepared with 0.5/0.5:PPA:FM ratio. The PPA imprinted polymers have higher affinities towards PPA compared to PSA.

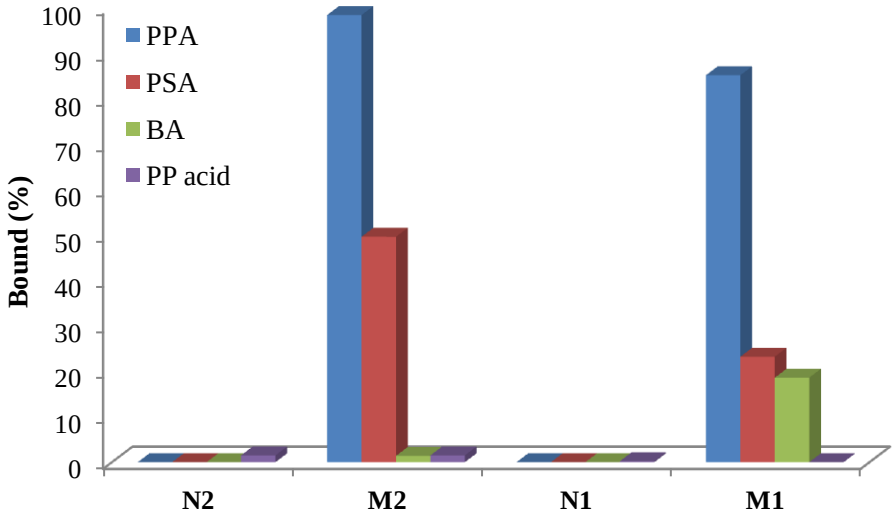

Figure 3.24 Percentage of bound PPA, PSA, BA and PP acid in the PPA imprinted column (M2, M1) and non-imprinted column (N2, N1) in 100 % MeCN mobile phase.

Next, these anions were injected onto the columns in an acetonitrile-rich mobile phase buffered with triethylamine (Figure 3.25). Under basic condtion, PPA and PP acid estabilish a better affinity to the urea group in the MIP hosts (Figure 3.24) as these anion exists in their anionic form (Table 5.3). On the other hand, PSA did not show affinity to the MIPs (M1, M2) in the same condition. A possible explanation might be that sulfate is highly hydrated anion in basic media [129]. Polymers N1 and N2 exhibited no affinity to all anions. The polymer M2 showed stronger affinity to PPA compared to M1. This is because of differences resulting from the number of urea-group donors from the MIP. M2 has two urea moieties in the binding sites whereas M1 has only one urea moiety. Figure 3.25 shows that imprinted polymers (M1, M2) have shown preferential high affinity towards the template PPA than PP acid, inspite of having the same functionalities. This result confirms that imprinted polymers have strong shape memories.

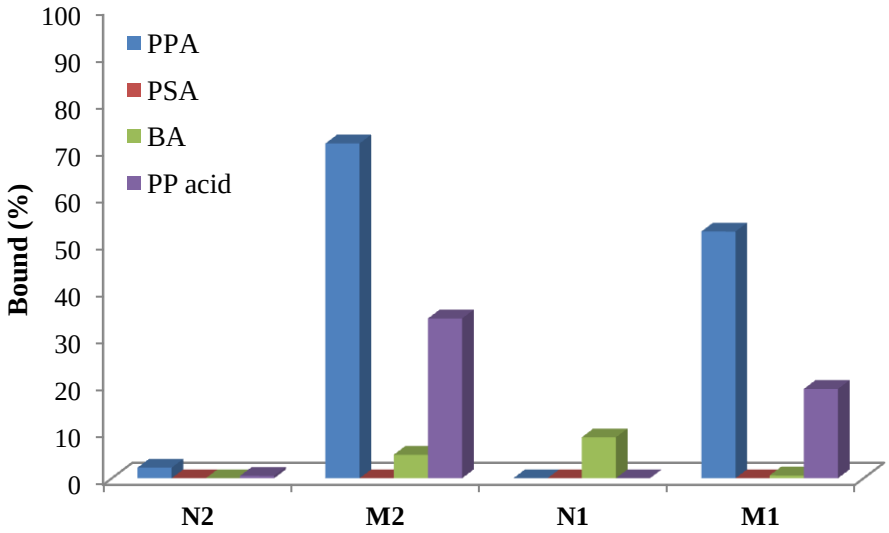

Figure 3.25 Percentage of bound PPA, PSA, BA and PP acid in the PPA imprinted column (M2, M1) and non-imprinted column (N2, N1) in MeCN:Water/90:10 (0.1% TEA) mobile phase.

Finally, all anions were injected onto PPA imprinted column using acteronitrile mobile phase buffered with the acidic modifier trifluoroacetic acid (TFA). In an acidic mobile phase, the PSA anion was bound strongly to the PPA imprinted column (M2) whereas no such affinity was observed for the other templates such as PPA, PP acid and BA. The retention factor (k) was measured for all the anions by using acetone as void marker.

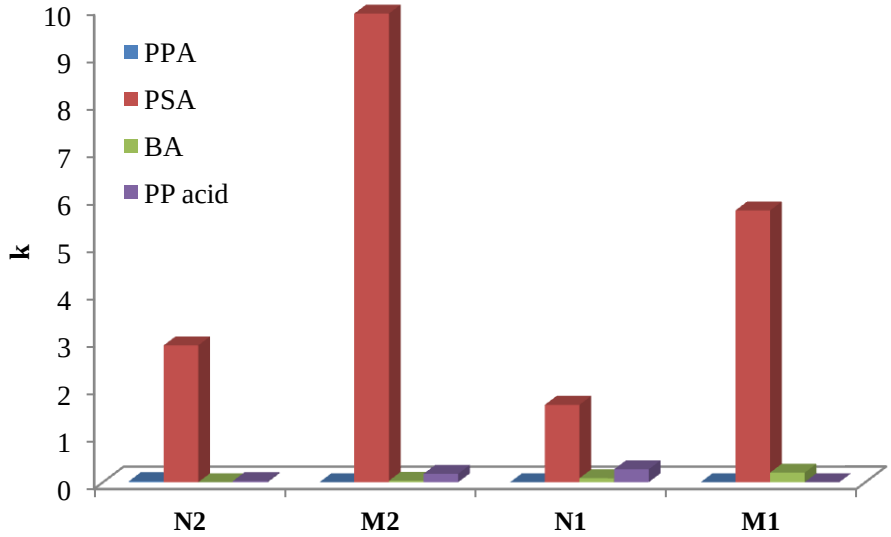

Figure 3.26 Percentage of bound PPA, PSA, BA and PP acid in the (M2, M1) and non-imprinted column (N2, N1) in MeCN:Water/95:5 (0.1% TFA) mobile phase.

In the acidic-buffered mobile phase, imprinted and non-imprinted columns showed weak affinity to PPA and PP acid (Figure 3.26) but showed affinity to PSA. This result further confirmed by injecting the PMP salt of PSA using neutral mobile phase. It iwas observed that the PMP salt of PSA has a stronger binding to M1, M2 compared to PSA when these anions were injected on the PPA imprinted polymer (M1, M2) in MeCN mobile phase (Figure 3.27). This observation confirmed that the PSA can have well fitted in the cavity of PPA imprinted polymer and it has the strong memory effect of counter ion. This results are similar to what B. Sellergen *et al.* found in a study where they found that IPR facilitates the access to template in the imprinted sites [108].

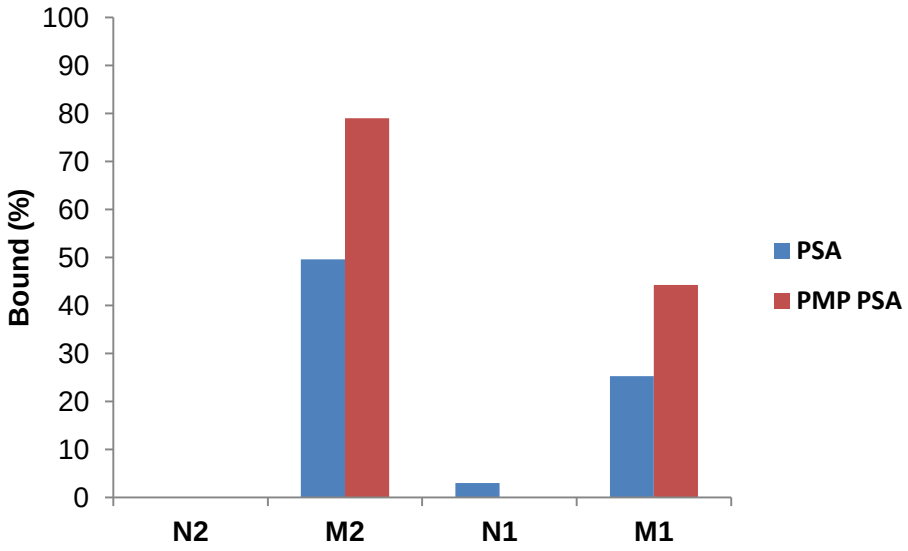

Figure 3.27 Percentage of bound PMP salt of PSA in the PPA imprinted column in MeCN mobile phase.

A directional hydrogen bond has been described as 'masterkey interaction' in supramolecular chemistry. In the present study, this hydrogen bond is the main interaction between neutral urea functionality in an imprinted site to the functional group of the oxyanion. In order to understand the hydrogen bonding interactions in more details, methyl tosylate and toluene sulphonate were injected onto PPA imprinted column (M2).

Toluene sulphonate has shown a stronger affinity to the PPA imprinted column where as there was no affinity for methyl tosylate. This was because sulphonate functionalities blocked by the methyl group in case of methyl tosylate, however the sulphonate group is accessible by the urea

functionality in the binding site of the imprinted polymer in case of toluene sulphonate. This observation gives evidence that the hydrogen bond interaction is a key parameter for recognition in the present study of imprinted polymer (Figure 3.28).

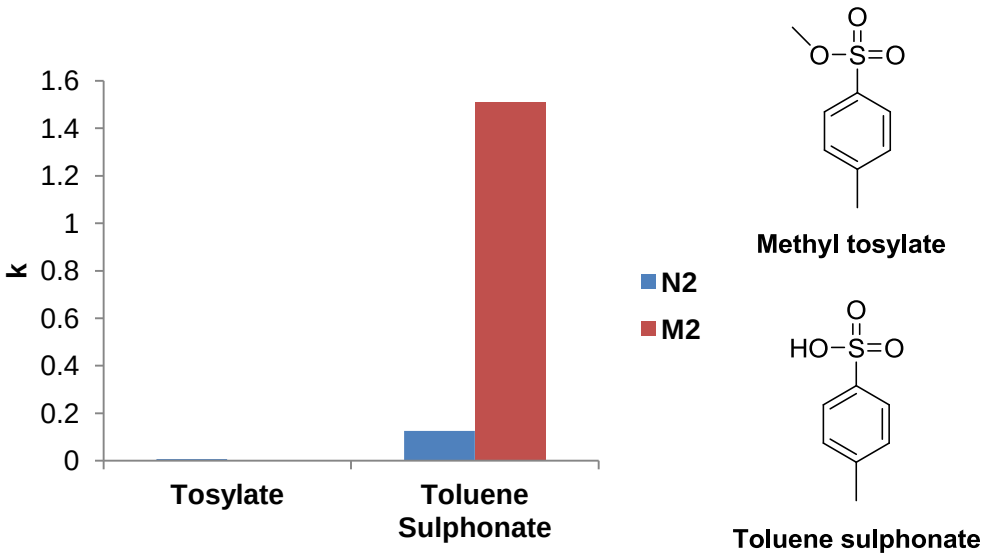

Figure 3.28 retention factor (k) of methyl tosylate and p- toluene sulphonate in the M2, N2 column in MeCN:Water/95:5 (0.1%TFA) mobile phase and structure of methyl tosylate and toluene sulphonate. Analytes used for proof of hydrogen bonds as key interaction in the recognition. HPLC conditions: 1mM of concentration in MeCN, injection volume: 5µl, flow rate:0.5 mL/min, DAD@205nm.

3.16.1 Testing of Fmoc-pTyr-OEt imprinted polymer for phenyl oxyanions

The anions (PPA, PP acid, PSA and BA) were injected into the columns P1, P_N1 (synthesis described as in section 4.4) in acetonitrile-rich mobile phase buffered with triethylamine (Figure 3.29A). An interesting observation was that P1 has preferential selectivity to PP acid compared to PPA. The reason is that PP acid is a substructure of Fmoc-pTyr-OEt used as a template in the preparation of imprinted polymer P1. Other anions (PSA and BA) were not retained in the P1 column. No anions showed any affinity to the P_N1 column.

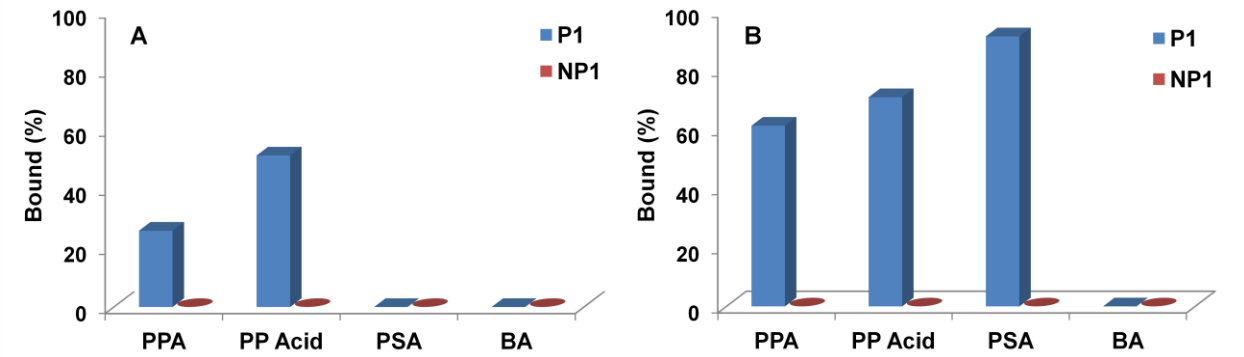

Figure 3.29 Percentage of bound PPA, PP acid, PSA and BA in the P1, P_N1 column in mobile phases. MeCN: Water/90:10 (0.1% TEA) (A) and MeCN:Water/95:5 (0.1% TFA) (B).

The same anions (PPA, PP acid, PSA and BA) were injected into the columns (P1, P_N1) in acetonitrile-rich mobile phase buffered with trifluroacetic acid (TFA) (Figure 3.29B). Another interesting observation was that PPA, PSA and PP acid were retained in the pTyr imprinted column (P1), but not BA. None of the anions was retained in P_N1. This polymer can be applied in chemical sequencing experiments where analysis is generally carried out under low pH conditions [130].

3.17 Conclusions

The results show that a combination of host-guest chemistry with conventional imprinting is very rewarding. Thus, the stable complexes formed between anion and the diaryl host monomers result in an exceptionally tight binding selective site when imprinted. The high affinity binding of the polymerizable monomer capable of strong interaction improved imprinting property within the resulting materials.

The successful non-covalent molecular imprinting for the phenyl phosphonic acid using a urea based functional monomer was demonstrated. When a stoichiometric amount of template PPA and functional monomer were used to create MIPs, this leads to a high imprinting effect. The polymer prepared with functional monomer (FM) to template (T) ratio 2:1 produce three fold increase of imprinting sites when compared to the polymer prepared with FM:T/1:1 ratio and binding energy was found to be in the range of 10^6 M^{-1}.

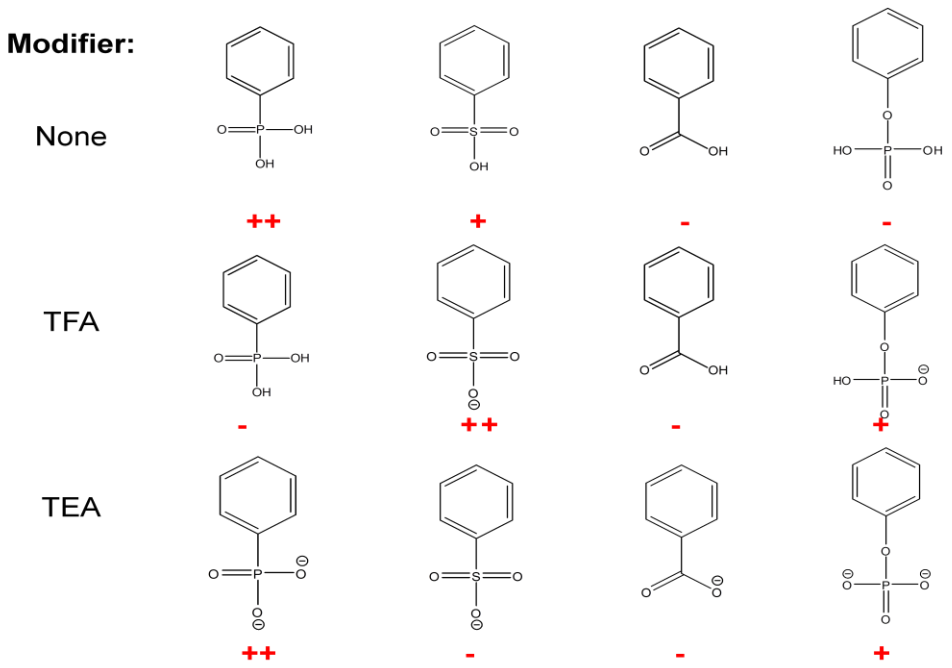

Figure 3.30 Oxyanion binding to PPA MIP (M1 and M2) in MeCN mobile phase with modifiers. ++, + and – is strength of binding (++: stronger binding, +: medium to weak binding, -: no binding).

The effect of the functional monomer on the imprinted polymers was well correlated with physical characteristics like morphology (surface area and pore size distributions) and binding parameters (total number of binding sites and polymer-template association energy, capacity). The MIPs selectively recognized their anion templates over other similar oxyanions MIPs showed, a pronounced sensitivity to the presence of acidic and basic mobile phase additives (Figure 3.30). Hydrogen bonding is the key parameter for the recognition of the oxyanion, which has been demonstrated for the imprinted polymer. To the best of my knowledge, this is first in-depth study of the oxyanion imprinted polymers and will be further explored for the recognition of phosphorylated/sulfated amino acids and peptides.

3.18 Experimental Section

3.18.1.1 Materials

Ethylene glycol dimethacrylate (EGDMA) were obtained from Aldrich (Milwaukee, USA), 1,2,2,6,6-pentamethylpiperidine from Fluka (Buchs, Switzerland), acetonitrile and methanol from J.T. Baker (Phillipsburg, NJ, USA). N,N'-azo-bis(2,4-dimethyl)valeronitrile (ABDV) was purchased from Wako.

EDMA was purified by the following procedure prior to use: The received material was washed consecutively with 10% aqueous NaOH, water, brine and finally water. After drying over $MgSO_4$, pure, dry EDMA was obtained by distillation under reduced pressure. All other reagents were used as received. DMSO-d_6, deuterated THF was purchased from Deuterio-GmbH (Kastellaun, Germany). Anhydrous solvents tetrahydrofuran, were stored over appropriate molecular sieves. benzene phosphonic acid (98%), benzene sulphonic acid (90%) from Aldrich and Benzoic acid (99%) from Across-Organic were used after recrystillzation from water. Methyl tosylate was received from Sigma Aldrich and p-toluene sulphonate monohydrate was received from Merck. Other solvents were of reagent grade or higher.

3.18.1.2 Apparatus and methods

HPLC: The HPLC measurements were carried out on Hewlett-Packard HP 1050 or 1100 instruments (Agilent Technology, Waldbronn, Germany).

Elemental analysis:These were performed at the Department of Organic Chemistry, Johannes Guttenberg Universität Mainz using a Heraeus CHN-rapid analyser (Hanau, Germany).

FT-IR spectroscopy: This was performed using a NEXUS FT-IR spectrometer (Thermo Electron Corporation, Dreieich, Germany).

3.18.1.3 N-3,5-bis(trifluoromethyl)phenyl-N´-4-vinylphenyl urea

The functional monomers (FM) 1-(4-Vinylphenyl)-3-(3,5-bis(trifluromethyl)phenyl)-urea monomer was synthesized according to reported procedure Hall *et al.*[106]. To a stirred solution of desired 4-amino styrene (20 mmol) in THF (50 mL) under an inert atmosphere was added the 1,3-bis(trifluoromethyl) phenyl isocyanate (20 mmol) as a neat. The solution was allowed to stir at room temperature overnight and then solvent was evapourated under reduced pressure. The resulting solid residue was dissolved in $CHCl_3$ and treated with charcoal to remove unreacted reactant was resulted into white compound.

Yield: 65 % of white solid ^{1}H NMR (DMSO-d6) 400 MHz; δ: 5.16 (d, 1H), 5.72 (d, 1H), 6.67 (dd, 1H), 7.40 (d, 2H), 7.47 (d, 2H), 7.64 (s, 1H), 8.13 (s, 2H), 9.07 (s, 1H), 9.40 (s, 1H); ^{13}C NMR (101 MHz, DMSO-d6) 112.44, 117.98, 118.76, 121.97, 124.68, 126.69, 130.22, 130.54, 131.51, 136.16, 138.18, 141.81, 152.31; Calculated for $C_{17}H_{12}F_6N_2O$: C 54.55, H 3.23, N 7.48 found C 54.59, H 3.07, N 7.58.

3.18.1.4 Mono-tetrabutylammonium salt of PPA, PSA

To 0.316 g (2 mmol) of PPA and PSA in 10 mL dry methanol 2 mL of a 1M solution of tetrabutylammonium hydroxide in methanol (1eq.) was added and the solution was stirred at room temperature for 2h. The solvent was removed under vacuum and the solid residue dried over P_2O_5.

3.18.1.5 Phenyl Phosphate (PP acid)

Sodium phenyl phosphate dibasic dihydrate (Sigma, Japan) was dissolved in ethyl acetate, neutralized by using 1N hydrochloric acid, and subsequently washed with water. The ethyl acetate was evaporated to dryness to a white product. The product was dried in a vacuum oven at room temperature and characterized by NMR spectroscopy.

^{1}H NMR: (200 MHz, DMSO) 7.08-7.19 (m, 3H), 7.29-7.39 (m, 2H); ^{31}P (81 MHz, DMSO) (s, -5.08)

3.18.1.6 ^{1}H NMR titrations and estimation of complex stoichiometry and association constants

All ^{1}H NMR spectroscopic titrations were performed in dry deuterated DMSO. The association constant (K) for the interaction between hosts and guests were determined by increasing amount

of guest components such as, mono -TBA salt of PPA into constant amount of functional urea monomer. The concentration of the functional monomer is 1 mM and the amount of added guest were 0, 0.25, 0.5, 0.75, 1.0, 1.5, 2.0, 4.0, 6.0 and 10.0 equivalents respectively. The Complexation Induced Shifts (CISs) of the host urea protons were followed and titration curves were constructed of CIS verses guest concentration. The raw titration data were fitted to 1:1 binding isotherm by non-linear regression from which association constant could be calculated. Complex stoichiometry was first assessed using a Jobs method of continuous variation.

3.18.1.7 NOESY NMR Study

0.0178 mM of (2.82 mg) PPA and (3.11 mg) PP acid were filled in separate NMR tubes and 0.6 ml of deuterated THF were added. In situ bis-PMP salts were prepared by addition of 0.035 mM (6.46 µL) pentamethyl piperidine. To this NMR tubes, 0.035 mmol (13.4 mg) of functional urea monomer was added in order to produce 1:2/T: FM complex respectively. The complex T: FM/1:2 and the pure functional urea monomer were scanned using 500 MHz NMR spectrophotometer by keeping parameters constants (Parameters: NS=8, TD1=512, SW=20 ppm).

3.18.1.8 Isothermal Titration Calorimetric

ITC titrations were performed with mico-caloriemeter VP-ITC at 25^{o}C. In all the titrations, the urea monomer solution was used a host in the cell and TBA salt of template were injected as a guest. 15 mM of TBA salt of guest and 0.2 mM of functional urea monomer in dry DMSO was used for titration. The dilution effect of the guest was measured as a reference and subtracted from the titration before evaluating the binding constant. In most of the cases the incorporated evaluation method “one set of sites” was used in order to get a good fitting.

3.18.1.9 Solubilization of PMP salts of PPA by functional urea monomer

0.027 mmol of PPA (4.4 mg) were taken in the 0.31 ml of dry THF and 0.0278 mmol (5 µL) and 0.055 mmol (10 µL) of PMP were added separately in HPLC vials to make mono and bis PMP salts respectively. (0.0278 mmol) 10.4 mg and 20.8 mg (0.055 mmol) of the functional urea monomer were added to the HPLC vials containing the respective salts.

3.18.1.10 Polymer preparation:Crushed monliths

Imprinted polymers were prepared in the following manner. The bis-pentamethylpiperidine and mono-pentamethylpiperidine salt of phenyl phosphonic acid (PPA), phenyl sulfonic acid (PSA) (0.5mmol), urea monomer (0.5 mM and 1 mmol) and EGDMA (20 mmol) were dissolved in THF (5.6 mL). To the solution was added an initiator ABDV (1% w/w of total monomers). The solution was transferred to a glass ampoule, cooled to 0^{o}C and purged with a flow of dry nitrogen for 10 minutes. The tubes were then flame-sealed while still under cooling and the polymerization initiated by placing the tubes in a thermostatted water bath pre-set at 50^{o}C. After 24h the tubes were broken and the polymers lightly crushed. They were thereafter washed 3 times with MeOH and extracted in a Soxhlet-apparatus with methanol:0.5N HCl/80:20 for 24h. This was followed by further crushing and sieving, whereby the fraction from 25-36 µm was used to evaluate their binding properties. A non-imprinted polymer (N1, N2) was prepared in the same way as described above, but with the omission of the template molecule from the pre-polymerization solution. Before extraction and after extraction of the template, elemental analyses of polymers were measured.

3.18.1.11 Rebinding of PPA in presence of PMP

The effect of PMP on rebinding of PPA was carried out using the same procedure as above with increasing percentage concentration of PMP (0 to 1%) in the acetonitrile. In this experiment, concentration of PPA, PSA was kept constant (0.6 mM) in each vial with corresponding MIPs and NIPs. The vials were kept at room temperature for more than 24 hours. Then supernatant concentrations [C_f (mg/mL)] were measured by HPLC.

3.18.1.12 HPLC Evaluation

The 25-36 µm particle size fraction was repeatedly sedimented (80/20: methanol /water) to remove fine particles and then slurry-packed into HPLC columns (30 mm x 4.6 mm i.d.) using the same solvent mixture as pushing solvent. Subsequent analyses of the polymers were performed using an Agilent HP1050 or HP1100 system equipped with a diode array-UV detector and a workstation. Analyte detection was performed at 205, 220 and 260 nm, depending on the analyte and mobile phase used at a flow rate of 0.5 mL/min. The retention factor (k) was calculated as $k=(t-t_0/t_0)$, where t= retention time of the analyte, t_0 = retention time of the void

marker (acetone). PPA, PSA, PP acid was monitored at 205 nm and BA was at 220 nm in MeCN mobile. PPA, PSA, PP acid was monitored at 263 nm and BA was monitored at 272 nm in TFA and TEA containing mobile phases. Concentration of the analyst was 0.5 mM, the flow rate was at 0.5 ml/min.

3.18.1.13 Reverse phase HPLC Conditions

Chromatographic analysis was carried out with an HPLC 1050 instrument (Agilent) equipped with a quaternary pump auto-injector and DAD detector. The analytical column was a polar endcapped C18 reverse phase Luna (250 mm x 4.6 μL). The mobile phase consisted a mixture of methanol and water (0.1 % of TFA) 32/68 for PPA and PSA and 50/50 for BA at a flow rate of 1 mL/min. The injection volume was 5 μL. The column was kept at room temperature. The absorbance wavelength was 205 nm for PSA and 225 nm for PPA. For quantification purposes calibration standards were prepared in the same conditions that the, rebinding experiments were made. The calibration curve was prepared in 0-1.2 mM concentration range after incubation of anions more than 24 hours. The retention time of anions PPA and PSA was 5.8 min, 3.9 min respectively.

3.18.1.14 Rebinding study

The 25-36 μm particle size fraction was repeatedly sedimented (80/20: methanol /water) to remove fine particles and then approximately 10 mg of polymers weighed in the 1.5 mL of HPLC Vial and 1 mL acetonitrile containing 0.1% PMP with different concentration of PPA (0 to 2 mM) were added to each vial corresponding MIPs and NIPs. The vials were kept at room temperature for more than 24 hours. Then supernent supernatant concentrations [C_f mg/mL] were measured by HPLC. The rebinding curves were created by plotting bound amount (μmol/g) versus free concentration in mM of template.

3.18.1.15 Nitrogen sorption

Nitrogen adsorption isotherms were measured at -196 ^{o}C (77K) using Quantachrome Nova 4000 adsorption analyzer (Quantachrome Corporation, Boynton Beach, FL). Prior to adsorption measurements, each polymer sample was degassed at 70^{o}C under high vacuum for at least 12 hours. The total pore volume was calculated by converting the amount of nitrogen adsorbed at a relative pressure of about 0.99 to the volume of liquid adsorbate. Adsorption and desorption were

recorded using 68-point pressure table. The surface areas were evaluated using the BET method and the average pore diameter and pore size distribution were calculated using the Barrett, Joyner, Halenda (BJH) analysis of the desorption branch.

3.18.1.16 Measurement of swelling

In order to better elucidate the difference between the dry and swollen state of the polymers, swelling tests were performed in acetonitrile. The swelling was measured in graduated NMR tube by allowing a known volume (1 cm) of dry polymer to equilibrate in acetonitrile, where after the volume of the swollen particles was measured. The swelling ratio, given as volume of the swollen polymer to volume of dry polymer, was measured by equilibration for at least 24 hours.

4 A phosphotyrosine-imprinted polymer receptors for recognition of tyrosine phosphorylated amino acid and peptides

4.1 Introduction

As tyrosine phosphorylation is a sub-stoichiometric modification often occurring in low-abundance proteins, the presently used separation and detection techniques based on antibodies or chelating chromatographic materials often exhibit insufficient selectivity and sensitivity for the modified proteins to be individually determined (Chapter 2, Figure 2.6) [131]. Thus, there is a general need for simple and robust techniques capable of separating or sensing this PTM in proteins or peptides. Apart from being a generic fractionation tool capable of isolating all pY, pS or pT-containing peptides over nonphosphorylated peptides, other levels of selectivity are equally important [108] (Figure 4.1). Thus, receptors that can recognize the amino acid sequence around the phosphorylation site would find use in diagnostic applications in case of identified reliable biomarker. In this area molecularly imprinted polymers (MIPs) could play an important role, complementing currently used immunological and chemical methods.

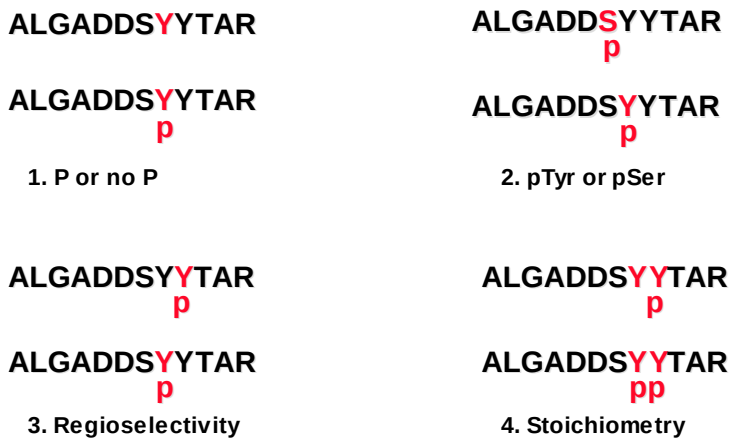

Figure 4.1 Different levels of phosphopeptide discrimination in the design of a pY-imprinted polymer [108].

This chapter is the continuation of work developed by M. Emgenbroich. C. Borrelli *et al.*[108]. In the current chapter, epitope imprinting strategies have been adopted to create a tight binding site for phosphotyrosine residue in the imprinted receptor. These receptors can be generic,

capable of selectively capturing phosphotyrosine containing amino acids and peptides. In a attempt to meet these requirements, diaryl urea host monomer have been used to bind phosphate oxyanions, in combination with an N, O protected phosphotyrosine template as same approach developed by M. Emgenbroich *et al.* [108] with little modification.

4.2 Template selection for imprinting

The choice of template is very crucial for preparation of MIP in this project because phosphorylated amino acids are hydrophilic in nature and are insoluble in polymerization solvent. N- and C- terminal protected phosphorylated tyrosine template as N-(9-fluorenylmethoxycarbonyl)-O'-phosphonotyrosine-ethyl ester (Fmoc-pTyr-OEt) were selected as template (**1e**). The advantage of these protecting groups are they provide enough hydrophobicty to the template so that it is soluble in organic solvent as well as it is easy to monitor during analysis. This approach thus allows potent receptors for modified peptides to be prepared using a single amino acid as template.

4.2.1 Synthesis of template

Emgenbroich *et al*. have used N-(9-fluorenylmethoxycarbonyl)-O'-phosphonotyrosine-methyl ester (Fmoc-pTyr-OMe) template in previous report. [108] N and C terminal is protected by Fmoc and methyl group respectively [108]. Fmoc-pTyr-OMe template was synthesized by phosphorylating Fmoc-Tyr-OMe with phosphorous oxychloride and after that hydrolysed phosphoric acid dichloride ($POCl_3$ method).[132] In the present work, N-(9-fluorenylmethoxycarbonyl)-O'-phosphonotyrosine-ethyl ester (Fmoc-pTyr-OEt) template have used and was synthesized by phosphoramidate chemsitry,[133, 134] which has advantages in term of stability, purity comparative to previous synthetic method.

At first, intermediate phosphorylating reagent diisopropylphosphordichloride (**1a**) was prepared from phosphorous trichloride and diisopropylamine by addition at -10°C as shown in Scheme 1. The compound **1a** was purified by distillation under reduced pressure and obtained as single peak at 170.5 ppm on ^{31}P NMR spectroscopy[134]. Bis[2-(methyldiphenylsilyl) ethyl] N,N-diisophosphoramidite [135] (**1b**) was synthesized by using commercially available methyldiphenylsilyl ethanol and phosphoramidite (**1a**). This reagent is fully compatible with Fmoc/*tert*-butyl strategy. The (methyldiphenylsilyl) ethyl-phosphate (MDPSE) group is stable

under the conditions used for repetitive removal of Fmoc group, readily removable by TFA and stable at room temperature for several months [133].

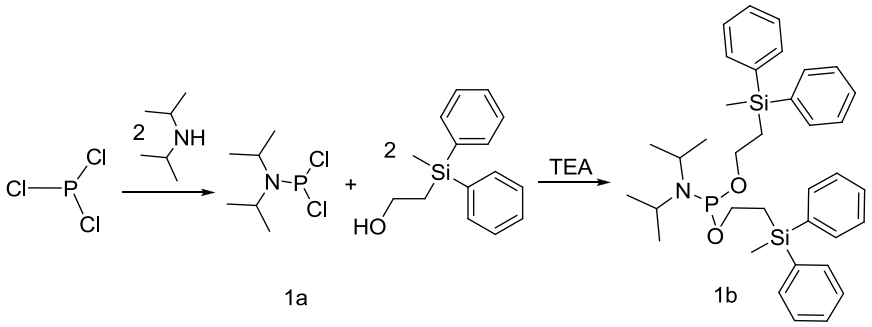

Scheme 1 Synthesis of Bis[2-(methyldiphenylsilyl) ethyl] N,N-diisophosphoramidite.

Synthesis of Fmoc-Tyr(PO_3MDPSE_2)-OEt: For the introduction of the phosphate group, the P^{III}-P^{V} technique was used. A phosphite triester was generated by addition of Bis [2-(methyldiphenylsilyl) ethyl] N, N-diisopropylphosphoramidite to Fmoc-Tyr-OEt (**1c**) in the presence of tetrazole. To receive the phosphate the phosphite triester was oxidized by *tert*-butylhydroperoxide in the second step. Fmoc-Tyr(PO_3MDPSE_2)-OEt (**1d**) was purified by silica gel column chromatography and characterized by ^{1}H, ^{13}C and ^{31}P NMR spectroscopy.

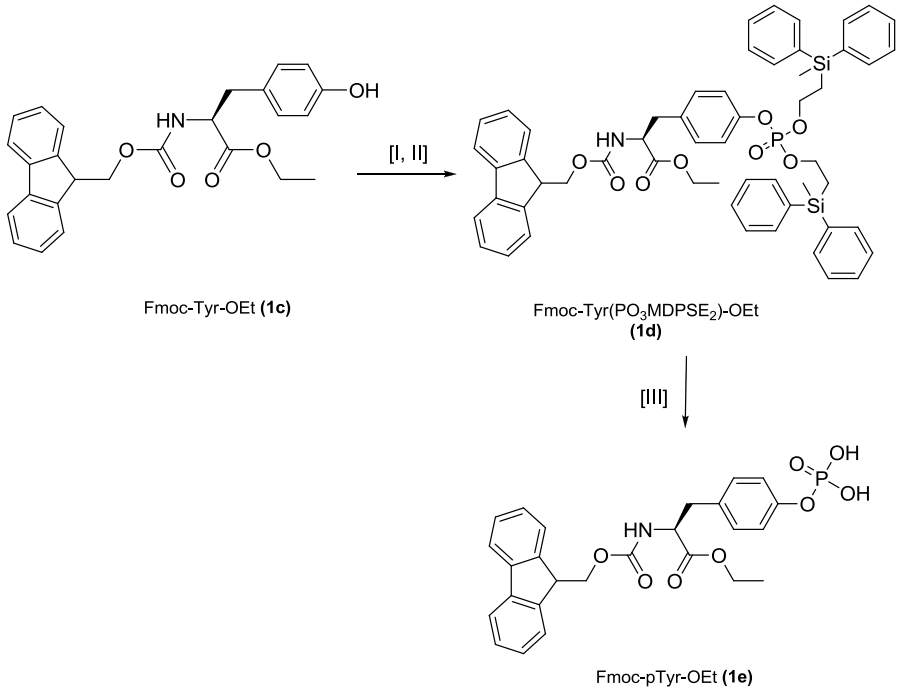

Scheme 2 Synthesis of template Fmoc-pTyr-OEt; reaction conditions:[I] Bis[2-(methyldiphenylsilyl) ethyl] N,N-diisophosphoramidite [II]t-BuOOH; [III] DCM:TFA/50:50.

Synthesis of Fmoc-Tyr(PO_3H_2)-OEt: methyldiphenylsilylethyl (MDPSE) group from Fmoc-Tyr(PO_3MDPSE_2)-OEt (**1d**) was readily cleaved in trifluoroacetic acid in dichloromethane. Fmoc-Tyr(PO_3H_2)-OEt (**1e**) was purified by silica gel column chromatography and characterized by characterized by ^{1}H, ^{13}C and ^{31}P NMR spectroscopy and mass spectroscopy.

4.3 Functional urea monomer and template (Fmoc-pTyr-OEt) complexation

The urea motif of host monomers can bind the carboxylate anions or the (di)phosphate anion in a stoichiometric manner according to previous chapter (chapter 2). As results from previous chapter and reports [73, 106, 108], anticipated that these neutral hydrogen bond receptors would provide sufficient binding energy while not suffering from the charge dependent sequence bias commonly observed for positively charged chelating receptors.[136] For instance, urea monomer **27** was used to prepare MIPs against the model template, the bis-PMP salt of N-Fmoc-pTyr-OEt. The bis-PMP salt of Fmoc-pTyr-OEt was insoluble in THF but became soluble upon addition of urea monomer. This is a visual indication of complex formation between monomer and the template.

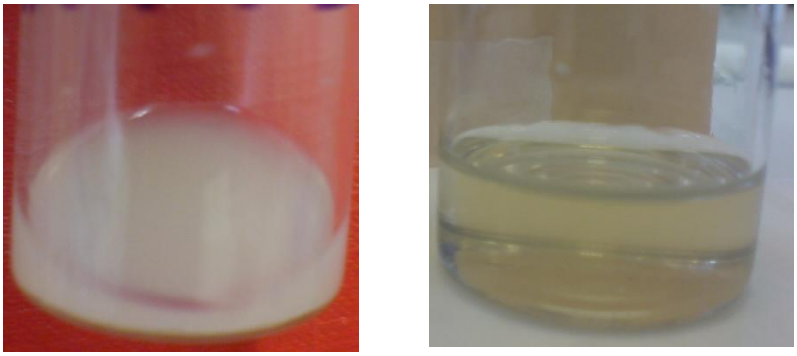

Figure 4.2 Prepolymerization solution of the bis-PMP salt of Fmoc-pTyrOEt in THF prior to (left) and after (right) addition of monomer.

Complexation of monomer and template was prepared using urea monomer in a 2:1 stoichiometric ratio to the template Fmoc-pTyr-OEt (Scheme 3) as a same polymerization protocol [108]. Each urea group establish cyclic hydrogen bonds with the phosphate anion.

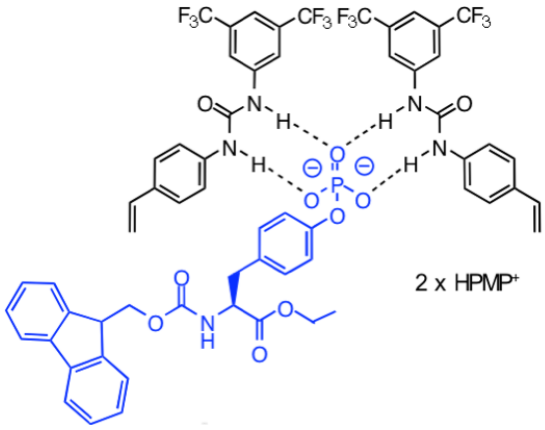

Scheme 3 The imprinted polymer (MIP) was prepared using functional urea monomer (FM) in a 2:1 stoichiometric ratio to the template Fmoc-pTyr-OEt [108].

4.4 Polymer preparation

Methacrylamide (MAAm) was added as a supplementary monomer to provide additional hydrogen bond stabilization and all monomers polymerized via free radical initiation, with ethylenglycoldimethacrylate (EGDMA) as crosslinking monomer and THF as solvent. The polymerization protocol was prepared according to previously described procedure [108] but with a few modifications. The resultant urea monomer-template complex was soluble in the polymerization solvent. Conventional azoinitiated thermal polymerization at 50°C subsequently afforded the imprinted (P1) and nonimprinted (P_N1) polymers. The lightly crushed polymer was subjected to template removal by extraction with acidic methanol using a Soxhlet apparatus. Particle size of 25-36 µm was obtained by crushing and sieving.

4.5 Physical properties of polymers

In order to investigate whether the imprinted and control polymers were otherwise comparable in terms of morphology and composition the polymers were characterised by elemental analysis (Table 4.1), IR-spectroscopy (Figure 4.9). Elemental analysis showed slightly lower carbon content in all the materials, possibly related to their hygroscopic nature, but reasonable agreement with the theoretical concentrations for the other elements and was found to be similar in previous results [108].

Table 4.1 Elemental composition of imprinted polymer P1 and corresponding non-imprinted polymer P_N1

Polymer		%C		%H		S (mL/mL)[a]	S (mL/mL)[b]
	Calc.	Found	Calc.	Found	Calc.	Found		
P1	60.6	56.46	6.73	6.73	1.05	0.98	1.93	1.9
P_N1	60.0	57.22	6.81	7.01	0.95	0.95	1.42	1.2

Calc. means assuming complete removal of template. Swelling ratio (s): [a]:Water; [b] :MeCN:Water/90:10 (1% TEA).

The irregular bulk imprinted polymer in particle size 25-36 µm was studied by scanning electron microscopy (SEM). The representative picture of P1 and P_N1 is shown in Figure 4.3 at different magnifications. The porous properties of material (specific surface area (S), specific pore volume (V_p) and average pore diameter (D_p)) were determined by nitrogen absorption techniques (Table 4.2) and details are reported in experimental procedure (3.18.1.15). The polymer exhibited mesoporous morphology with surface area larger than 200 m^2g^{-1} and average pore diameters of roughly at 4 nm. These morphologies of P1 and P_N1 are comparable in dry state with slightly lower surface area in P1 compared to P_N1. On the other hand, swelling ratio of P1 is higher compared to P_N1, when tested in the solvents MeCN:Water/90:10 (1% TEA) and water as shown in Table 4.2.

Table 4.2: Physical properties of Fmoc-pTyr-OEt imprinted and non-imprinted polymers. The BET specific surface area (S), Specific pore volume (Vp) and average pore diameter (Dp) were determined.

Polymer	S (m^2/g)	V_p (mL/g)	D_p (nm)
P1	307.412	0.153	3.519
P_N1	359.883	0.174	3.706

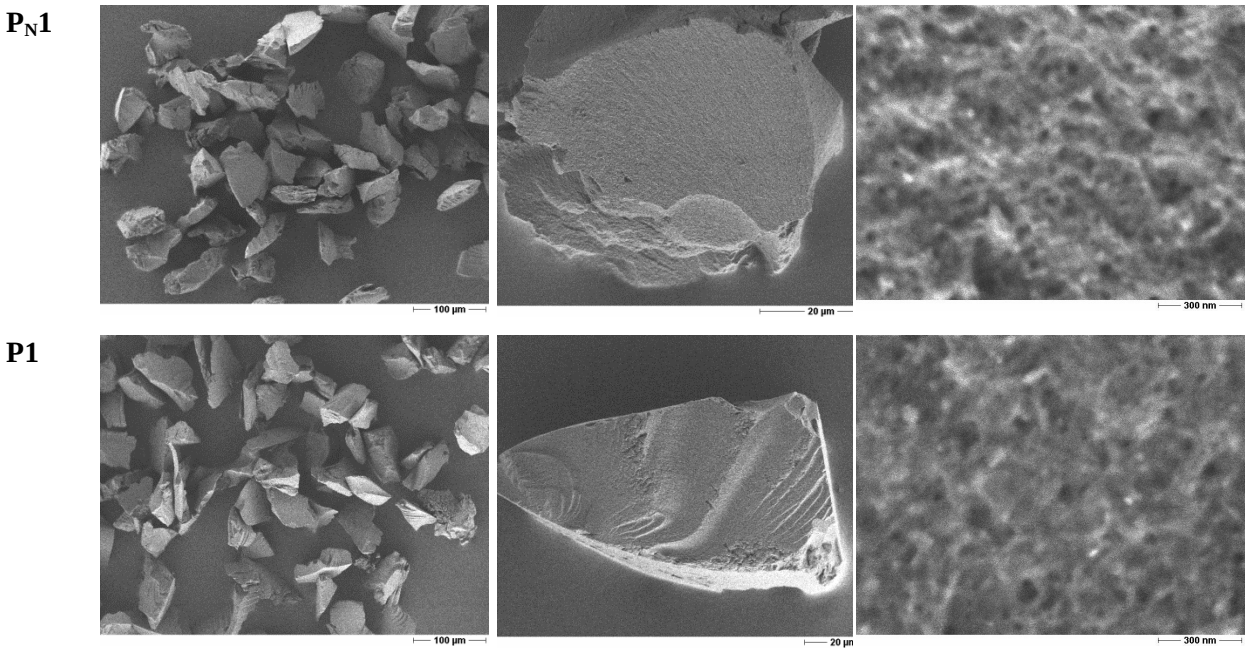

Figure 4.3 Scanning electron microscopy (SEM) picture of P1 and P_N1 (particle size: 36-50 µm) at different magnifications.

4.6 HPLC evaluation

The 36-50 µm particle size fraction was sedimented repeatedly (80/20: methanol/water) to remove fine particles and then slurry-packed into HPLC columns (30 mm x 4.6 (i.d.) mm) using the same solvent mixture as pushing solvent. Subsequent analyses of the polymers were performed using an Agilent HP1050 system equipped with a diode array-UV detector and a work station .Analyte detection was performed at 254 nm for amino acids and 220 nm for peptides with a flow rate of 0.5 mL/min.

4.6.1 Selectivity for Fmoc amino acid derivatives

Imprinting effects were first assessed by chromatography using the crushed polymer monoliths as stationary phases. In the first test, Fmoc amino acid derivative was injected on to column in an acetonitrile rich mobile phase buffered with TFA. The P1 exhibited a strong affinity for the low molecular weight template (Fmoc-pTyr-OEt) and the non-phosphorylated counterpart (Fmoc-Tyr-OEt) was only weakly retained. The template did not elute out from P1 column even after 1

hour (Figure 4.4A), however the NIP (P_N1) displayed no retentivity for both the analytes (Figure 4.4B).

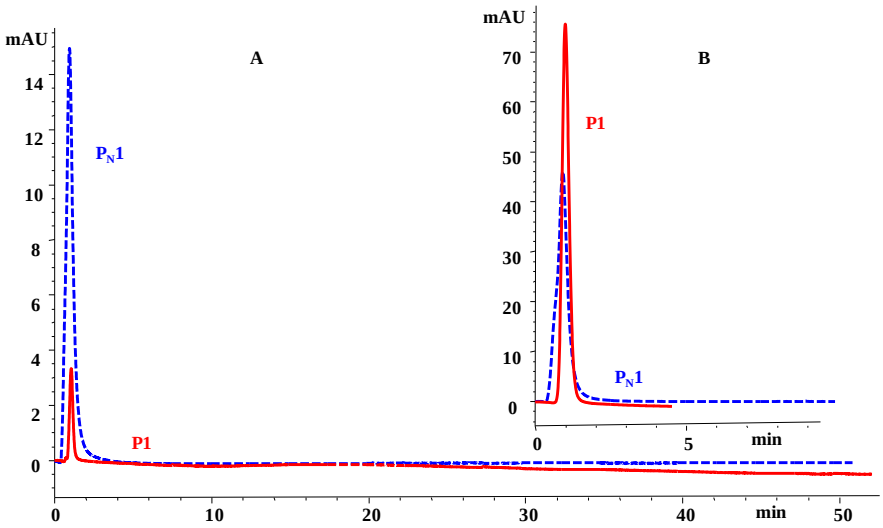

Figure 4.4 LC evaluation of P1 and P_N1 packed in HPLC column. Fmoc-pTyr-OEt in P1 and P_N1 (A); Fmoc-Tyr-OEt in P1 and P_N1 (B) [column size: 4.6 (i.d.) x 30 mm, mobile Phase: 95:5/MeCN:Water (0.1% TFA); DAD @260 nm; injection volume:5 µL, flow rate:0.5 mL/min.

Further selectivity of imprinted polymers assessed by injecting pTyr, Tyr and pSer (Fmoc-derivatives) were injected on to columns at two different concentrations as 0.5 mM and 0.1 mM. At high concentration, P1 showed preferential higher retention factors compared to pSer derivatives (Figure 4.5). Encouraging observation was found, when 0.1 mM of pSer, pTyr derivatives were injected, pTyr analyte was fully retained in the P1, however pSer analyte eluted out from P1 column within few minutes (Figure 4.5, Table 4.3). P_N1 did not show any affinity to all these analytes.

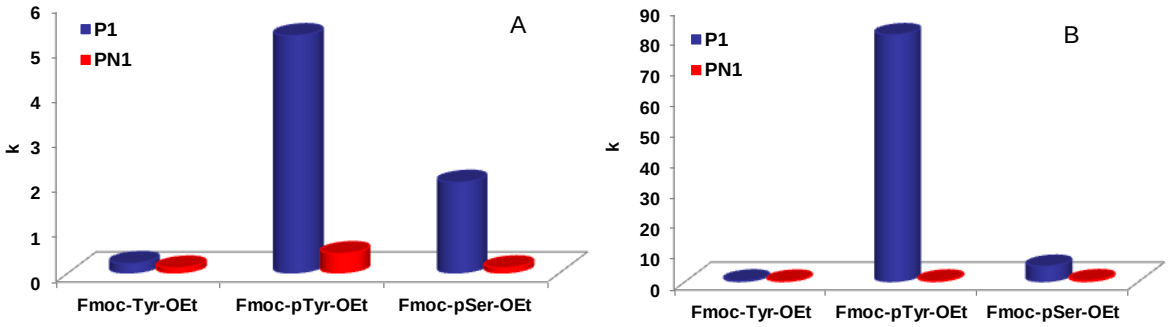

Figure 4.5 HPLC retention factors (k) for the pTyr template analogues in a water poor mobile phase; A) 0.5 mM amino acids, B) 0.1 mM amino acids. Fmoc-pTyr-OEt in MeCN:Water/80:20, 0.1 mM of Fmoc-Tyr-OEt in MeCN:Water/95:5, 0.1 mM of Fmoc-pSer-OEt in MeCN:Water/80:20. column size: 4.6 x 30 mm, mobile phase:95:5/MeCN:Water (0.1% TFA), DAD@260 nm, injection volume: 5 µl, flow rate: 0.5 mL/min.

4.6.2 Phosphoangiotensin peptide enrichment

The polymer P1 was synthesized from Fmoc-pTyr-OEt (template) and diaryl urea monomer complex. After removal of template, the resultant imprinted polymer was expected to possess p-Tyr selective sites and this can extent to capture pTyr modified peptides containing this epitope (Scheme 4).

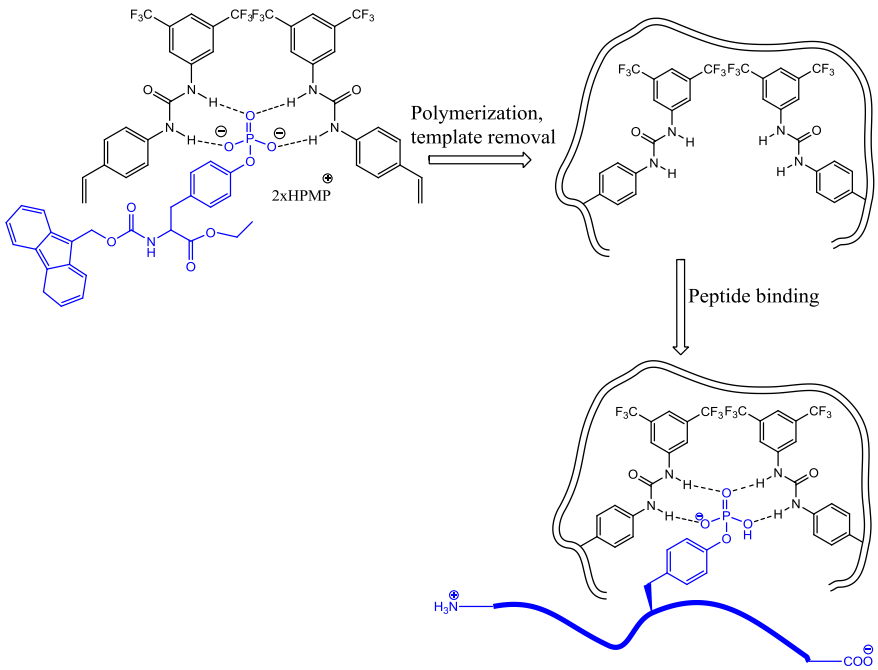

Scheme 4 Epitope imprinting. MIP synthesized from pTyr modified amino acid is selectively capture peptide containing pTyr.

To prove epitope imprinting concept, the stable nuropeptide angiotensin II (Ang), containing an internal tyrosine residue present in both the non-phosphorylated (Ang) and monophosphorylated (pAng) (DRVpYIHPF) forms were chosen for the present study. To understand the retention mechanism of the peptides, peptides were injected onto P1 and P_N1 column using a TFA modified binary actonitrile mobile phase mixture. pAng peptide was selectively retained in the P1 column, however no retention of Ang peptide on P1 was observed (Figure 4.6). Peptide observed weak affinity to P_N1 (Figure 4.6).

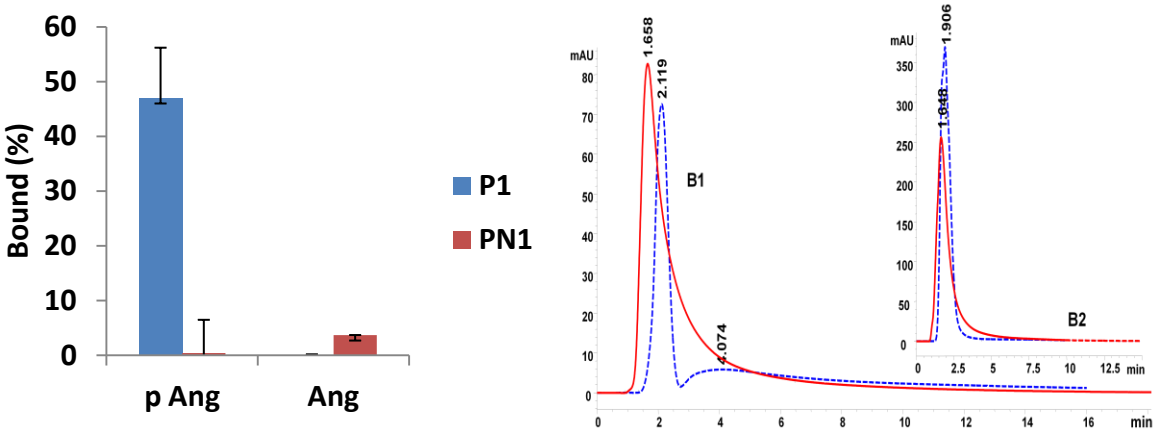

Figure 4.6 LC evaluation of P1 and P_N1 packed in HPLC column. Percentage of bound Angiotensin and phosphoangiotensin-II peptide in P1 and P_N1 (left); LC chromatogram corresponding B1) pAng traces (B1), Ang traces (B2) with P1 blue dotted line and P_N1 red line (right) (conditions concentration: 1 mg/mL in water, flow rate: 0.3 mL/min, injection volume: 5µl, DAD@220 nm, column: 4.6 (i.d.) x 30 mm).

Imprinted (P1) and non-imprinted polymer (P_N1) were packed in the HPLC column of size 4.6 (i.d.) x 30 mm and concentration of peptides was used in the range of µM to mM. In approaching towards real life applications in proteomics, major limitations are amount of samples and low abundant analyte (possible lowest concentration) from complex mixture. To overcome this limitation, quantity of materials (P1, P_N1) were scaled down and solid phase extraction (SPE) was performed pipette tip experiment in the group of Prof. Katrin Marcus, Medical Proteome Center, Ruhr Universität Bochum, Germany [137].

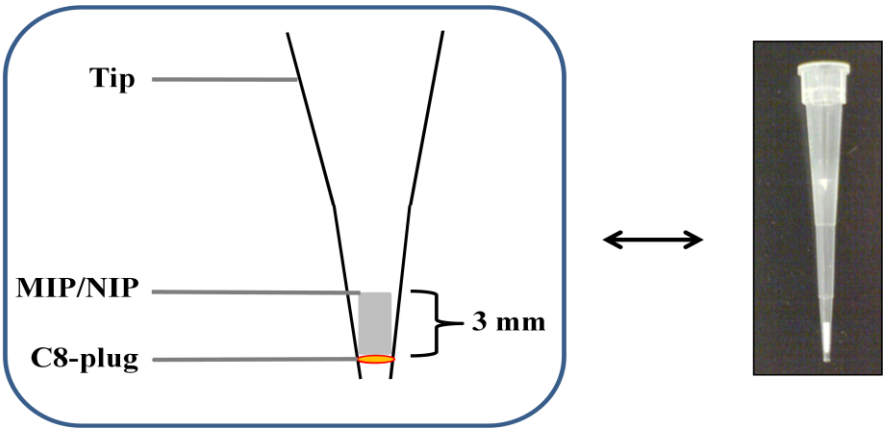

Figure 4.7 General schematic representations of pipette tips used for enrichment experiment.

4.6.3 Proof of concept for the use of a pTyr-MIP in Proteomics

Further selectivity and sensitivity of P1 and P_N1 was tested in more complex samples with lowest detectable concentration (1 fmol) of Ang peptides by Helling *et al*.[137].

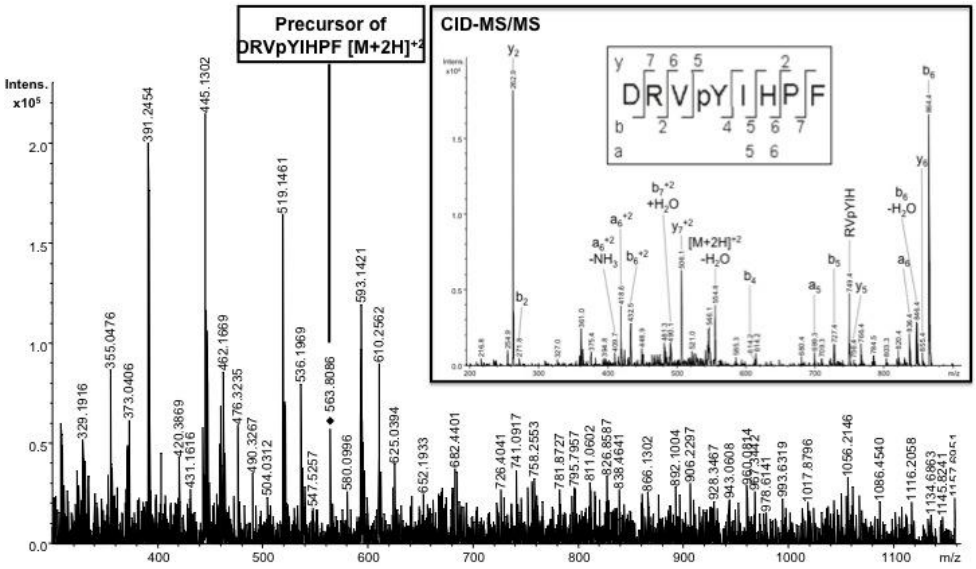

Figure 4.8 Nano-LC-ESI MS after pTyr-MIP SPE of a 10 pmol tryptic digest of fetuin spiked with 1 fmol phosphoangiotensin. The peptide was identified after 58 min by HPLC by measuring the masses of the precursor ion and its fragment ions [137].

These MIPs found high enrichment factors, pTyr versus pSer selectivity, solvent compatibility and high robustness. Figure 4.8 shows analyte detection by nanoLC-MS/MS after pTyr MIP enrichment of 1 fmol of a pTyr containing peptide (phosphoangiotensin) spiked in 10 pmol of a tryptic digest of Fetuin containing abundant pSer-peptides. Whereas the peak corresponding to the pTyr peptide was clearly observable, pSer peptides were not visibly enriched using this protocol.

In further tests on model peptide mixtures it was found that MIP-SPE method could be used for extracting multiply phosphorylated peptides. Thus a peptide corresponding to a phosphorylated sequence of Insulin receptor I (TRDIpYETDpYpYRK) was significantly enriched on the P1, this peptide had a strongly impaired recovery in the SPE using TiO_2 sorbent [137].

4.7 Short conclusion

Urea-mediated imprinting of N,O-protected phosphotyrosine (pTyr) led to a synthetic receptor capable of selectively extracting pTyr-amino acids and peptides.

4.8 Materials and Methods

4.8.1.1 Chemicals

Acetonitrile and methanol from J.T. Baker (Phillipsburg, NJ, USA). N,N'-azo-bis(2,4-dimethyl)valeronitrile (ABDV) was purchased from Wako, tatrazole solution, triethyl amine, diisopropyl amine from Fluka, diethyl ether extra dry and tetrahydrofuran extra dry from Across Organic, 2-(methyldiphenylsilyl) ethanol from Sigma Aldrich. H-Tyr-OEt and Fmoc-Cl were received from Bachem. Anhydrous solvents, dichloromethane and tetrahydrofuran, were stored over appropriate molecular sieves. Other solvents were of reagent grade or higher. The substrate Fmoc-Tyr-OEt was synthesized by previously reported procedure[138]. The peptides angiotensin and phospho-angiotensin were obtained from Calbiochem-Merck (Darmstadt, Germany). N-(9-Fluorenylmethyloxycarbonyl)-O-phosphoserine-ethyl ester *(*Fmoc-pSer-OEt) was synthesized in-house and purity was about 80% based on ^{31}P NMR spectroscopy (described in chapter 6).

4.8.1.2 Experimental Methods

^{1}H NMR spectroscopic data were recorded on Brucker Advance DRX spectrophotometer at room temperature. NMR spectroscopic data were calibrated to the solvent signal of $CDCl_3$ and DMSO (d_6) at 7.26 and 2.50 respectively. TLC was performed on Merck Silica gel 60 F_{254} aluminium sheet. For flash chromatography, MN silica gel 60M (40-63 µm) was used.

4.8.1.3 (Diisopropylamino) dichlorophosphine (1a)

(Diisopropylamino) dichlorophosphine compound was synthesized according to previously reported procedure [134, 139]. To a solution of phosphors trichloride (9.15 ml, 105 mmol) in 100 mL of anhydrous diethyl ether (29 ml, 210 mmol) of diisopropyl amine in 20 mL anhydrous diethyl ether was added drop wise within 2.5h at -10°C and followed by additional stirring for 1 hour at room temperature. The precipitated salt was removed by filtration and the filtrate was evaporated to give a slightly yellow crude liquid. (Note: The temperature of reaction mixture was maintained by using dry ice and acetone). Purification was done by distillation at 40°C afforded colorless liquid (BP 28°C /0.084 mbar). Yield: 74 % ^{1}H NMR (400MHz $CDCl_3$) δ 1.25-1.28 (d, 12H J_{HP}=12 Hz), 3.85-3.98 (m, 2H); ^{13}C NMR (100MHz $CDCl_3$) 48.06, 48.25 (d, CH, J_{PC}= 19

Hz), 23.36, 23.47 (d, CH_3 J_{PC} = 11 Hz), ^{31}P NMR ($CDCl_3$) δ 170.5 Elemental analysis calculated for $C_6H_{14}C_{l2}NP$ C, 35.66; H,6.98; N, 6.93; found C, 35.48; H, 6.97; N, 7.09.

4.8.1.4 Bis[2-(methyldiphenylsilyl)ethyl] N,N-diisophosphoramidite (1b)

Chao *et al*.[133] have synthesized phosphrylated tyrosine containing peptides using 2b and in this current study 2b was synthesized according to reported protocol [135]. To a solution of (4.21 gm, 98 mmol) of (dichlorodiisopropyl amino) Phosphine in 40 mL of dry ether at 0°C was added dropwise in a solution of 80 mL of dry ether containing (10 gm, 196 mmol) 2- (methyl diphenylsilyl)ethanol and (5.91 mL, 200 mmol) of triethylamine. After addition was completed, the resulting solution was allowed to gradually warm to room temperature and stirred overnight. The precipitated salt was removed by filtration and washed thoroughly with excess of ether. The combined organic phase was washed with 10% $NaHCO_3$, water and brine. After removal of solvent, the residue was purified by silica gel column chromatography with elution of solvent by Hexane: EtOAc: TEA / 90:10:4. Yield 64.59% as clear viscous liquid. ^{1}H NMR (400MHz $CDCl_3$) δ 0.57 (s, 6H), 1.06, 1.08 (d, J= 8Hz, 12H), 1.51-1.64 (m, 4H), 3.45-3.58 (m, 2H), 3.68-3.83 (m, 4H) 7.31-7.41 (m, 12H) 7.50-7.53 (m, 8H); ^{13}C NMR (100MHz $CDCl_3$),-4.20, 17.92, 18.00 (d, J_{PC}=8 Hz), 24.47, 24.56 (d, J_{PC}=9 Hz), 42.73, 42.57 (d, J_{PC}=16 Hz), 60.23,60.47 (d, J_{PC}=24 Hz),127.86, 129.26, 134.41, 136.54; ^{31}P NMR ($CDCl_3$) δ143.87 (s).

4.8.1.5 N-(9-Fluorenylmethyloxycarbonyl) tyrosine- ethyl ester (Fmoc-Tyr-OEt) (1c)

To a solution of 5.41 gm (0.0220 mole) tyrosine ethyl ester hydrochloride in 30 mL of water a solution of 6.33 gm (0.0458 moles) potassium carbonate in 12 mL of water was added at 0^{O}C. 45 mL dioxane was added to dissolve the precipitant. To this mixture, 5.0 gm (0.0193 mole Fmoc-Cl) were added portion wise and stirred at 0^{O}C for 4 hours. Afterwards product was extracted 3 times with each 60 mL of ethyl acetate. The combined organic phase were dried and evaporated. After removal of solvent, the product was purified by a column chromatography ($CHCl_3$:Acetone/19:1) and further recrystallization from cyclohexane/ethyl acetate yielded 91.3% white compound. (7.60 gm) ^{1}H, 400 Hz $CDCl_3$ δ 1.23 (t, 3H), 3.02 (m, 2H), 4.17 (m, 2H), 4.31-4.62 (m, 3H), 6.70 (d, 2H), 6.93 (d, 2H), 7.24-7.75 (m, 10H); ^{13}C, (100 Hz $CDCl_3$) δ 14.07, 37.42, 47.05, 54.87, 61.58, 66.94, 115.39, 119.89, 124.98, 127.07, 127.64, 130.41, 141.21, 143.54, 154.91, 155.54, 171.66.

4.8.1.6 N-(9-Fluorenylmethyloxycarbonyl)-O- Bis[(methyldiphenylsilyl) ethyl] phosphono] tyrosine ethyl ester (Fmoc-Tyr(PO_3MDPSE_2)-OEt) (1d)

Bis[2-(methyldiphenylsilyl)ethyl] N,N-diisophosphoramidite (1.535 g, 2.5 mmol) in 5 mL of anhydrous THF was added to a solution of Fmoc-Tyr-OEt (0.5389 g, 1.25 mmol) and tetrazole (8.3 mL of a 0.45M solution in MeCN) in 20 ml of anhydrous THF. The resulting solution was stirred at room temperature for 4 hours and cooled to 0 °C. To this mixture tert-BuOOH (0.75 mL of a 5-6M solution in decane) was added followed by stirring for two hours at 0 °C and further stirring at room temperature for another 1 hour. After aqueous workup, the residues were purified by silica gel column chromatography eluting with n-Hexane/Acetone: 80/20 (v/v). This resulted in 63% yield of the product as a white powder. ^{1}H NMR, (400 MHz DMSO d6) δ 0.53 (s, 6H), 1.10 (t, 3H), 1.56 (t, 4H, J= 8Hz), 2.85-3.30 (m, 2H), 4.02-4.27 (m, 10H), 6.97 (d, 2H, aromatic), 7.22-7.92 (m, 30H, aromatic) ^{13}C NMR, (100MHz, DMSO d6) δ -4.20, 14.35, 16,85, 16.90 (d, J_{PC} = 5 Hz), 35.91, 46.92, 55.82, 60.96, 65.97, 66.43, 66.36 (d, J_{PC}=7 Hz), 119.87, 119.91 (d, J_{PC} = 4 Hz) 120.46, 125.52, 127.92, 128.36, 129.88, 130.85, 134.39, 135.92, 141.05, 144.05, 156.27, 172.12; ^{31}P NMR (DMSO d6) δ -5.74 (s), MALDI-TOF observed m/z: M+Na+2H^{+} = 983.453.

4.8.1.7 N-(9-Fluorenylmethyloxycarbonyl)-O- phosphonotyrosine- ethyl ester (Fmoc-pTyrOEt (1e)

Fmoc-Tyr(PO_3MDPSE_2)-OEt (0.961 g) was dissolved in an icecooled solution (0 °C) of DCM/TFA: 1/1 (v/v) (18 mL) and stirred at room temperature for 3 hours. After removal of solvent and aqueous workup, the residues were purified by silica gel column chromatography eluting with chloroform/methanol: 95/5 (v/v) (0.1 % acetic acid). This resulted in 51% yield of the product as a white powder. ^{1}H NMR, (400 MHz DMSO d6) δ ^{1}H, δ 1.12 (t, 3H), 2.83-3.01 (m, 2H), 4.03-4.30 (m, 6H), 7.09 (s, 2H), 7.18-7.89 (m, 12H); ^{13}C NMR ^{13}C, (100MHz, DMSO d6) δ 14.38, 35.86, 36.02, 46.92, 56.06, 60.95, 65.97, 120.07, 120.47, 125.51, 128.00, 130.29, 141.05, 143.48, 144.07, 156.29, 172.22; ^{31}P NMR (DMSO d6) δ -5.185 (s). HPLC Conditions: C18 Luna column, Mobile phase: H_2O/MeOH: 80:20 (v/v) (1% TEA), DAD@ 254 nm, flow rate: 1 mL/min, Injection volume: 10 µL, stock solution: 1mg/mL in Methanol; ESI-MS: 512.14,

529.17. MALDI-TOF observed m/z: $M+H^+$, $M+Na^+$, $M+K^+$, $M+Na^++K^+$= 512.98, 534.96, 551.14, 573.19 respectively.

4.8.1.8 Polymer Preparations

The pTyr-imprinted polymer (P1) was prepared as previously described [108] but with a few modifications. The bis-pentamethylpiperidine (PMP) salt of Fmoc-pTyrOEt (**2**) (template) (0.5 mmol), functional urea monomer (**27)** (1 mmol), methacrylamide (1 mmol) and EDMA (20 mmol) were dissolved in THF (5.6 mL). To the solution was added the initiator ABDV (1% w/w of total monomers). The solutions were transferred to a glass ampoule, cooled down to 0 ^oC and purged for 10 min with a flow of dry nitrogen. Then afterword the procedure was adopted as reported in the previous chapter. The non-imprinted polymer (P_N1) was synthesized as imprinted polymer only with omission of template.

Table 4.3 HPLC retention factors (k) for the pTyr template and its non-phosphorylated analogue in a water poor mobile phase.

	P1	P_N1
Fmoc-Tyr-OEt	0.21	0.14
Fmoc-pTyr-OEt	> 50	0.20
Fmoc-pSer-OEt	5.0	0.30

Injection: 5 µL of 0.1 mM stock solutions, Mobile Phase: ACN/Water: 95/5 (v/v) (0.1% TFA)

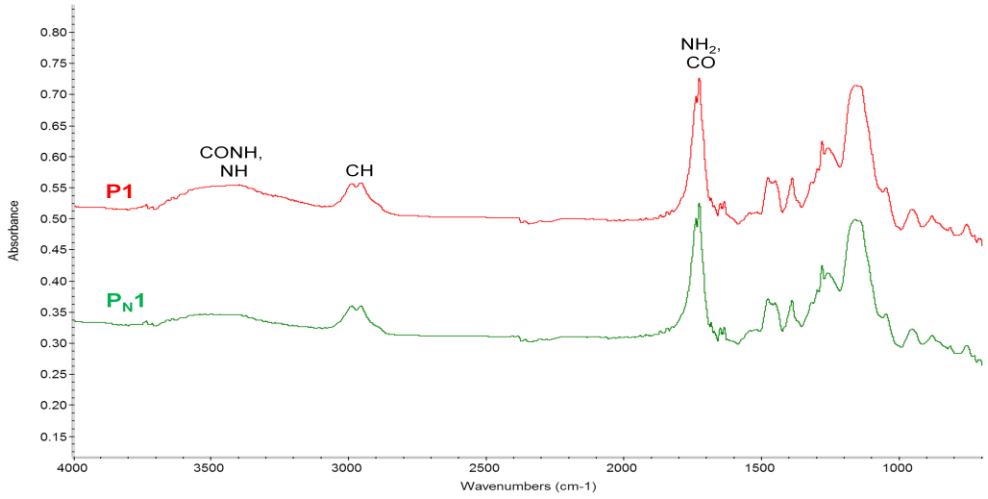

Figure 4.9 Infra-red spectra of P1 and P_N1.

5 Imprinted polymers tragetting sulfated protein fragments

5.1 Introduction

Tyrosine sulfation is a PTM of underestimated importance known targets are membrane proteins which are e.g. involved e.g. blood coagulation, cell adhesion and hormone regulation [140],[63, 64]. The analysis of these modifications is complicated by the lability of sulfotyrosine and the isobaric masses of phospho/sulfo tyrosine [69, 70]. Sulfotyrosine readily decomposes at elevated temperature and at low pH conditions. This is the major reason excluded it from being analyzed by chemical sequencing experiments. Localization of tyrosine sulfation, however, has remained a daunting challenge for mass spectrometry analysis because sulfotyrosine is labile in both positive and negative ion MS/MS experiments, yielding unmodified tyrosine[141],[142].

Both modifications phosphorylation and sulfation give rise to 80 Da nominal mass increase. In principle, they can be distinguished by ultra high accuracy mass measurements due to their 9.5 mDa mass difference (sulfotyrosine: m/z = 79.9568 Da; phosphotyrosine m/z = 79.9663 Da)[143]. However, this approach is not generally applicable because the Fourier transform-ion cyclotron resonance (FT-ICR) mass spectrometers required for this type of measurements are not available in most MS facilities.

Recently Leary *et al*.[65], has been used a subtractive approach in which a highly specific and efficient derivatization reaction allows the acetylation of unmodified tyrosine residues as shown in Figure 5.1 Upon MS/MS, the sulfate residues of the sulfotyrosine cleaved, resulting a free tyrosine group. Therefore, the information of the sulfation site is preserved as all other tyrosine residues have an additional acetyl group, which is stable in positive ion MS/MS. Thus the detection of an unacetylated tyrosine(s) indicates the site of sulfation [65].

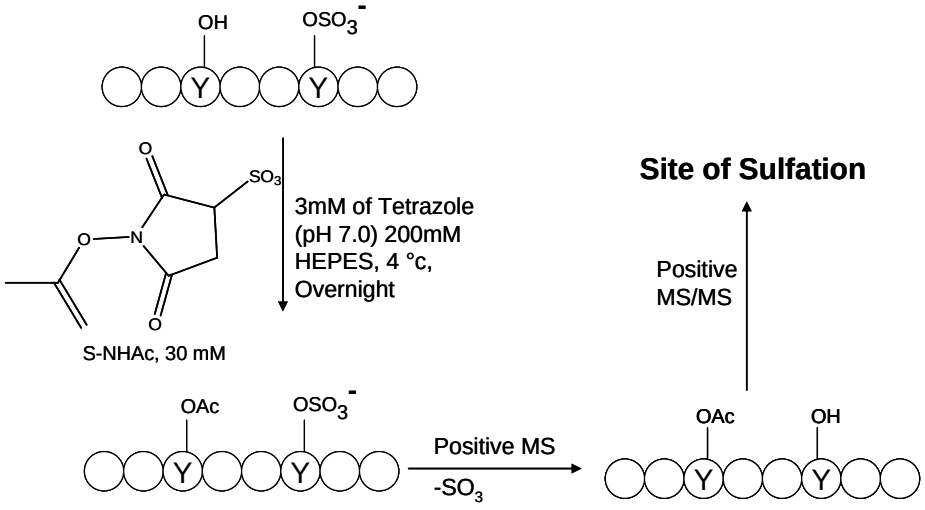

Figure 5.1 Subtractive strategy for site determination of protein tyrosine sulfation. Unmodified tyrosyl hydroxyl and primary amino groups are acetylated quantitatively by reacting with S-NHSAc using imidazole as a catalyst. During mass spectrometry analysis in the positive ion mode the sulfuryl groups of sulfotyrosine residues are lost but the acetyltyrosine is stable. The site(s) of tyrosine sulfation is then inferred from positive MS/MS experiments (adapted from [65]).

The scarcity of reports of this PTM is thus more due to the lack of general, unambiguous analytical methods than to a limited occurrence or relevance. One approach to address the problem is to develop selective enrichment techniques which effectively could fractionate the various modified proteins or protein fragments [70]. Sulfotyrosine antibodies or more recently antibody fragments generated by in vitro display technologies have proven promising in this regard [144] but these are biological receptors which suffer from their inherent problems related to robustness and cost.

In the previous chapter, selective enrichment of phosphotyrosine peptides by phosphotyrosine imprinted polymers (MIPs) are demonstrated at ultra trace levels from proteolytic digests [137]. This MIPs, which can be used to selectively enrich sulfopeptides in a strongly pH dependent manner will be discussed in this chapter.

5.2 Polymer preparation

5.2.1 Phosphotyrosine and sulfotyrosine imprinted polymer

The polymer P1 and P_N1 were synthesized (Table 5.1) and were investigated in the chapter 4. Fmoc-sTyr-OEt was obtained by Fmoc-Tyr-OEt sulfation using sulfur trioxide complex in N,N dimethyl formamide as reported by Futaki et al.[145] and Ukei et al[146]. sTyr template was transferred to a TBA salt which had been isolated and dried by lyophilisation prior to polymerization. The polymers P1S was prepared in the similar way to P1 (according to Table 5.1) using the urea host monomer (FM) 1:1 (sTyr) stoichiometric ratio to the template Fmoc-sTyr-OEt in its monoanionic form using EGDMA crosslinking monomers and Methacrylamide (MAAM) as a co-monomer.

5.2.2 Pentaerythritol triacrylate (PETA) as cross-linking monomer

Pentaerythritol triacrylate (PETA) is in comparsion to EGDMA, a hydrophilic cross-linker. The combination of its hydrophilic character and rigidity has proven benefits in the synthesis of imprinted polymers. MIPs synthesized using PETA as crosslinker have improved imprinting properties and binding performance in aqueous media. This has been shown shown superiors in many examples, for instance amino acid derivatives [147] and ephedrine.[148], riboflavin[149, 150] etc.

Polymer P2 was synthesized by polymerizing functional monomer complex with Fmoc-pTyr-OEt using PETA as crosslinking monomer and acrylamide (AA) as a supplementary monomer (Table 5.1). Nonimprinted polymers (P_N1 and P_N2) were prepared identically to the imprinted polymers but omitting the template.

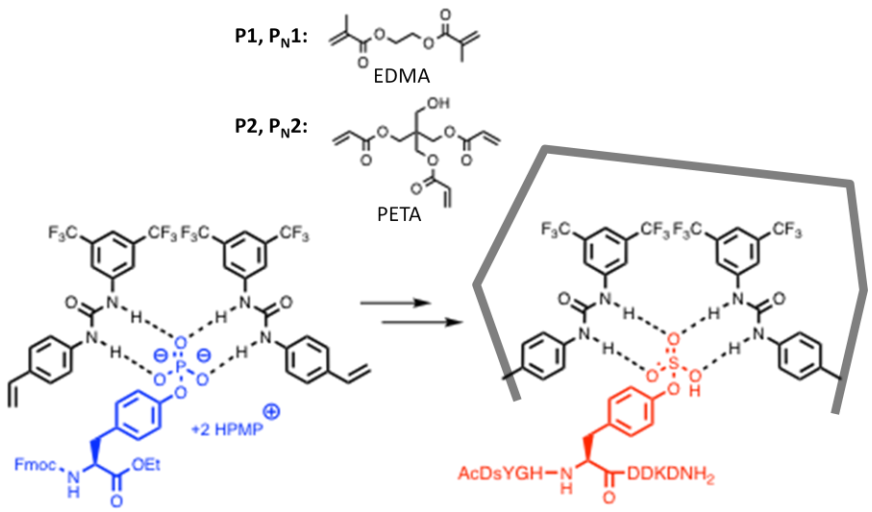

Figure 5.2 Possible prepolymerization complex of monomer and Fmoc-pTyr-OEt and recognition of an sTyr containing peptide by the resulting MIP [151].

Table 5.1 Monomer composition used to prepare imprinted and nonimprinted polymers

Polymer	Template	Host monomer	Co-Monomer	Crosslinker
P_N1	-	1 (1)	MAAm (1)	EGDMA (20)
P1	Fmoc-pTyr-OEt (0.5)	1 (1)	MAAm (1)	EGDMA (20)
P1S	Fmoc-sTyr-OEt (1)	1 (1)	MAAm (1)	EGDMA (20)
P_N2	-	1 (1)	Aam (1)	PETA (13.3)
P2	Fmoc-pTyr-OEt (0.5)	1 (1)	Aam (1)	PETA (13.3)

All polymers were prepared using the indicated templates and monomers, THF as porogen and ABDV as initiator by thermal homolysis of the initiator at 50°C. The molar composition has been indicated in parentheses.

Conventional azo-initiated thermal polymerization at 50°C subsequently provided the imprinted and non-imprinted polymers. The polymers were lightly crushed and then subjected to template removal by extraction with acidic methanol using a Soxhlet apparatus. The polymer were crushed and sieved to particle size of 36-50 µm. As shown in Table 5.2, the elemental

composition indicated efficient template removal from P1 whereas P2 still contained residual template.

Table 5.2. Elemental composition of all polymers after solvent extraction and drying (Found) compared with the nominal elemental composition assuming no template removal (Calc.)

	% C		% H		% N		% S	
	Calc.	Found	Calc.	Found	Calc.	Found	Calc.	Found
P1	60.60	56.46	6.72	6.73	1.05	0.98		
P_N1	60.00	57.22	6.81	7.01	0.95	0.95		
P1S	60.11	54.98	6.62	7.49	1.14	0.72	0.65	-
P2	56.40	52.68	5.82	6.29	1.05	1.07		
P_N2	56.13	53.10	5.86	6.39	0.95	0.94		

5.3 Chromatographic characterization

Imprinting effects were thereafter assessed by chromatography using the crushed polymer monoliths as stationary phases for HPLC. Fmoc amino acids were injected into the columns in an acetonitrile rich mobile phase buffered with either triethylamine or trifluoroacetic acid to investigate discrimination ability of template from other control analytes. Figure 5.3 shows that P1 and P2 exhibited strong affinity for the Fmoc-pTyr-OH in this mobile phase with nearly 70% of injected analyte remaining bound on the column. Meanwhile, the other amino acids were only weakly retained and P_N1 and P_N2, exhibited no affinity for any of the analytes.

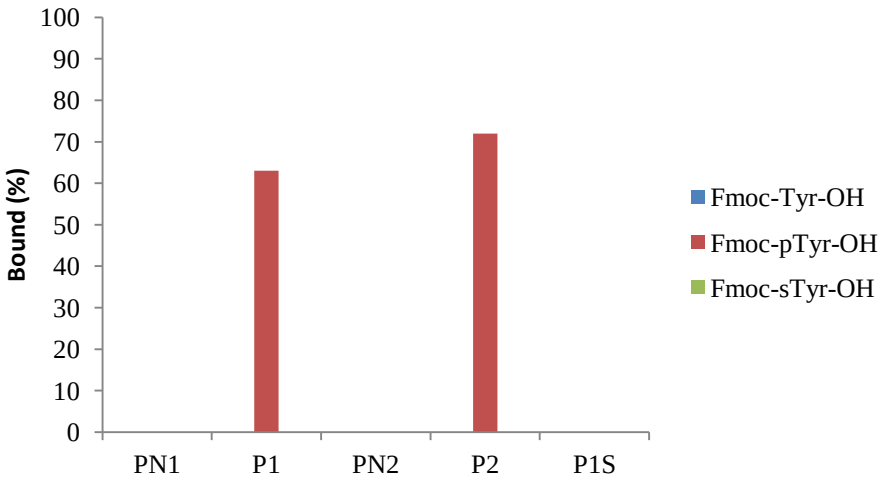

Figure 5.3 Fraction of injected Fmoc-amino acids which was fully retained on the Fmoc-pTyr-OEt imprinted polymers and the corresponding non-imprinted control polymers. The mobile phase was MeCN:Water 93:7 (1% TEA).

In basic mobile phases, anions are in the anionic form (Table 5.3). Thus, phosphomonoester have shown highest affinity among the anions to urea donors in the imprinted sites. This also corroborates the relative stabilities of the complexes obtained from the NMR titrations and ITC especially if the latter features two ureas offering quadruple hydrogen bonding. On the other hand, sulfate was not retained by P1 and P2. sTyr analyte did not enter in the imprinted sites because it is a strongly hydrated anion (Table 5.3). The sTyr anaylte was only weakly retained by polymer P1S in spite of this polymer being synthesized using sTyr template (Figure 5.4B and D). When the sTyr analyte was injected into an acidic mobile phase, it was found to be retained by the column P1, P2 (Figure 5.4 and Figure 5.5). These results are in good agreement with the results presented in chapter 3, where PPA imprinted polymer have shown affinity to PSA model oxyanion. The polymer was showed a pronounced selectivity for pTyr over Tyr in acidic mobile phases (0.1% TFA). This result is previously explained based on the relative strengths of the acids involved (Table 5.3) in the mobile phase.

The pH of a 0.1 % TFA solution is not sufficiently low to protonate the phosphate group fully, which still carries one O-localized partial negative charge, a potent hydrogen bond acceptor, for interacting with the binding site [108]. MIPs prepared using the hydrophilic cross-linking monomer PETA (P2) displayed highly enhanced retentivition and selectivity than those prepared

using the hydrophobic monomer EGDMA (P1). Moreover, the polymer P2 establishes a to four fold higher imprinting factor in organic mobile phase compared to P1 which is made from EGDMA crosslinker. This reflects an enhanced fidelity of the imprinted sites (Figure 5.5C and D), presumably involving an active participation of the matrix OH groups (from PETA) in interacting with the guest. Similar imprinting effect enhancement has reported in case of riboflavin application when PETA crosslink monomer was used [149, 150].

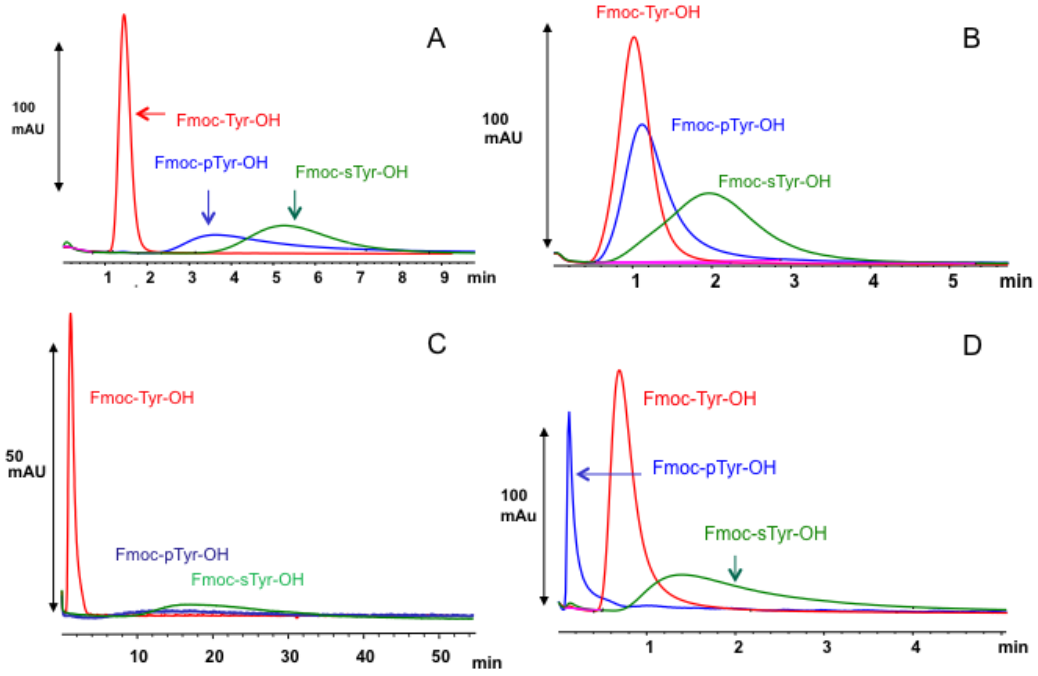

Figure 5.4. Elution profiles of control analytes Fmoc-Tyr-OH (red elution profiles), Fmoc-pTyr-OH (blue elution profiles) and Fmoc-sTyrOH (green elution profiles) injected on P1 (A) P_N1, (B) P2 (C), P1S (D) using MeCN:Water/95:5 (0.1% TFA) as mobile phase.

The sTyr analyte injected onto P2 column, showed strong retention in the acidic mobile phase. Both pTyr and sTyr analytes have shown nearly identical retention factors in the P2 column. They were eluted as broad peak from P2 after ca 10 min elution time. The retention behavior contributed from non-specific binding. This interesting retention behavior is also linked to the protonation state of the functional groups (Table 5.3). In the TFA mobile phase, sTyr analyte is in its neutral form and is less strongly hydrated. In this condition, the sTyr analyte easily enter in the binding cavities of the imprinted polymer.

Table 5.3 pKa values and protonation states of relevant acids and hydration energies of their nonsubstituted anions[151]

Acid	pK_a 1	pK_a 2	Charge in presence of TEA[a]	Charge in presence of TFA[b]	Anion hydration energy[c] (kJ/mol)
$PhOPO_3H_2$	0.90	6.28	-2	> -0.5	-498
$PhOSO_3H$	< 1	-	-1	> -0.5	-1130

a) pKa=10.7

b) pKa=0.5

c) Values reported for SO_4^{2-} and PO_4^{3-} [129].

The EGDMA based polymers (P1 and P_N1) displayed a decrease in retention when changing from organic to a more aqueous mobile phase. The opposite behavior was observed for the more hydrophilic polymers (P2 and P_N2) where the retention factor showed a strong increase on both the imprinted and non-imprinted polymers. Increase in non-specific interactions can be explained by in the overall decrease in imprinting factor. Over all, polymers synthesized from PETA have shown improved water compatibility compared to EGDMA polymers.

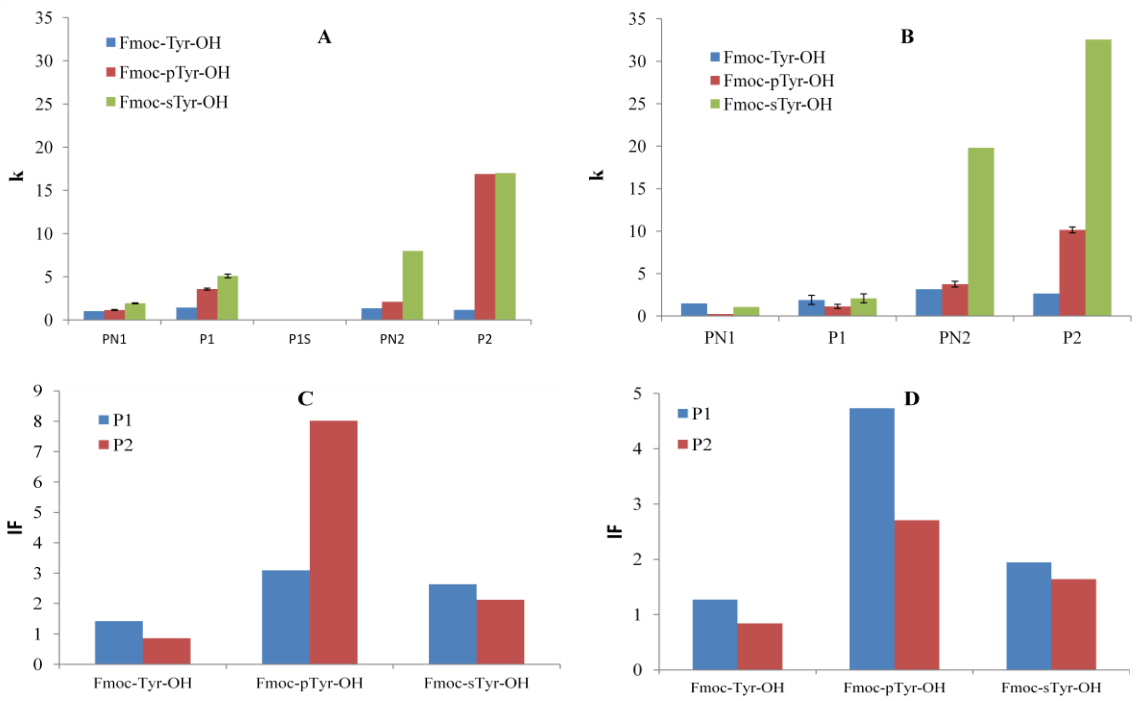

Figure 5.5. Retention factors (A, B) and imprinting factors (C, D) for pTyr and sTyr imprinted polymers and nonimprinted control polymers. The mobile phase was in (A and C) MeCN:Water - 95:5 (0.1% TFA) and in (B and D) MeCN:Water -50:50 (0.1% TFA).

The polymers P1 and P2 made using pTyr template have successfully retained pTyr and sTyr analytes in acidic mobile phases, however in basic mobile phases, these polymers were able to retain but no affinity was found for sTyr analyte.

5.4 Enrichment of sulfopeptide by imprinted polymer

The imprinting strategy was applied to explore whether sTyr selective MIPs can retain sulfated peptides. Therefore, a synthetic sulfated peptide ($C5aR_{10\text{-}18}S_2$) [152] (Figure 5.7), featuring two sulfated tyrosine residues sTyr-11 and sTyr-14 have taken for the study. This sulfation of CCR5 is also mimicked by the human immune system in this case, tyrosine sulfated antibodies against gp120 were identified in two HIV-1 infected patients[153]. “HIV-1 infection starts by binding of viral glycoprotein gp120 to CD4 host cell. Glycoprotein gp120 is connected to the virus via a gp41 transmembrane protein. Subsequent conformational arrangements of gp102 lead to binding to the chemokine receptor CCR5. The binding of gp120:CD4 complex to this CCR5 co-receptors

allows gp41 to bind to the membrane of host cell and promote fusion and the entry of viral content" Figure 5.6 [154].

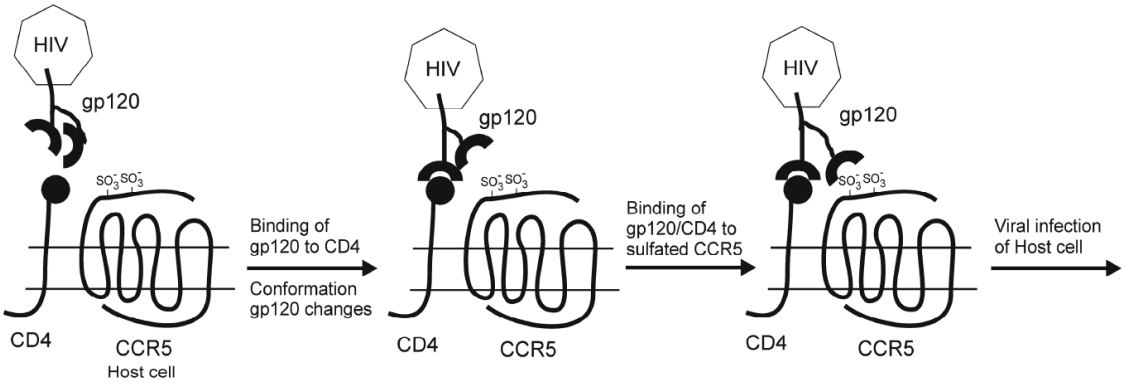

Figure 5.6 HIV-1 infection of a host cell. Gp 120 binds to CD4, upon which a binding site for the N-terminus of CCR5 is exposed. Binding of gp 120:CD4 will lead to viral entry [154, 155].

The N-terminus of the CCR5-receptor contains four tyrosine residues surrounded by acidic amino acids of which especially tyrosine 10 and 14 are sulfated and crucial for promoting the binding of CD4/gp120 and finally viral infection[156]. This sulfation of CCR5 is also mimicked by the human immune system. In this case, tyrosine sulfated antibodies against gp120 were identified in two HIV-1 infected patients[153]. C5aR is a G-protein coupled receptor involved in inflammatory response in the presence the proinflammatory agent C5a. The two sTyr residues are located near the N-terminus and are essential for high affinity binding of C5a by C5aR. This sequence is hence a target for inflammation inhibitors [157].

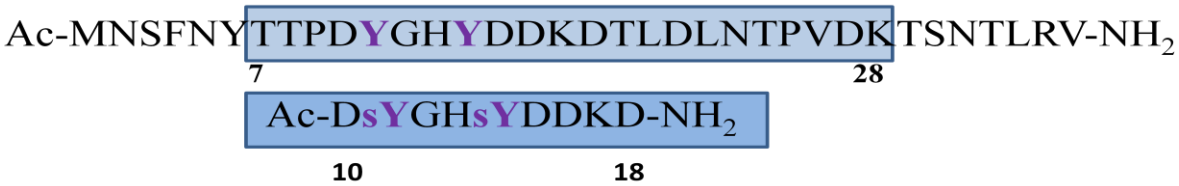

Figure 5.7 Amino acid sequence of residues 1–35 of the human C5aR (numbering according to Swiss-Prot entry P21730). The sequence of peptide $C5aR_{7–28}$ S_2 is indicated in color (upper) and the positions of tyrosine residues 11 and 14. Synthetic analogue $C5aR_{10-18}S_2$ (lower sequence) is used in the current study [157].

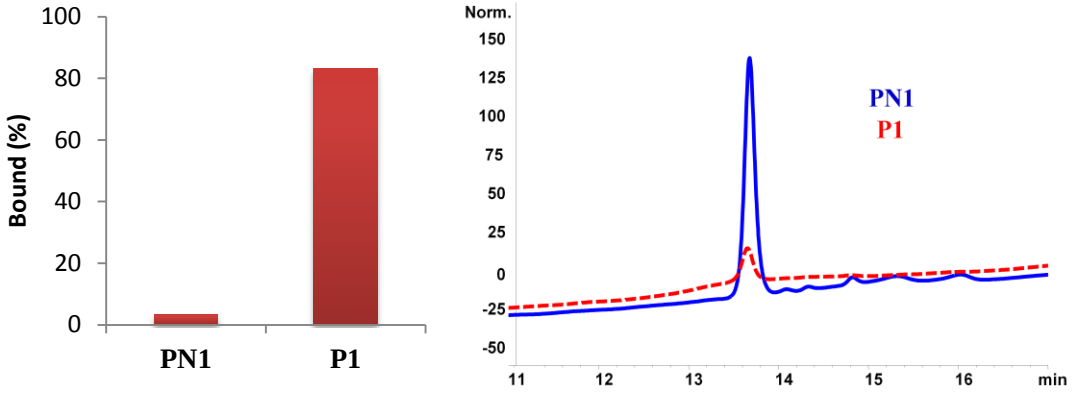

A. B.

Figure 5.8 A) Uptake of the C5aR peptide to P1 and P_N1; B) HPLC-UV chromatograms of supernatant fractions after incubation of the C5aR peptide with P1 and P_N1, respectively.

Polymers P1 and P_N1 were incubated with $C5aR_{10\text{-}18}S_2$ in MeCN:water 80:20 (0.1% TFA) under equilibrium conditions and measured the specific binding to each of the polymers by C18-HPLC quantification of the nonbound peptide. A strong imprinting effect was observed with more than 80% of the peptide bound to P1 whereas P_N1 showed only a minimal affinity for the peptide as shown in Figure 5.8. This uptake corresponds to a specific binding of *ca* 0.8µmol/g sorbent.

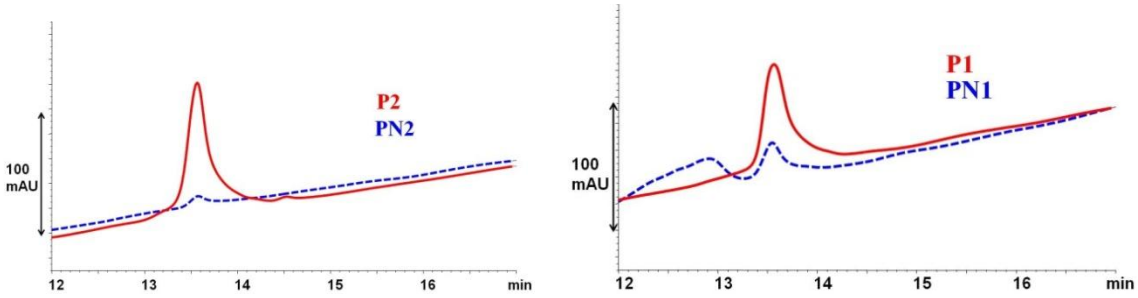

A) B)

Figure 5.9 HPLC-UV chromatograms of elution fractions corresponding to Figure 5.10 after SPE on $P2/P_N2$ (A) and $P1/P_N1$ (B).

Approximately 20 mg polymer was taken in the cartridge and applied for solid phase extraction (SPE). The simple SPE protocol has developed, which consist of one loading and one elution step. The acidic MeOH was used for the elution and elution fractions were quantified by reverse phase HPLC.

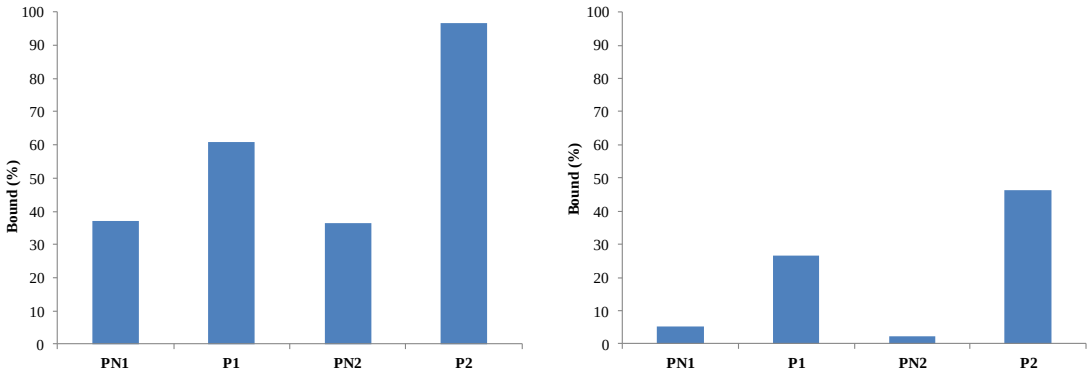

A) B)

Figure 5.10 Recoveries of C5aR obtained on P1, P2 and the corresponding nonimprinted polymers (P_N1 and P_N2) after percolation of 1 mL (A) 7.5 µM and (B) 15µM solutions of the peptide in MeCN followed by one single elution step (0.4 mL) with the MeOH (0.1% TFA) solvent. The sample were analyzed in duplicate.

The recovery of the model peptide after SPE on P1 and P2 using an optimized extraction protocol is shown in Figure 5.9 and Figure 5.10. The P2 showed the superior performance with a near quantitative recovery of the peptide at lower sample loads significantly exceeding the recoveries obtained on the other polymers. These results are in agreement of Fmoc amino acids results (Figure 5.5).

5.5 Selective enrichment of sulfopeptide from mixture of peptides

The model peptide mixture was prepared and was taken for solid phase extraction for P2, P_N2 polymers. The model peptide mixture made up of $C5aR_{10\text{-}18}S_2$, its desulfated parent peptide and methylated peptides resulting from hydrolytic treatment of C5aR in acidified methanol (2% TFA in MeOH) (see Table 5.4). When an applied mixture of peptides for SPE on to the polymers, the recoveries of the different peptides in the elution fraction after SPE on P2 and P_N2 are seen in Figure 5.11.

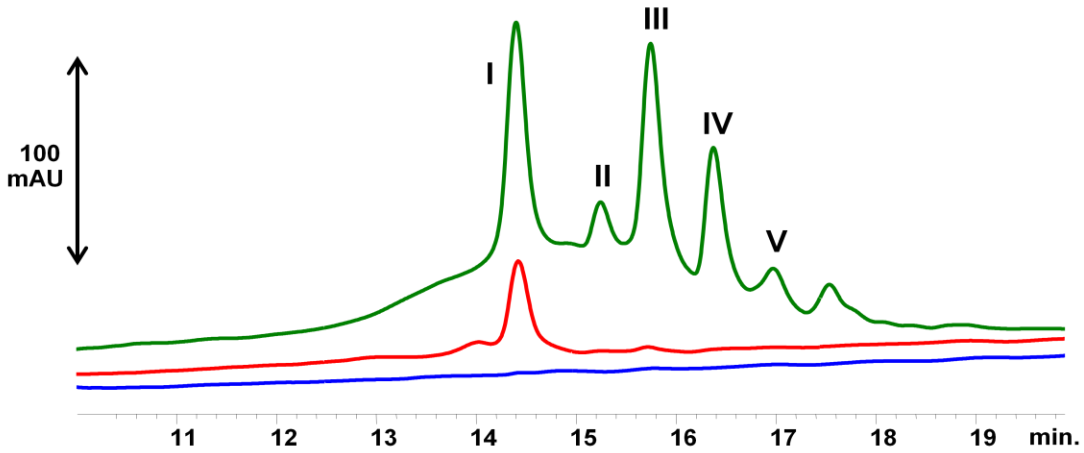

Figure 5.11 Reversed phase HPLC chromatogram of a mixture of $C5aRS_2$ and its hydrolysis and esterification products.

Table 5.4. LC-MS characterization of the C5aR peptides resulting from hydrolysis and esterification in MeOH (2%TFA)

Peptide	Sequence	Calc. Mass (m/z)	Exp. Mass (m/z)	t (min)[a]	t (min)[b]
I. $C5aR_{10\text{-}18}\ S_2$	Ac-DsYGHsYDDKD	664.7	584.7*	11.45	14.4
II. $C5aR_{10\text{-}18}$	Ac-DYGHYDDKD	585.7	585.7	12.30	15.2
III. $C5aR_{10\text{-}18}$ (Me)	Ac-DYGHYDDKD (Me)	591.7	591.7	12.85	15.7
IV. $C5aR_{10\text{-}18}$(Me)	Ac-DYGHYDDKD (Me)	591.7	591.7	13.01	16.3
V.$C5aR_{10\text{-}18}(Me)_2$	Ac-DYGHYDDKD $(Me)_2$	598.7	598.7	13.41	16.9

Sulfated tyrosine residues are indicated by sY and desulfated mass* $[M\text{-}2SO_4]^{2+}$ observed during MS measurement. The masses given refer to mono isotopic mass $[M+2H]^{2+}$ and $[M]^{2+}$.

a) Retention time t using reversed phase method 2 described in the experimental section (5.9.1.9).
b) Retention time t using reversed phase method 1 described in the experimental section (5.9.1.8).

Under the competitive conditions, P2 can effectively retain the sTyr peptide, with minimal retention of the non-sulfated counterparts and that it can be cleanly eluted with a moderate recovery (ca. 38%). Under these conditions, non-imprinted polymer did not retain any of these peptides.

5.6 Desulfation of sulfopeptide during MS measurement

When two peptides $C5aR_{10\text{-}18}S_2$ and $C5aR_{10\text{-}18}$ have taken for mass measurement, mass spectroscopy cannot distinguish (Table 5.4). Desulfation was occurred during MS measurement resulting both the peptides have same masses, whereas the imprinted sorbents are capable of discriminate these peptides.

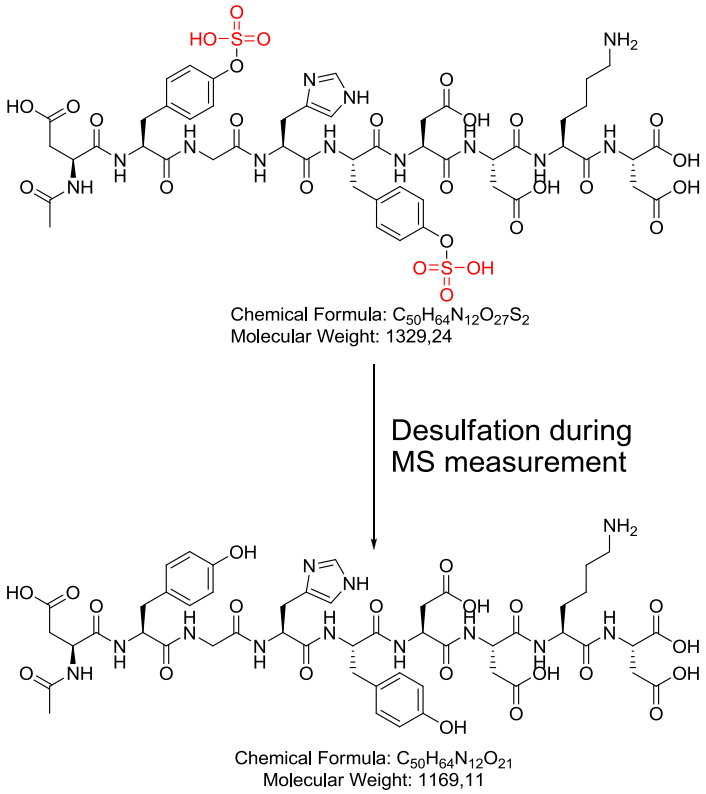

Figure 5.12 Desulfation of $C5aRS_2$ peptide during (LCMS and MALDI-TOF) mass measurements (Described in 5.9.1.9 and 5.9.1.10).

The characterization challenges have been observed in many reports that desulfation was occurred during MS measurement in both positive and negative ion MS/MS experiments, yielding unmodified tyrosine [141, 142].

MALDI-TOF MS measurement is known for soft ionization method, expecting to observe molecular masses without desulfation. The peptides pYY-ZAP70 (Gly-Ala-Asp-Asp-Ser-Tyr(PO_3H_2)-Tyr-Thr-Ala-Arg) and $C5aR_{10\text{-}18}S_2$ (Ac-Asp-Tyr(SO_3)-Gly-His-Tyr(SO_3)-Asp-Asp-Lys-Asp-NH_2) were subjected to MALDI-MS measurement study found that masses 1199.85 ($M+H^+$) (Figure 5.14) and 1169.17 $[M-2SO_3]^+$.(Figure 5.13) was observed for these peptide respectively.

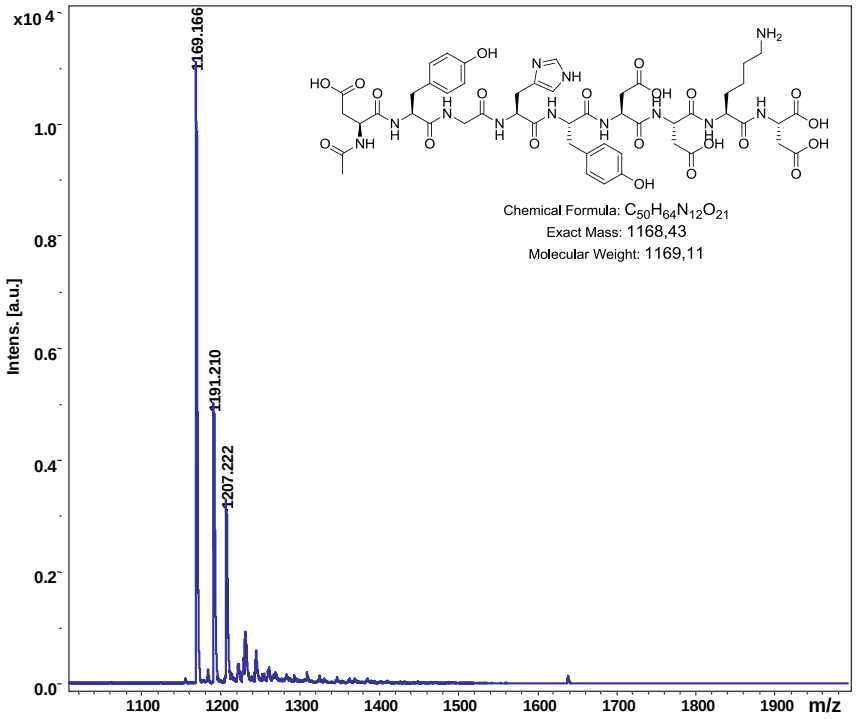

Figure 5.13 MALDI-MS spectra of $C5aR_{10\text{-}18}$ S_2 The m/z is corresponding to the desulfated peptide.

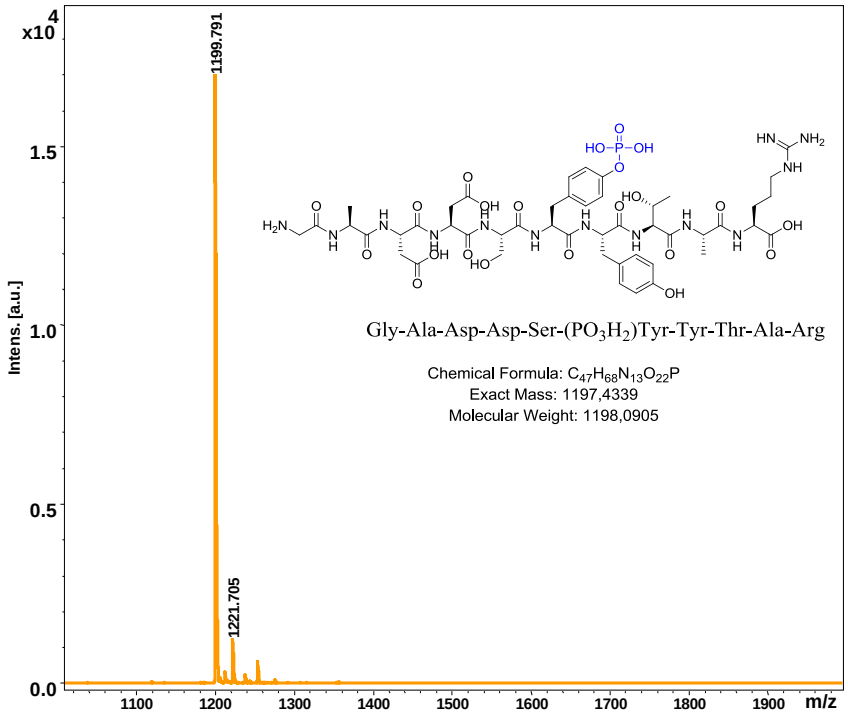

Figure 5.14 MALDI-MS spectra of pYY-ZAP70. MS of pYY: $[M + H]^+$

5.7 Competitive enrichment of phosphorylated and sulfated peptides

An equimolar mixture of the monophosphorylated peptide pYY-ZAP70 and $C5aR_{10\text{-}18}S_2$ were loaded and SPE performed according to two different protocols. In the first protocol, the SPE consisted only a load and an elution step whereas the second protocol contained an intermediate aqueous wash step. Figure 5.15A shows the chromatograms of the elution fractions and Figure 5.15B, Figure 5.16 the corresponding MALDI-TOF mass spectra. The load/elute SPE resulted in a ca 40% total peptide recovery was observed with both peptides present in roughly equal amounts (Figure 5.15). This suggests that no binding site competition occurs under these conditions. In the load-wash-elute SPE on the other hand, the sulfated peptide was strongly enriched in the final elution fraction with the phosphorylated peptide nearly quantitatively removed in the washing step. The recovery in the elution fraction, estimated from the peak areas (UV), were ca 20% for $C5aR_{10\text{-}18}S_2$ and <1% for pYY-ZAP70.

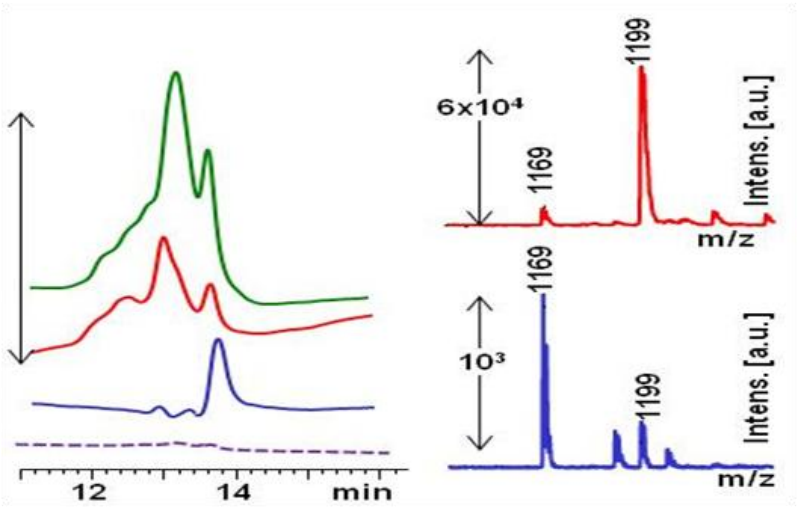

A B

Figure 5.15 (A) an equimolar mixture of C5aRS$_2$ and pYY-ZAP70 (green trace) and the elution fraction after SPE on P2 (SPE1: red trace; SPE2: blue trace) and P_N2 (black dashed trace). SPE1 conditions: Loading: MeCN; Elution: MeOH (0.1%TFA). SPE2: Loading: MeCN; Washing: MeCN:Water 90:10 (0.1% TFA); Elution: MeOH (0.1%TFA).(B) MALDI-MS spectra of the elution fraction after SPE P2 (SPE1: red ; SPE2: blue).

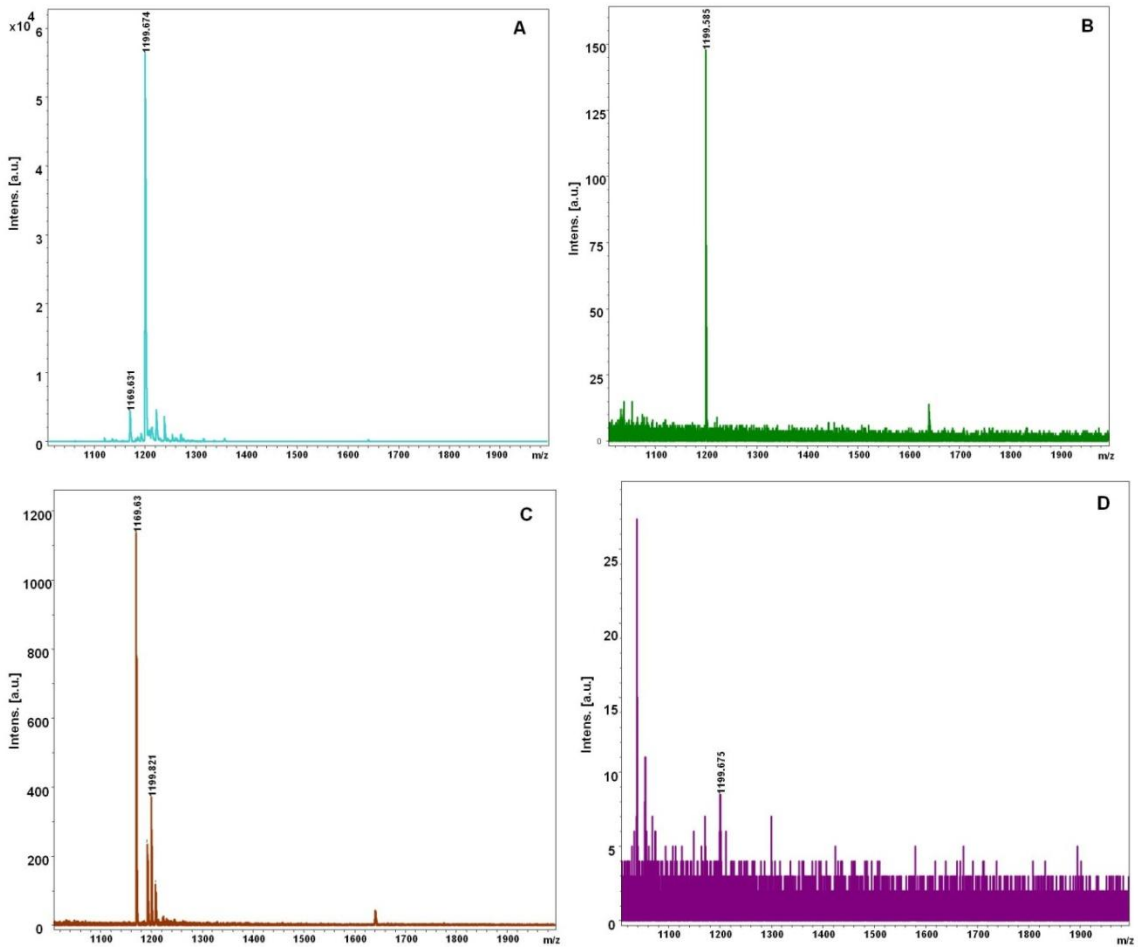

Figure 5.16 MALDI-MS spectra of elution fractions of $C5aR_{10\text{-}18}S_2$ and pYY ZAP70 after SPE on P2 (A, C) and non-imprinted polymers P_N2 (B, D) (Described in the experimental section 5.9.1.10).

5.8 Conclusions

In summary, the MIPs described in this work are potent receptors for sulfotyrosine and/or phosphotyrosine containing amino acids and peptides. This is to my knowledge the first example of synthetic polymers capable of cleanly and selectively extracting and discriminating sulfated peptides from nonmodified peptides.

The MIPs were capable of selectively capturing both a phosphorylated and a sulfated peptide in a mixture and could release the peptides separately based on elution conditions.

5.9 Materials and Methods

5.9.1.1 Materials

Fmoc-Tyr-OH, Fmoc-Tyr(SO_3H)-OH. Na salt, Fmoc-Tyr(PO_3H_2)-OH, were received from Bachem AG Switzerland and purity are > 97 %. Pentaerythritol triacrylate (PETA) were purchased from Sigma-Aldrich (Steinheim, Germany). N, N-dimethylformamide (DMF) (extra dry): Across Organics, UK; Pyridine: Aldrich, Germany; 1,4 dioxane: Fischer Scientific, UK; Sulfurtrioxide:Dimethylformamide complex (DMF:SO_3) 97% Fluka Switzerland. The base 1,2,2,6,6-pentamethylpiperidine (PMP) was purchased from Fluka (Buchs, Switzerland). The initiatior *N,N´*-Azo-bis-(2,4-dimethyl)valeronitrile (ABDV) was purchased from Wako Chemicals (Neuss, Germany). Methanol (MeOH) of HPLC grade and MeCN of HPLC grade, were purchased from Acros (Geel, Belgium). Details concerning the synthesis of the template Fmoc-pTyr-OEt and polymer P1 were already reported [137]. The LC-MS of Fmoc-sTyr-OEt was carried out in mixture acetate buffer and MeCN mobile phase. Doubly sulfated C5a sulfopeptide Ac-Asp-Tyr(SO_3)-Gly-His-Tyr(SO_3)-Asp-Asp-Lys-Asp-NH_2 was prepared as described before [152, 157]. The LC-MS of Fmoc-sTyr-OEt was carried out in mixture acetate buffer and MeCN mobile phase. The monophosphorylated regulatory sequence 487-496 of human protein kinase ZAP-70 (Gly-Ala-Asp-Asp-Ser-Tyr(PO_3H_2)-Tyr-Thr-Ala-Arg (87.68 % pure) (pYY-ZAP70) was received from Lifetein, USA.

5.9.1.2 Synthesis of Fmoc-Tyr ($SO_3N^nBu_4$)-OEt

Fmoc-sTyr-OEt was synthesized as reported by Futaki et al.[145] and Ukei et al[146] with a few modifications. Fmoc-Tyr-OEt (0.2155 g, 0.05 mmol) was dissolved in DMF-Pyridine (4:1; 1 mL) and then DMF-SO_3 (0.382 g, 5 equivalents) was added. The mixture was stirred overnight at room temperature. After removal of solvent, the residue was dissolved in water and extracted with ethyl acetate. The unmodified reactant is soluble in ethyl acetate and water soluble compound was treated with saturated sodium hydrogen carbonate solution and tetrabutylammonium hydrogen sulfate. The solution was acidified with citric acid and extracted twice with chloroform. After removal of solvent, lyophilization of the residue from dioxane/water:50/50 (v/v) gave Fmoc-Tyr($SO_3N^nBu_4$)-OEt as stable colorless amorphous powder (0.22 g) 60% yield with purity more than 85% based on LCMS. Calculated $C_{26}H_{25}NO_8S$

m/z: 511.54; observed masses $[M+NH^4]^+$-529.54 MS-MS:Fmoc+NH_4^++H^+-242.37; MALDI-TOF (DHB Matrix) Found m/z: $M+Na^+$, $M+H^++Na^+$ - 534.7, 535.7 respectively.

5.9.1.3 Polymer preparation

P1 was prepared using the bis-PMP salt of Fmoc-pTyr-OEt as template, N-3,5-bis(trifluoromethyl)-phenyl-N'-4-vinylphenylurea as functional monomer, EGDMA as crosslinker and THF as porogen as reported in chapter 4. **P1S** was prepared in an analogous manner. Thus TBA salt of Fmoc-sTyr-OEt (62.7 mg, 0.083 mmol), monomer (**1**) (31.19 mg, 0.083 mmol), methacrylamide (7.09 mg, 0.083mmol), EDMA (330.4 mg 1.667 mmol) and initiator ABDV (3.69 mg, 1% w/w of total monomers) were dissolved in THF (0.466 mL). The solution was transferred to a glass ampoule, cooled to 0^oC and purged with a flow of dry nitrogen for 10 minutes. The tubes were then flame-sealed while still under cooling and the polymerization initiated by placing the tubes in a thermostated water bath pre-set at 50^oC. After 24h the tubes were broken and the polymers lightly crushed. They were thereafter washed 3 times with MeOH and extracted in a Soxhlet-apparatus with methanol : 0.1N HCl/50:50 for 24h. This was followed by further crushing and sieving, whereby the fraction from 36-50µm was used for packing the HPLC-columns to evaluate their binding properties. **P2** was prepared in the following manner. The template Fmoc-pTyr-OEt (100 mg, 0.196 mmol) was dissolved in dry THF (2.39 ml). The corresponding Bis-PMP salt was then prepared in situ by the addition of two equivalents of PMP (60.7 mg, 0.39 mmol) followed by addition of monomer (**1**) (146.4 mg, 0.39 mmol), acrylamide (27.79 mg, 0.39 mmol), PETA (1.5514 g, 5.20 mmol) and initiator ABDV (17.25 mg, 1% w/w of total monomers). Otherwise, the procedure described above for the preparation of P1S was followed. Non-imprinted polymers (P_N1 and P_N2) were prepared in the same way as described above, but with the omission of the template molecule from the pre-polymerization solution.

5.9.1.4 HPLC Evaluation

The 36-50 µm particle size fraction was sedimented repeatedly (80:20/MeOH: Water) to remove fine particles and slurry packed into HPLC column (30 x 4.6 mm) using a same solvent mixture as a pushing solvent. Subsequent analyses of the polymers were performed using an Agilent HP1050 or HP1100 system equipped with a diode array-UV detector and a workstation. Analyte

detection was performed at 260 nm, the flow rate was 0.5 ml/min and 5 µl of stock solutions of the analytes in MeCN:Water (80:20) was injected unless otherwise mentioned. The retention factor (k) was calculated as $k = (t-t_0)/t_0$, where t is retention time of analyte and t_0 = retention of void marker (acetone) (Eq.1 2). Imprinting factor (*I*) of analyte was calculated as k_{MIP}/k_{NIP} (Eq 1.3). Prior to each run the columns were washed with MeOH (0.1% TFA) for at least 2 hours and equilibrated for at least 20 minutes with mobile phase. In the case of the TEA modified mobile phases, the columns were conditioned with MeOH for more than 4 hours prior to each run.

5.9.1.5 Sulfopeptide enrichment

The polymer particles P1 and P_N1 (25 mg, particle size < 25 µm) were suspended in MeCN/Water:80:20 (0.1% TFA) (0.5 mL) containing C5a peptide (50 µM) followed by incubation of the mixtures for 24 hours at room temperature. After incubation, the supernatant was collected and analyzed by reversed phase HPLC as indicated below to determine the free (F) and bound (B) solute concentration.

5.9.1.6 Optimized solid phase extraction (SPE) procedure

Solid-phase extraction cartridges (1mL, Varian, Spain), were packed with 20 mg of the pTyr imprinted (36-50 µm) and the corresponding nonimprinted polymers. The cartridges were equilibrated with 0.6 mL of MeCN:Water/95:5 (0.1% TFA), and the sample containing the peptide, dissolved in MeCN, was percolated at a constant flow rate of 0.6 mL min^{-1} with the aid of a peristaltic pump. The cartridges were thereafter subjected to an elution step by percolating 400 µl of a MeOH (0.1% TFA). Before reuse, the cartridges were washed with 1 mL of MeOH (1% TFA) and reequilibrated with 1 ml of buffer MeCN:Water/95:5 (0.1% TFA). The elution fractions from the SPE column were directly analyzed by reversed phase HPLC.

5.9.1.7 Reversed phase HPLC-method 1

Chromatographic data were acquired with an HPLC 1100 system from Agilent Technologies that consisted of a quaternary pump, an autosampler and a diode array detector. Chromatographic separations of the peptides were performed using a Luna C18 (155 mm× 4.6mm I.D., 5µm) HPLC column protected by a C-18 guard column (4.0mm×3.0mm I.D., 5µm), both from Phenomenex (Torrance, CA,USA) in the gradient mode with a mobile phase composition

resulting from combining solvent A (95:5 Water: MeCN (0.1% TFA)) and solvent B (40:60 Water:MeCN (0.1% TFA)) as follows: 0% B, (2 min), 0-33.6 % B, (17.5 min), 100% B, (22 min). The flow rate was 1 ml/min and the column temperature was kept at room temperature 25◦C. The injection volume was 100 µl, and peptide was eluted at retention time 13.6 min. The diode array detector wavelength was set at 205nm for the peptide. Quantification was performed using the reference peptide as an external standard.

5.9.1.8 Hydrolysis of $C5aR_{10\text{-}18}S_2$ and solid phase extraction of a peptide mixture

Pure $C5aR_{10\text{-}18}S_2$ (2.4mg) was dissolved in 2 mL MeOH (2% TFA) and the solution allowed to stirr for ca 12 hrs. The solvent was evaporated (vacuum pump connected to desiccator) at room temperature and the resulting solid residue dissolved in MeCN:Water (50:50, v/v) (1.2 mL) resulting in a peptide mixture stock solution (2 mg/mL) which was characterized by reversed phase HPLC as outlined above.

Cartridges packed with P2 or P_N2 were equilibrated with MeCN (0.1% TFA) (2mL) and the sample containing the peptides (10 µl of pure $C5aRS_2$ and 20 µl of hydrolyzed $C5aRS_2$) dissolved in MeCN (0.1% TFA) (0.97 mL), percolated at a constant flow rate of 1 mL/min with the aid of a peristaltic pump. The cartridges were then washed with MeCN/Water:95/5 v/v (0.1% TFA) (1mL) to elute the non specifically retained peptides. Finally the peptides were eluted with 0.1% of TFA in MeOH (0.4 mL). The cartridges were extensively washed with 2 mL of MeOH (2% TFA) and re-equilibrated with MeCN (0.1% TFA) (2mL) before reuse. The elution fractions were directly analysed by reversed phase HPLC.

5.9.1.9 LCMS study of hydrolyzed peptides - Reversed phase HPLC-method 2

10 µl of (1 mg/mL) pure $C5aRS_2$ peptide and 20 µl of hydrolyzed C5aRS2 in 370 µl of MeOH (0.1%TFA) were used for LCMS characterization. The FT-fullscan spectra were obtained with an LTQ-Orbitrap Spectrometer (Thermo Fisher, USA) equipped with a HESI-II source. The spectrometer was operated in positive mode (1 spectrum s^{-1}; mass range: 200-1400) with nominal mass resolving power of 60 000 at m/z 400 with a scan rate of 1 Hz) with automatic gain control to provide high-accuracy mass measurements within 2 ppm deviation using an internal standard; Bis(2-ethylhexyl)phthalate : m/z = 391.284286. The spectrometer was attached to an Agilent (Santa Clara, USA) 1200 HPLC system consisting of the LC-pump, PDA detector

(λ = 270 nm), autosampler (injection volume 25 µl) and column oven (30°C). The following parameters were used for the experiments: spray voltage 5 KV, capillary temperature 200 °C, tube lens 110 V. Nitrogen was used as a sheath gas (50 arbitrary units) and auxiliary gas (5 arbitrary units). Helium served as the collision gas. The separations were performed by using a Nucleodur Isis column (50 x 3 mm, 1.8 µm particle size) from Macherey-Nagel (Düren, Germany) with a H_2O (+ 0.5% HCOOH/ MeCN (+ 0.1% HCOOH) (B) gradient (flow rate 500 µl min^{-1}). Samples were analyzed by using a gradient program as follows: 100% A isocratic for 2 min, linear gradient to 20% B over 20 min, after 100% B isocratic for 5 min, the system returned to its initial condition (100% A) within 0.5 min, and was equilibrated for 4 min.

5.9.1.10 MALDI-TOF mass spectrometry and SPE of a pY, sY peptide mixture ((Figure 6.13, and Figure 6.14)

Cartridges packed with P2 or PN2 were conditioned with MeCN (0.1% TFA) and MeCN (2 mL each) prior to the loading step. A sample (1mL) of a solution of $C5aR_{10\text{-}18}S_2$ (15µM) and pYY-ZAP70 (15µM) dissolved in MeCN was then percolated through the columns at a constant flow rate of 0.6 mL/min with the aid of a peristaltic pump. The peptides were then either eluted in one single step with MeOH (0.1%TFA) (0.4 mL) (SPE1) or after an intermediate washing step with MeCN:Water 90:10 (0.1% TFA) (1mL) also with MeOH (0.1%TFA) (0.4 mL) (SPE2). The cartridges were extensively washed with 2 ml of MeOH (2% TFA) and re-equilibrated with MeCN (0.1% TFA) and MeCN (2 mL each) before reuse. The elution fractions were directly analyzed by reversed phase HPLC and by MALDI-TOF-MS. The mass-spectrometric analysis of the fractions collected during the SPE experiments was performed using a MALDI reflector time-of-flight mass spectrometer (Autoflex II mass spectrometer, Brucker-Daltonics GmbH, Bremen, Germany) equipped with a Scout-384 source unless otherwise stated. Ions were generated by irradiation of analyte/matrix deposits by nitrogen laser at l=337 nm and analyzed with an accelerating voltage of 25 kV in the reflector mode and in the positive-ion mode. Data collection, in terms of the scanning conditions and the number of scans, was performed identically for all samples unless otherwise noted. The spectra were collected by accumulating 1000 laser shots, the scanning was performed by using the RP Pepmix_Par method, and the mass spectra were analyzed with flex Control software (Brucker Daltonic FLEXControl). The elution

fractions were directly taken to the MALDI experiments. The matrix solution was prepared by dissolving DHB (40 mg) in MeCN/water (1:1, v/v; 1 mL) 0.1% TFA. The matrix solution (1 µl) and the SPE aliquots (1 µl) were then deposited together on the target plate and evaporated at room temperature. Peptide masses: pYY-ZAP70 (Gly-Ala-Asp-Asp-Ser-Tyr(PO_3H_2)-Tyr-Thr-Ala-Arg): $M+H^+$=1199.85 and C5a$R_{10\text{-}18}S_2$ (Ac-Asp-Tyr(SO_3)-Gly-His-Tyr(SO_3)-Asp-Asp-Lys-Asp-NH_2): $[M-2SO_3]^+$ =1169.17.

6 Phosphoserine-imprinted polymer receptors for recognition of serine-phosphorylated amino acids and peptides

6.1 Introduction

Among the most common phosphorylation events, serine and theronine residues undergo phosphorylation much more often than tyrosine residues with the content ratio (pSer: pThr: pTyr) of 1800:200:1 in vertebrate cells. However, tyrosine phosphorylation gains more attention because of low abundant and regulated more strictly. Many enrichment techniques have developed for selective capture of phosphopeptides (Chapter 2; Figure 2.6). Tyrosine antibodies are more successful for selective enrichment however, it suffers from cost and stability. Hunter *et al* [158] has reviewed about antibodies and well explained why high-affinity antibodies for pSer and pThr antibodies are not developed? "This is mainly because of the lower immunogenicity of the phosphoserine and phosphothreonine side chains. The existing anti-phosphoserine and anti-phosphothreonine antibodies tend to recognize phosphate monoesters and they have to use in more carefully'' [158]. These limitations are compounded in many approaches by the greater cellular abundance of phosphoserine and phosphotheronine. Alternative to phosphospecific antibodies, chemistry based methods developed for enrichment particularly on base stability of these amino acids [159].

Under basic conditions, phosphoserine and phosphotheronine residues undergo an elimination reaction whereby phosphoric acid is lost and α, β unsaturated bond is formed. The end product are dehydroalanine and dehydroaminobutyric acid respectively as shown in Scheme 6.1. β-elimination reaction was optimized for complete reaction efficiency for pSer/pThr residue [160] so that pTyr residue was maintained in high recovery as pTyr residue is stable in condition.

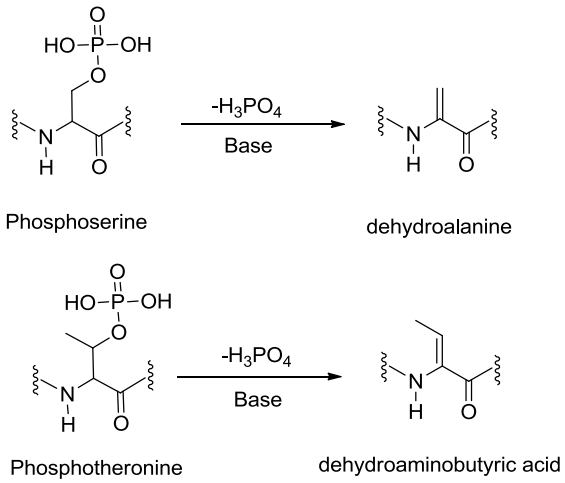

Scheme 6.1 Elimination reaction of phosphoserine and phosphthreonine in alkaline conditions.

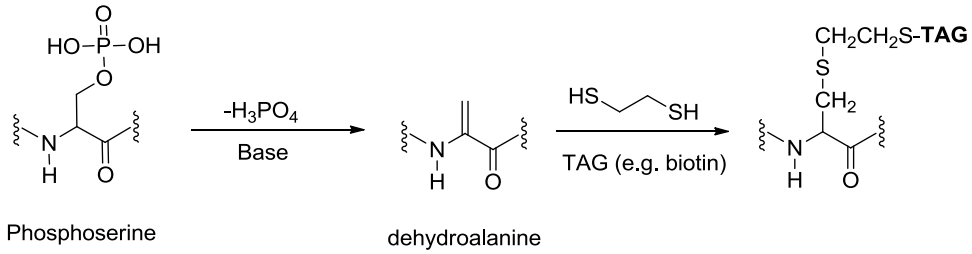

Scheme 6.2 Chemical modification based on β elimination.

Many chemical derivatization strategies have been devised to displace the phosphoryl group and binding tag to the peptide. Samples containing phosphoproteins were first treated with a strong base, leading to β-elimination reaction in the case of phosphoserine and phosphothreonine residues (Scheme 6.2). A reactive species containing an α,β unsaturated bond were formed. This serves as a Michael acceptor for the nucleophile (in this case, ethanedithiol or an isotopic variant may be substituted for quantitation purposes). The biotinylated reagent reacted with sulfhydryl (-SH) groups at acidic to neutral pH. Biotinylated phosphoprotein was then tagged for enrichment on avidin columns and these products were analyzed by mass spectroscopy [67].

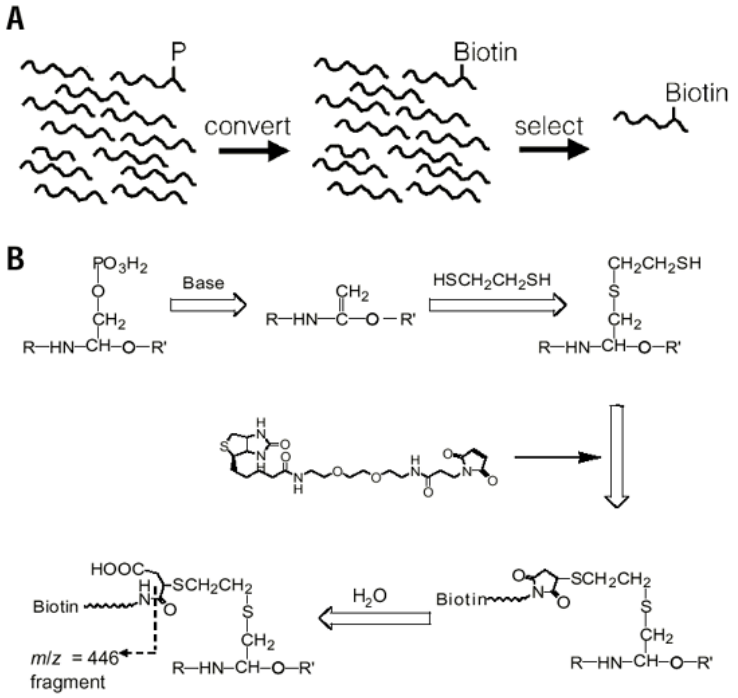

Scheme 6.3 Wavy lines represent proteins or peptides. Wavy line with "P" designates phosphoprotein or phosphopeptide (A); Scheme for chemical conversion of a phosphoserine residue to a biotinylated residue. Indicated by the dashed line is the position of the facile cleavage that produces the ion observed at *m/z* = 446 in the MS/MS spectra (B) (scheme adapted from[67]).

From the survey of enrichment methods emerges that no single technique is able to tackle the entire phosphoproteome. Some methods work in the direction of enriching only some species, like the antibodies for phosphotyrosine or the combination β-elimination/Michael addition selective for phosphoserine and phosphothreonine. Other methods, like calcium precipitation, SAX, SCX and HILIC, work better as pre-separation techniques to reduce sample complexity before more specific enrichment methods like IMAC, MOAC, SIMAC and PAC (Figure 2.6) but suffer from major limitations [45].

In general, a simple and straightforward strategy is desired, with few preparation steps and little sample handling in order to avoid loss of phosphopeptides. The efforts towards label free and unbiased quantification, synthesis of pSer imprinted polymer will be discussed in the current chapter and recognition properties of these materials will compare with phosphotyrosine (P2) imprinted polymer.

6.2 Synthesis of template

Fmoc-Ser(PO_3H_2)-OEt was synthesized from the symmetric phosphoramidite reagent Di-benzyl-N,N-diethylphosphoramidate [161, 162] and Fmoc-Ser-OEt was used as shown in the Scheme 6.4. Fmoc-Ser-OEt was synthesized from Fmoc-NHS ester and serine ethyl ester hydrochloride. Hydroxyl group of N and C protected serine was phosphorylated with tetrazole/phosphoramidite and subsequent oxidation of the resultant phosphate-triester intermediate with t-butyl hydroperoxide. Bis-protected phosphoserine has poor long-term stability because of beta-elimination with the loss of the phosphate group and formation of dehydroalaninyl derivatives. Both of the benzyl groups were removed by hydogenolysis using Pd-charcoal catalyst without purification of intermediate compound. Fmoc-Ser(PO_3H_2)-OEt compound was purified by silica gel column chromatography. The purity of the compound was checked by ^{1}H, ^{13}C, ^{31}P NMR and mass spectroscopy.

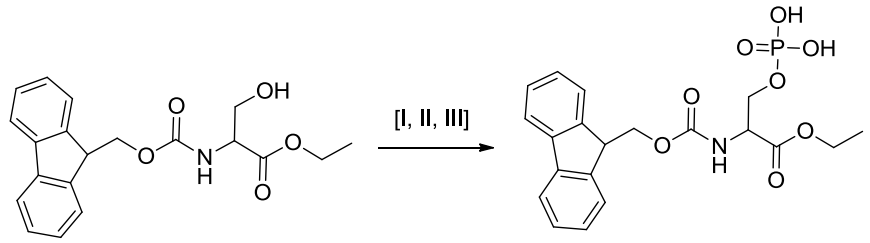

Scheme 6.4 Synthesis of Fmoc-pSer-OEt. [I] Di-benzyl-N,N-diethylphosphoramidate/tetrazole, [II] t-BuOOH, 0OC, [III] H_2/ 10% pd on Charcoal.

6.3 Synthesis and evaluation of imprinted polymers

Phosphoserine imprinted polymer (P3) was synthesized as similar protocol as phsophotyrosine (P2) imprinted polymer with the only difference of template Fmoc-Ser(PO_3H_2)-OEt. The difference in the P2 and P3 is the pre-polymerization complex between mono-urea monomer (FM) with Fmoc-pTyr-OEt and Fmoc-pSer-OEt respectively (Scheme 6.5). Otherwise, the polymerization compositions and conditions are identical for both the polymer except a difference of the template. The non-imprinted polymer (PN_2) was prepared identical way as imprinted polymer only by omission of template (described in section 5.9.1.3).

The template was removed with acidic MeOH by extraction with Soxhlet apparatus. The color change was observed in the imprinted polymer before and after removal of template (Figure 6.15

and work up described in section 6.10.4). Polymers in the size of 36-50 µm was packed in the LC column (30 mm x 4.6 (i.d.) and was evaluated imprinting properties. In the first test of evaluation, Fmoc-pSer-OH was injected onto the P3, P_N2 column in an acetonitrile rich mobile phase buffered with TFA. The P3 exhibited a strong affinity for the pSer derivative in contrast to P_N2 as shown in Figure 6.1. The base labile phosphoserine template was stable during polymerization conditions.

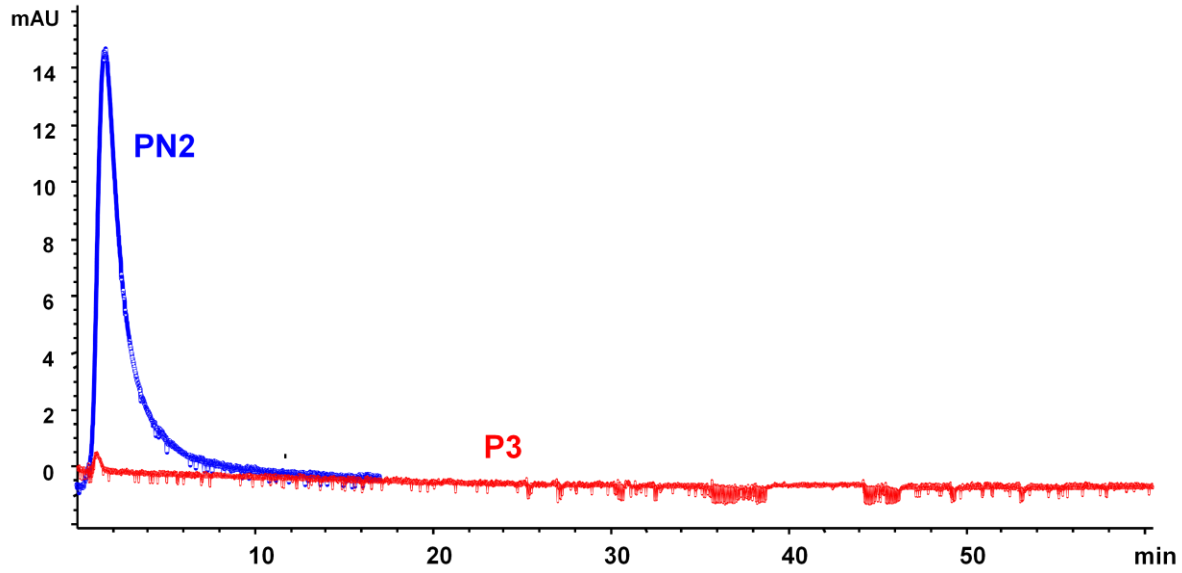

Figure 6.1 phosphoserine derivative was injected on to P3 and P_N2 polymer in acidic buffered mobile phase. (With extensive conditioning) Injection Volume: 5 µl, flow rate:0.5 ml/min, DAD@254 nm, analytes: 0.5 mM of Fmoc-pSer-OH in MeCN:water/95:5 (0.1% TFA).

Recognition properties of P2, P3 polymers were evaluated in term of selectivity towards pSer, pTyr containing amino acids and phosphopeptides will be discussed further in this chapter.

6.4 Comparison of phoshotyrosine (P2) and phosphoserine (P3) imprinted polymer

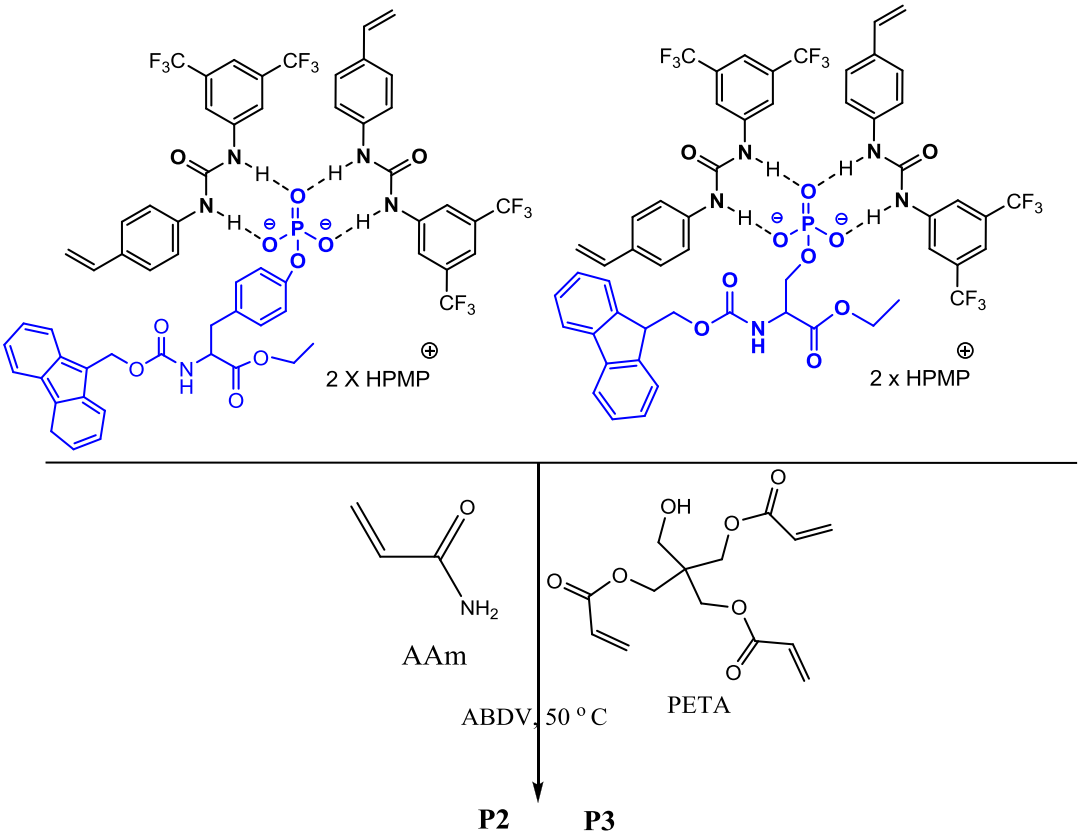

Scheme 6.5 Proposed prepolymerization complex formed between FM with Fmoc-pTyr-OEt (P2) Fmoc-pSer-OEt (P3) and the procedure for the preparation of imprinted polymers and corresponding non-imprinted polymer (P_N2).

6.5 Polymer Morphology

The polymers P2 and P3 exhibit no porosity in the dry state. Thus, the nitrogen sorption technique does not show the pore size distributions and morphologies of the P2 and P3 materials in dry state. For this purpose, the porosity in the swollen state has investigated by inverse size exclusion chromatography (ISEC), providing the exclusion volume for polystyrene standards of known molecular radii.

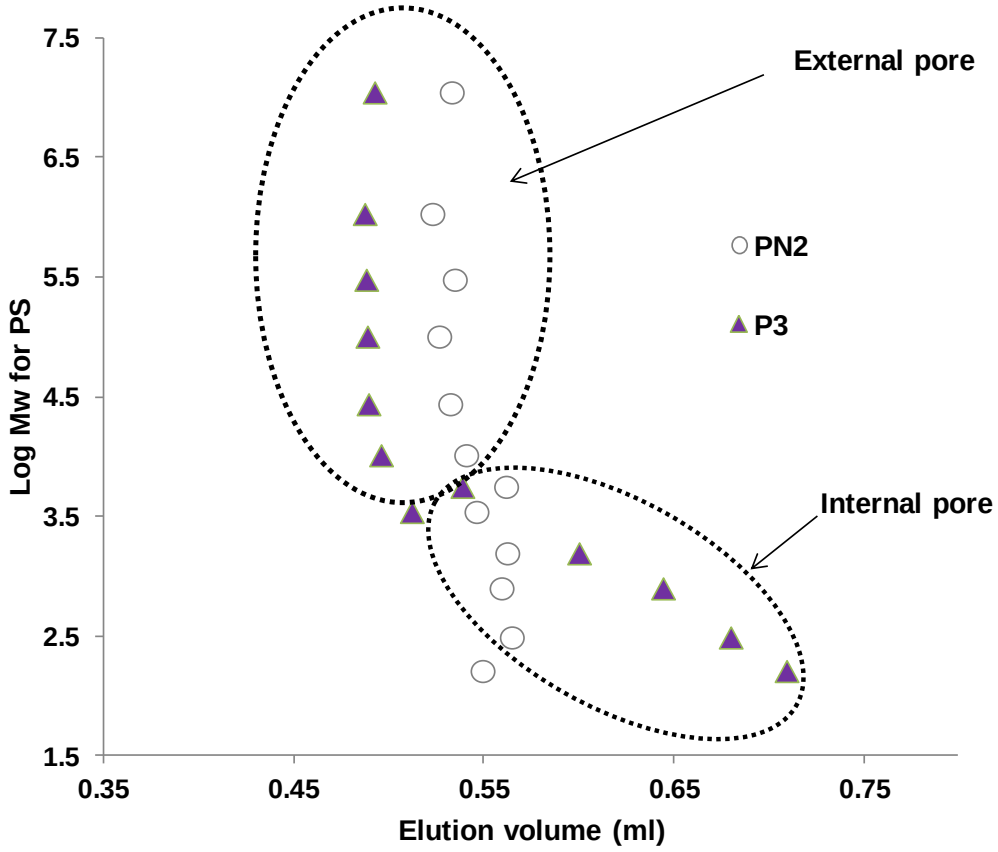

Figure 6.2 ISEC plot or plot of the logarithm of the molecular masses of the polystyrene (PS) standards versus their retention volume for the imprinted (P3) and non-imprinted column (P_N2).

6.5.1 Inverse Size Exclusion Chromatography

The P3 and P_N2 columns (30 mm x 4.6 (i.d.)) were used for the inverse size exclusion measurements. The measurements were performed using an Agilent 1100 HPLC system comprising a binary pump, an autosampler and a variable wavelength detector. THF was used as mobile phase at a flow rate of 0.2 mL/min. The wavelength of detection was again 254 nm. Polystyrene standards with a molecular weight ranging from 162 to 11,100,000 Da were from Polymer Standards Service, Mainz, Germany. 1 mg/mL solutions of polystyrene standards of different molecular weights were injected for the evaluation. Acetone was used as void marker. Retention volume of excluded molar mass is the volume corresponding internal and external pore zones in the calibration curves. The logarithm of the molecular masses of the polystyrene standards versus their elution volume for the imprinted (P3) and corresponding non-imprinted

column (P_N2) is plotted and denoted as ISEC plot [163]. Polymer P3 was observed two kinds of pores external pores and internal pores; however non-imprinted polymer P_N2 showed only one kind of pores in the region of the external pore as shown in Figure 6.2. The difference in the pore system between P3 and non-imprinted polymer P_N2 is related to the template effect.

6.6 HPLC Evaluations

In the first step of evaluation, slurry-packed into HPLC columns (30 mm x 4.6 (i.d.) mm) from polymer P2, P3 and P_N2 have taken for evaluation towards Fmoc derivatives of amino acids. For comparing imprinting efficiency and discriminative behaviour of all analytes, washing and equilibrating conditions were kept same for all the columns. Binary mixture of mobile phases of MeCN and H_2O buffered with either acid (TFA) or base (TEA) was used for chromatography

The first step of evaluation, 5 µl of 0.5 mM of Fmoc derivatives was injected onto the column with a flow rate of 0.5 mL/min in mobile phase MeCN:H_2O/93:7 (1% TEA). For basic mobile phase, the columns were washed with MeOH for 1 hour followed by equilibrated for 30 minutes with the mobile phase.

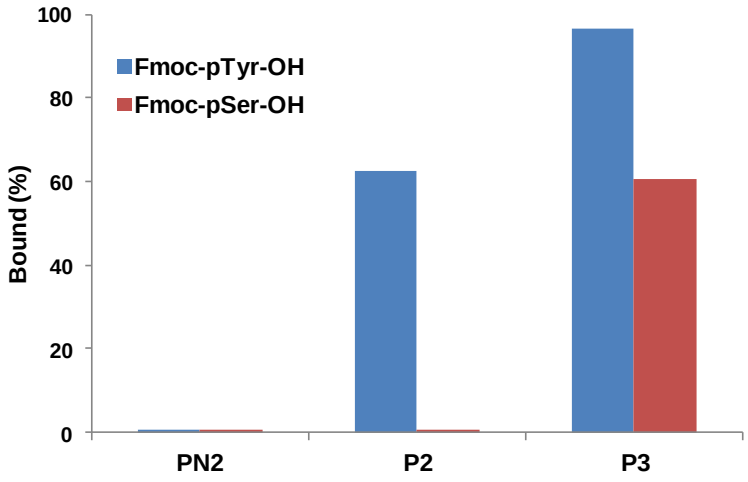

Figure 6.3 Fmoc derivatives were injected onto P2, P3 and P_N2 in the MeCN: Water/93:7 (1% TEA) mobile phases at 254 nm.

In the case of Fmoc derivative was fully or partially retained in the column P2 and P3 therefore, the results were plotted as percentage of bound amino acids versus column (Figure 6.3). In the basic mobile phase, pTyr and pSer analyte were injected in the P2, P3 column, expecting that

analyte are in dinionic form. The P2 have shown clear discrimination between pTyr and pSer amino acid, however P3 have shown selectivity to pSer amino acid over pTyr amino acid. pTyr analyte selectively retained in P2 but pSer anaylte showed a weak affinity. In contrast to P3, P2 have selective recognition for pTyr amino acid. This is related to differences in the structure of pTyr and pSer amino acid. In the second step of evaluation, Fmoc amino acid derivatives were injected onto column in MeCN:H_2O/95:5 (0.1% TFA) and MeCN:H_2O/50:50 (0.1% TFA) mobile phase with a flow rate of 0.5 mL/min. The columns were washed with acidic (0.1% TFA) MeOH for 1 hour followed by equilibrated for 30 minutes with mobile phase before injecting the analyte. Retention factor (k) for the analyte was calculated by using acetone as void marker.

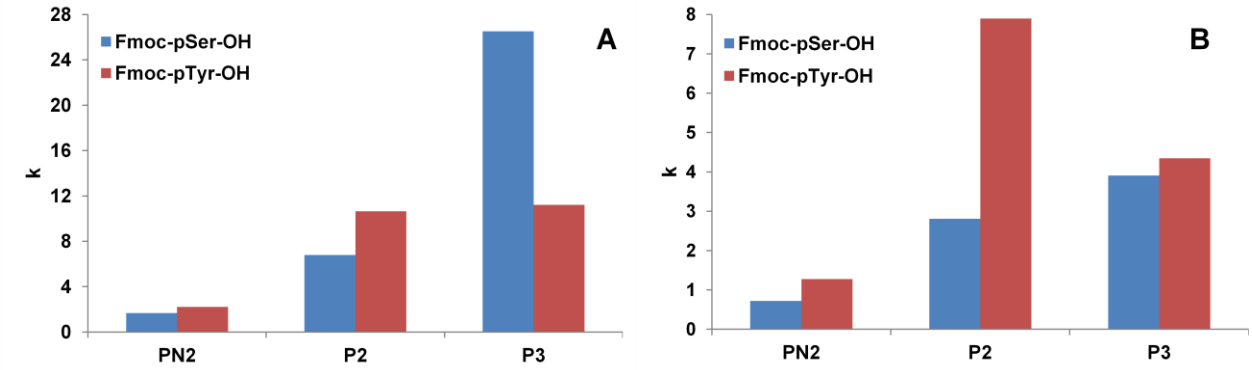

Figure 6.4 Retention factor (k) of Fmoc acids injected onto in P2, P3 and P_N2 column in mobile MeCN: Water/95:5 (0.1% TFA) (A) and MeCN: Water/50:50 (0.1% TFA) (B).

The polymer P2 and P3 have shown a good imprinting effect in the MeCN:H_2O/95:5 (0.1% TFA) and MeCN:H_2O/50:50 (0.1% TFA mobile phase (Figure 6.4). In organic mobile phase P3 have shown relatively superior imprinting effect compared to P2 but in aqueous mobile phase, P2 have relatively superior imprinting effect (Figure 6.4). P3 have a strong imprinting efficiency compared to P2 in organic rich mobile phase. In aqueous rich mobile phase (MeCN:H_2O/50:50 (0.1% TFA)), P2 have a strong imprinting efficiency compared to P3. In case of aqueous mobile phase, overall imprinting properties were reduced compared to organic mobile phase (Figure 6.4B). The reason is that H_2O competes with amino acids during the rebinding process.

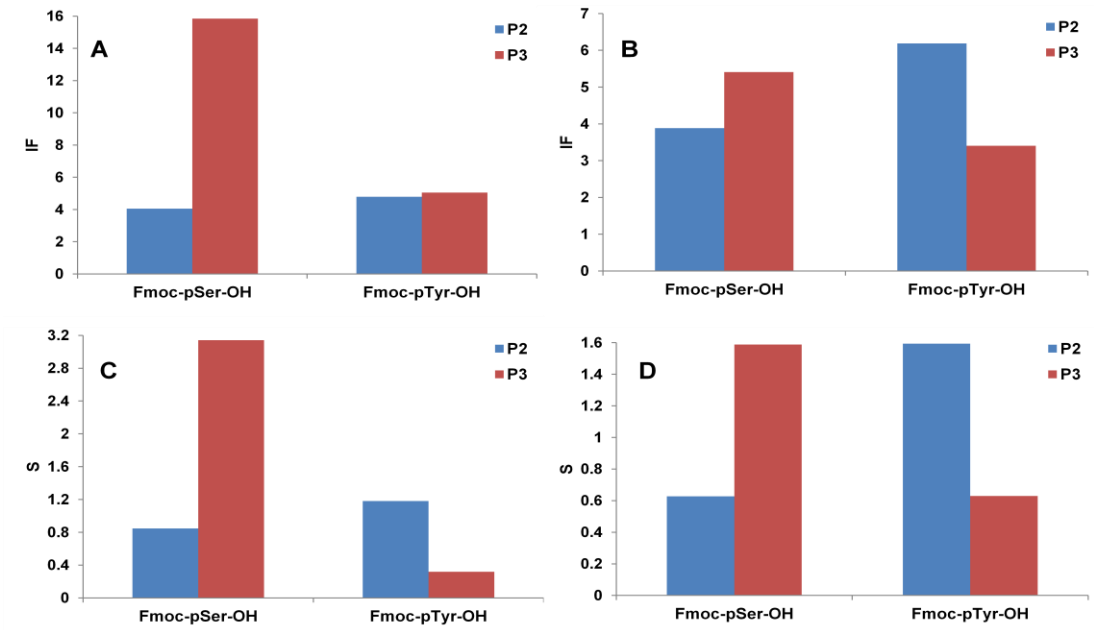

Figure 6.5 Retention factor (k) and specific selectivity factor (S) of Fmoc acids injected onto in P2, P3 and P_N2 column in mobile MeCN: Water/95:5 (0.1% TFA) (A,C) and MeCN: Water/50:50 (0.1% TFA) (B, D).

Further these imprinting properties were evaluated by calculating imprinting factor (IF) (Eq 1.3) and specific selectivity factor (S) (Eq.1 4). Specific selectivity factor (S) is the ratio of imprinting factor for two different substrate $S = IF_1/IF_2$. It is conventional to put a higher value in the numerator (which is usually imprinted substrate) and the lower value of the denominator and highly depend on the concentration of analyte. In this current study, Specific Selectivity Factor (S) has evaluated as the ratio of the IF of amino acids for sake of comparison (Figure 6.5). In 50:50/MeCN:Water (0.1% TFA) found that specific selectivity factor (S) for Fmoc-pTyr-OH and Fmoc-pSer-OH to P2 and P3 column are exactly same (1.5) respectively (Figure 6.5D).

6.7 Solid phase extractions

6.7.1 Optimization of Loading Solvents

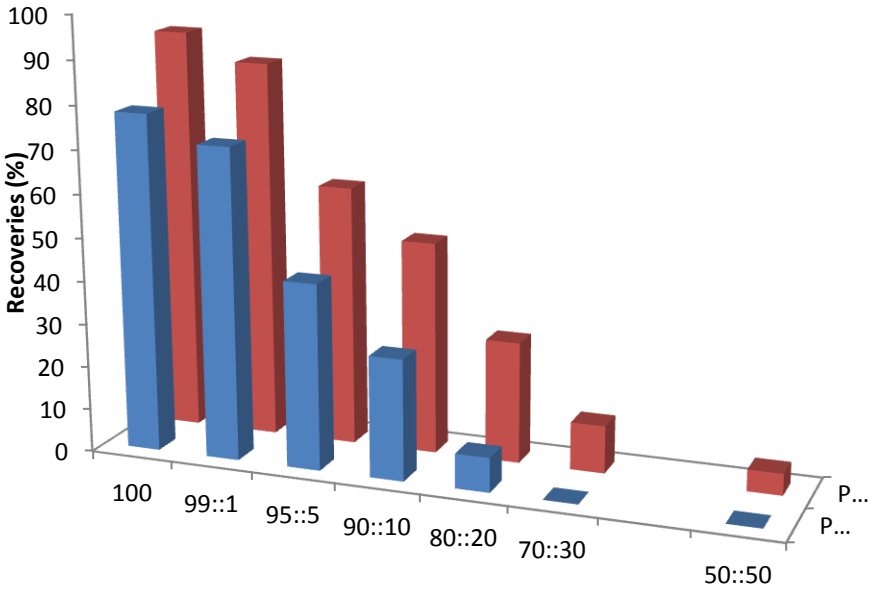

Figure 6.6 Recoveries obtained from P3 and P_N2 for VpSI after percolation 5 µg/mL of 1 ml 100% MeCN solution and subsequent washing using 0.5 mL of the MeCN:Water/99:1 mixture.

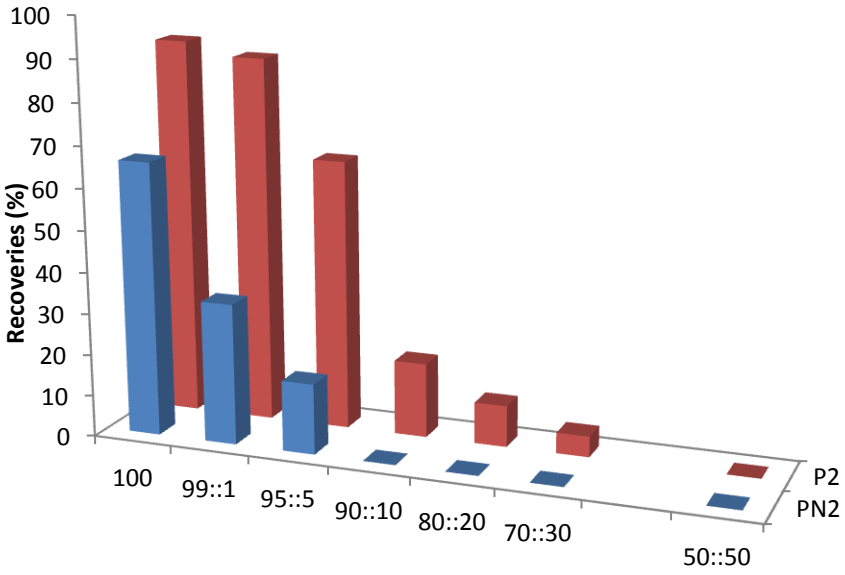

Figure 6.7 Recoveries obtained from P2 and P_N2 for VpYI after percolation of 1 mL 100% MeCN solution and subsequent washing using 0.5 mL of the MeCN:Water/99:1 mixture.

The nature of loading solution has a remarkable influence on the affinity of target analytes. The peptides VpYI and VpSI was loaded using a binary mixture of MeCN/H_2O and found that as the increase of H_2O in the loading solvent have better difference in the imprinted and non-imprinted polymer (Figure 6.6 and Figure 6.7). There is minor recovery found from MIP and NIP above the 50% H_2O in the loading step. In the mixture of MeCN:H_2O up to 20% water in loading condition found good recoveries with better difference in the MIP and NIP. This loading condition can be applied to further SPE study.

6.7.2 Selectivity Study

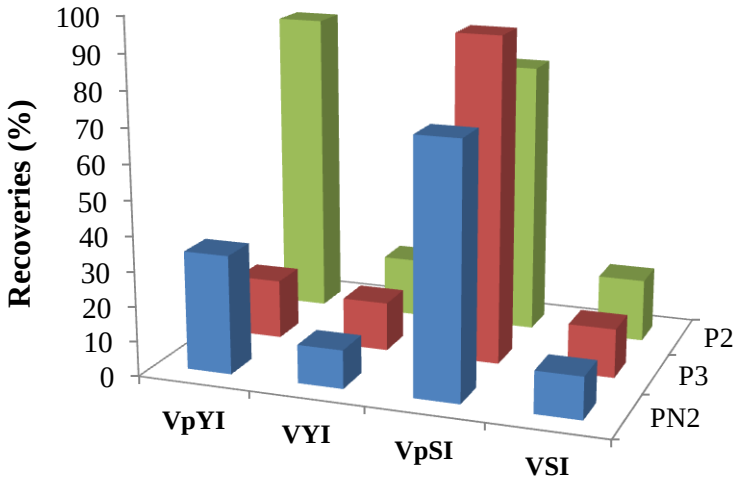

Figure 6.8 Recoveries obtained in all the polymers tested for VpYI, VYI, VpSI, VSI after percolation 5 µg/mL of 1 mL 100% MeCN solution and after washing with 0.5 mL of 99:1 /MeCN: mixture.

VpYI, VpSI and corresponding non-modified peptides (VYI, VSI) were dissolved in 1 mL of MeCN separately. These peptides were loaded on to these absorbent. Followed by washing step with 0.5 mL of MeCN:H_2O/99:1 mixture was found that p-Tyr peptide has selectively recovered from the P2 polymer. The VpSI peptide bound non-specifically on P2, P3 and P_N2, the selectivity can be obtained by optimizing the washing solvent. P3 have a marginally higher recovery of pSer peptide over P2, P_N2. However, there is minor recovery for the non-modified peptides VYI, VSI from all absorbents.

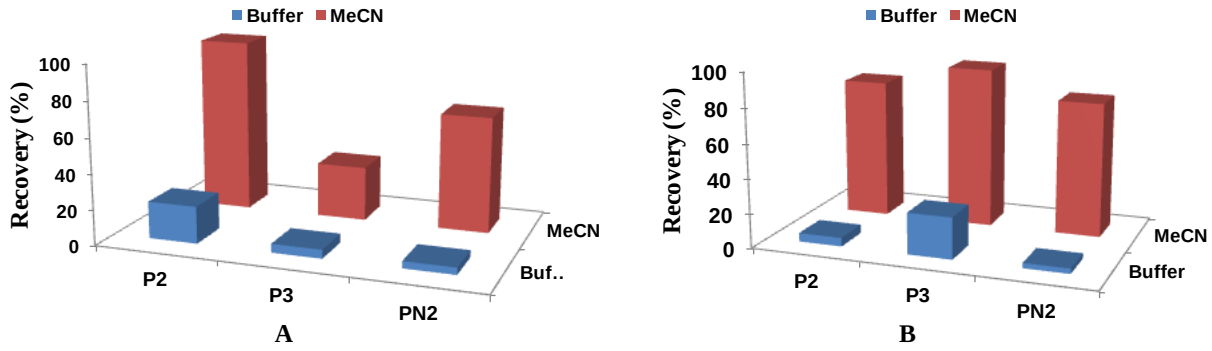

Figure 6.9 Recoveries obtained in all the polymers for VpYI (A); VpSI (B) after percolation 5 µg/mL of 1 mL loading solution of 100% AcN or 100% NH_4CO_3 buffer without washing step.

In order to study the retention behavior of the peptides in the organic and aqueous mobile phase, pY and pS tripeptide was spiked in MeCN and NH_4CO_3 buffer. These samples were subsequently loaded on the absorbent. It was found that in the NH_4CO_3 buffer, pTyr and pSer peptides were selectively recovered from P2 and P3 respectively although peptide recovery was less than 50% whereas no recovery of these peptides was found from non-imprinted column.

6.7.3 Sample Loading Volume

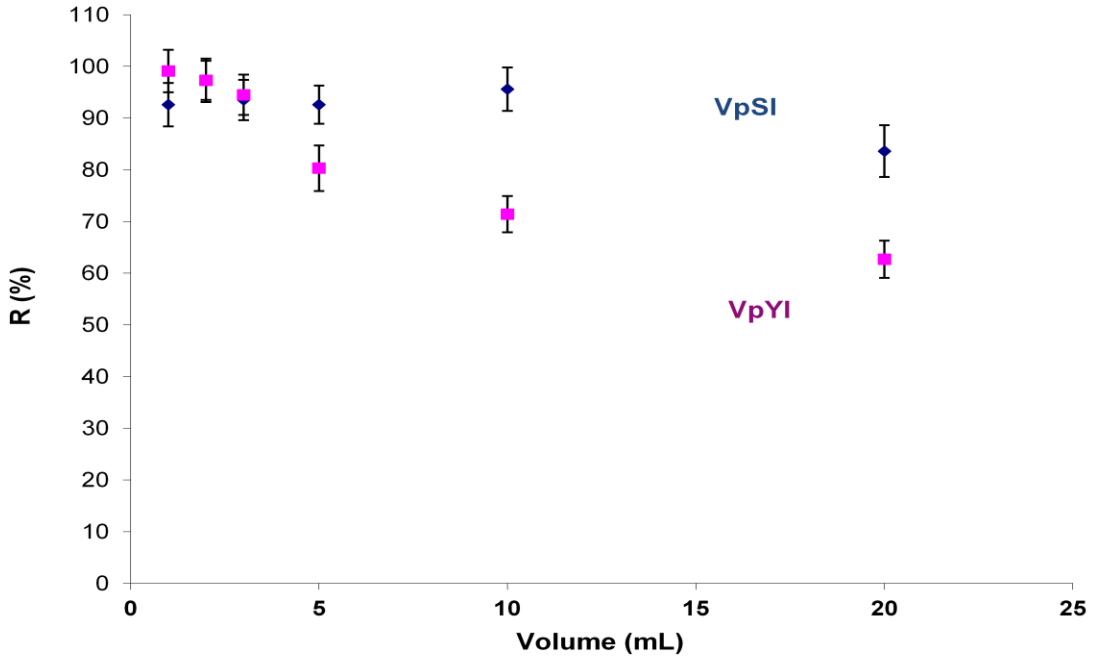

Figure 6.10 Recoveries obtained in MIPs for P2 and P3 with increasing amounts of the loading volume VpYI and VpSI peptides.

The influence of sample volume on the recovery of peptide VpYI and VpSI was investigated in the range from 1 mL to 20 mL. For this reason, the peptide was spiked in the MeCN solution was loaded on the column with flow rate of 0.5 mL/min. As shown in the Figure 6.10, there is no significant loss of peptide even after loading in the 20 mL of MeCN and corresponding recovery is in the range of 70 to 90 percentages. This result showed that MIP based absorbent has excellent capacity for the peptides.

Since goal of this work is the enrichment of pTyr and pSer modified peptides from biological complex samples, sample volume is important step can be useful for direct loading of biological sample in organic solvent after cell lysis for real life application.

6.8 Human cell lysate spiking experiments

To further check selectivity and specificity, mono and multi-phosphorylation at pTyr and pSer containing 10 peptides were spiked in the SH-SY5Y human dopaminergic neuroblastoma cell

lysate (Table 6.1). 8 µl (8 pmol) peptides have spiked in (27,5 µg proteins digested by trypsin in 20 µl H_2O) cell lysate. This mixture was diluted up to 2 mL with organic solvent (1980 µl MeCN + 0.1% TFA) and further used for offline solid phase extraction (SPE). Approximately 1 mg of pTyr (P2) and pSer (P3) imprinted sorbent was packed in the micro column (Figure 4.7). The self-made micro column was prepared using pipette tip. Lower end of the tips was packed with C18 plug prior to MIP sorbent. In evaluation, simple loading and two elution steps were utilized to check efficiency of SPE method. In elution steps, (100 µl) MeOH-0.1% TFA was used. Two elution steps were used in such a way that in the first elution, loosely bound peptide elute out and second elution step, strongly bound peptide elute out. Eluted fractions was evaporated to dryness and re-dissolved in 10 µl of H_2O (0.1% TFA) and further masses of peptides were measured with MALDI-TOF/TOF-MS spectrophotometer (Figure 6.11).

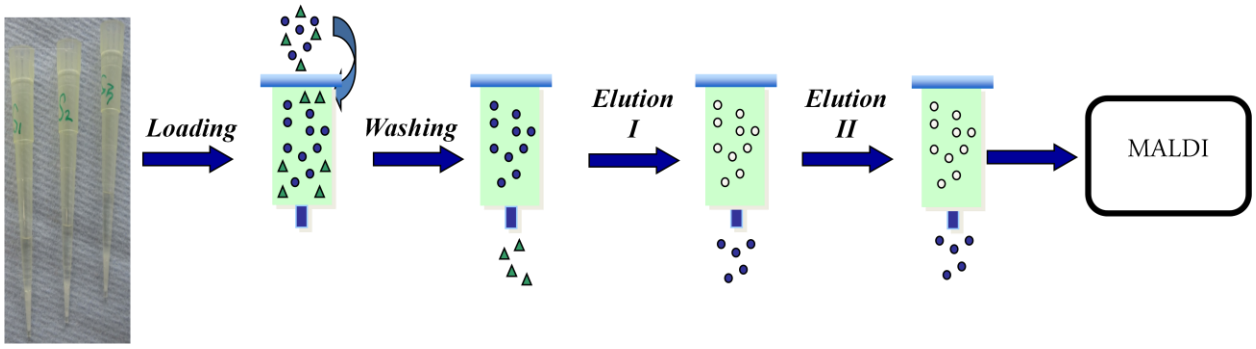

Figure 6.11 Schematic representation of offline solid phase extraction (SPE) using MIP based absorbent.

Table 6.1 Tyr and Ser-containing model peptides used for to probe the phospho- selectivity of the polymer.

No.	Peptide Sequence	Average Mass	modific -ations	Observed mass
1	DRVYIHPF	1046,54	Y	1046.8
2	DRV**pS**IHPF	1049.5	pS	1050.6
3	DRV**pY**IHPF	1126,51	pY	1126.7
4	TRDIYETDYYRK	1623,77	3Y	1623
5	TRDI**pY**ETD**pYpY**RK	1862,68	3pY	1862.9
7	GADDSYYTAR	1118,47	2Y	1118.6
8	GADDS**pYpY**TAR	1278,41	2pY	1278.6
9	GADDSY**pY**TAR	1198,44	YpY	1198.6
10	WWGSGPSGSGGSGGGK	1419,62	4S	1420.8
11	WWGSGP**pS**GSGG**pS**GGGK	1580,42	2S2PS	1580.8

Note: The phosphorylated peptides are indicated by the letter p; for example pY: phosphorylated tyrosine and pS: phosphorylated serine.

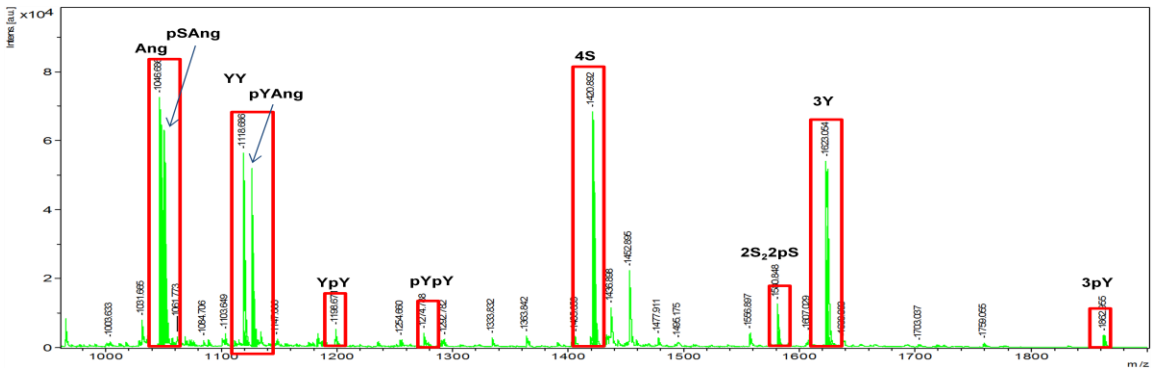

Figure 6.12 MALDI-TOF/TOF-MS spectra of mixture of standard peptides mentioned in Table 6.1.

In preliminary observations, pTyr and pSer imprinted materials showed high affinity and selectivity for pY and pS peptides in complex samples (lysate of SH-SY5Y neuronal cell line). It is possible to use biological samples like lysates with dilutions with organic solvent (for instance

MeCN) and directly use for solid phase extraction experiments. In these experiments, two elution steps were used. In the first election, lightly bound peptide can elute out and in second elution, tightly bound pepide elute out. When these peptides were loaded on to polymers, masses and intensity from loading and elution fractions were measured using MALDI instrument (Figure 6.11).

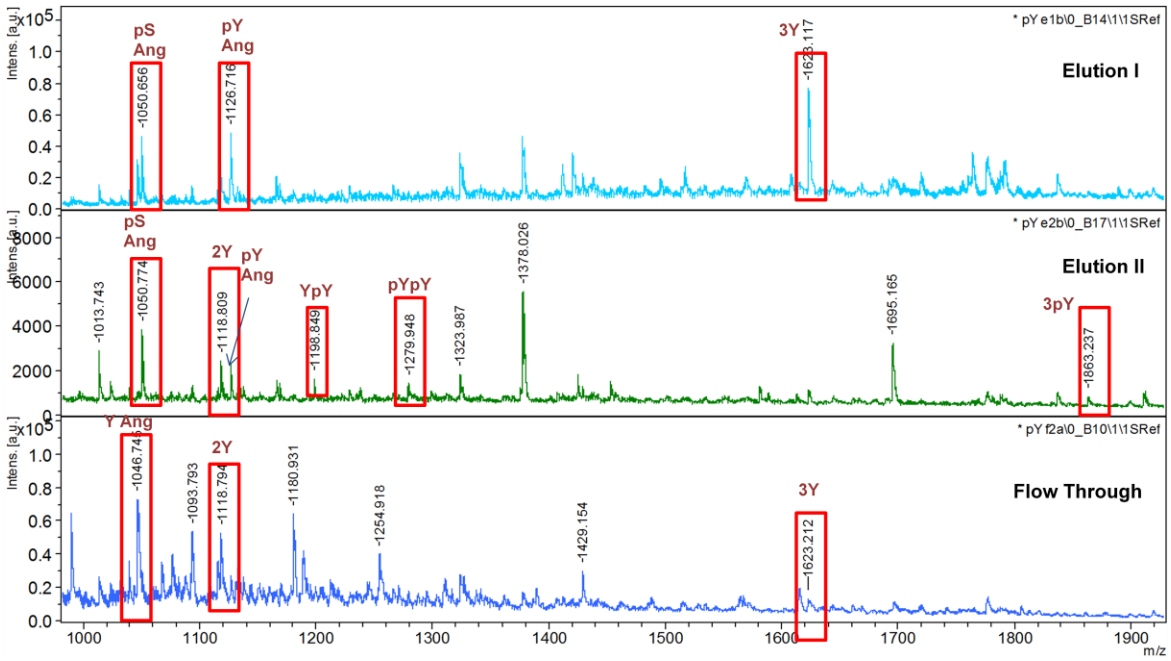

Figure 6.13 MALDI-TOF/TOF-MS spectra of peptide mixture spiked in after SPE from P2. (pY-imprinted) polymer.

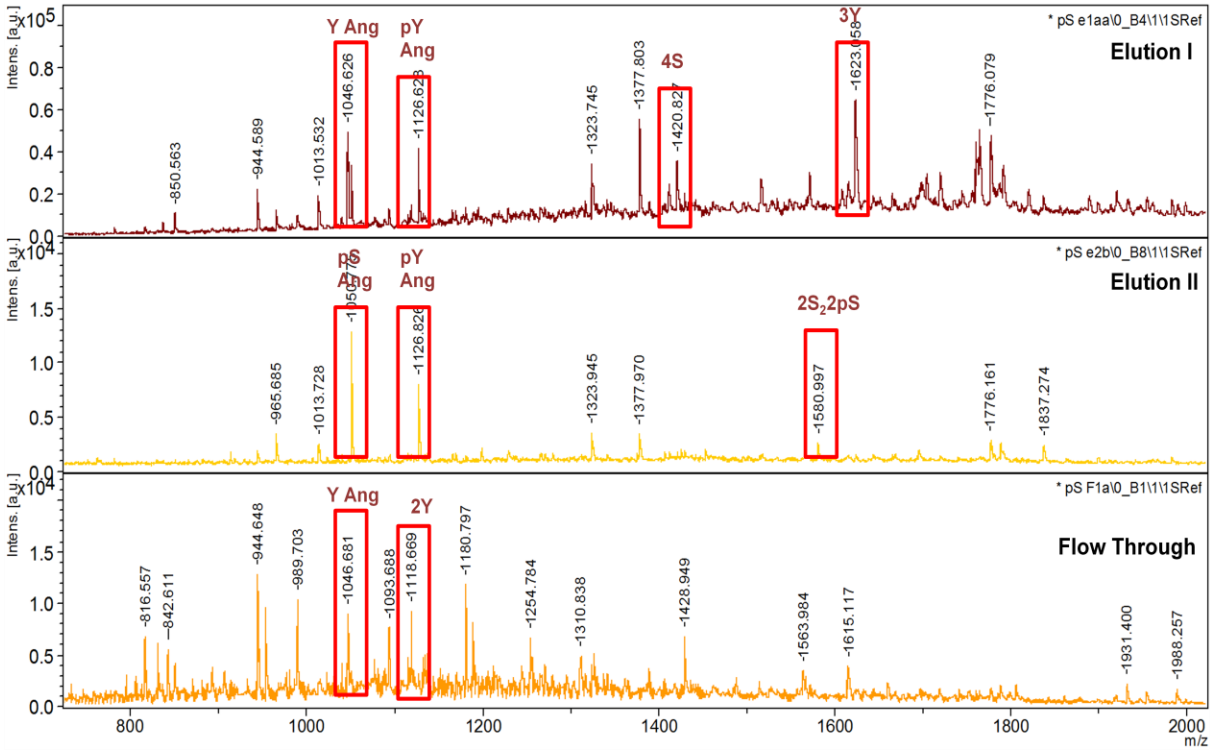

Figure 6.14 MALDI-TOF/TOF-MS spectra of peptide mixture spiked in after SPE from P3 (pS-imprinted) polymer.

These materials have shown high selectivity towards imprinting motifs (pTyr, pSer) containing peptides in the preliminary experiments. Non-modified peptides were found in the flow through from P2, P3 polymer (Figure 6.13 and Figure 6.14). The majority of mass peaks were obtained pTyr peptides from P2 and pSer peptides from P3 in the second elution step. This is very preliminary results showed a trend of the affinities of peptides towards materials. Further optimization of protocol needed for SPE washing conditions can show pTyr and pSer discrimination by imprinted polymers and may forward unique polymeric antibodies for selective discrimination.

6.9 Conclusion

A simple and straightforward approach for specific isolation of phosphotyrosine and phosphoserine has been developed based on MIP based absorbent and enrichment is based on pTyr or pSer. pTyr and pSer imprinted materials have shown high affinity and selectivity for pTyr and pSer containing peptides in complex samples, when (spiked with lysate of SH-SY5Y

neuronal cell line. With further optimization, the method may uniquely discriminate of pTyr and pSer modification and has the potential to apply large-scale phosphopeptide isolation.

6.10 Materials and methods

Fmoc-OSu, Serine ethyl ester hydrochloride (Ser-OEt HCl) from Bachem; Benzyl alcohol (99%) from Across Organics, N, N-diisopropylethyl amine (DIEA) and tert-butyl hydroperoxide 5.0-6.0M solution in decane, tetrazole solution from Fluka. VYI, VpYI, VpSI and VSI tripeptides was received from LifeTein USA and purity are 98.31%, 92.04%, 95.36% and 89.53% respectively.

GADDSYYTAR, GADDSpYpYTAR, GADDSpYYTAR and GADDSYpYTAR are received from LifeTein USA and purity are 89.14%, 93.89%, 87.68% and 92.88% respectively. WWGSGPSGSGGSGGGK, WWGSGPpSGSGGpSGGGK are gift samples received from Prof. Karl Mechtler from Institute of Molecular Pathology (IMP), Vienna, Austria.

DRVYIHPF Angiotensin II peptide was received from Sigma Aldrich, DRVpYIHPF phosphor-Angiotensin II Human peptide (purity 97%) is received from Calbiochem-Merck (Darmstadt, Germany). DRVpSIHPF peptide (purity 88%) received from LifeTein USA. The purity of above all these peptides is based on HPLC. The triply phosphorylated Insulin receptor peptide TRDIpYETDpYpYRK (pInsR), and the non-phosphorylated peptides TRDIYETDYYRK (InsR) are obtained from Mobitech (Göttingen, Germany).

6.10.1 Synthesis of N-(9-Fluorenylmethyloxycarbonyl) serine ethyl ester (Fmoc-Ser-OEt)

Fmoc-OSu (5 gm, 14.822 mmol) and serine ethyl ester hydrochloride (2.5139 gm, 14.822 mmol) weretaken in the 20 ml of dry dichloromethane and stirred under nitrogen atmosphere. The DIEA (2.579 gm, 14.86 mmol) were added to the reaction mixture at $0^{O}C$ and reaction mixture were stirred at room temperature more than 12 hrs and reaction mixture were washed with 1M HCl, Sat. $NaHCO_3$, water, brine and dried over Na_2SO_4. The solvent was evaporated and compound was precipitated from n-hexane. Yield 68.6% ^{1}H NMR (400MHz $CDCl_3$) δ 1.21-1.31 (t, 3H), 3.94-3.99 (d, 2H), 4.21 (m, 3H), 4.43-4.44 (m, 3H), 5.76-5.78 (d, 1H), 7.30-7.78 (m, 8H, Aromatic); ^{13}C NMR (100MHz $CDCl_3$) δ 14.28, 47.25, 56.22, 62.14, 63.52, 67.31, 120.12, 120.14, 125.20, 127.19, 127.22, 127.87, 141.41, 141.45, 143.77, 143.93, 156.38, 170.58; (LCMS) observed mass m/z: M+18 (355.14+18) 373.17.

6.10.2 Synthesis of Di-benzyl-N,N-diisopropylphosphoramidate

Di-benzyl-N,N-diisopropylphosphoramidate was synthesized according to procedure reported by Perich *et al.* [162] and Li *et al.* [164]. A solution of 0.02 mol of BzlOH and 0.04 mole of Et_3N in absolute Et_2O (20 ml) was added slowly to a solution of 0.01 mol of (diisopropylamino) dichlorophosphine in 10 ml of absolute diethyl ether such that the reaction temperature was maintained under 0^OC. After complete addition, was stirred at room temperature for 3 hours. The reaction mixture was washed 5% sodium bicarbonate and brine respectively. After dried with anhydrous Na_2SO_4, filtered and evaporated under reduced pressure. The crude product was obtained and used further reaction without purification (more than 90%, purity based on ^{31}P). ^1H NMR (400MHz $CDCl_3$) δ 1.20-1.22 (d, 12H), 3.66-3.75 (m, 2H); 4.67-4.89 (m, 4H); 7.24-7.38 (m, 10H) ^{13}C NMR (100MHz $CDCl_3$) 24.60, 24.67, 43.00, 43.12, 65.25, 65.43, 126.95, 127.19, 128.20, 139.45, 139.53; ^{31}P NMR ($CDCl_3$) δ 148.55.

6.10.3 Synthesis of N-(9-Fluorenylmethyloxycarbonyl)-O-Phosphoserine ethyl ester (Fmoc-Ser (PO_3H_2)-OEt)

(1.22 gm, 3.532 mmol) of (Di-benzyl-N,N-diisopropylphosphoramidate) phosphoramidate in 5 ml of anhydrous THF was added to a solution (0.5 gm, 1.40 mmol) of Fmoc-Ser-OEt and 9.38 ml, (0.45M in acetonitrile, 4.22 mmol) tetrazole in 15 ml of anhydrous THF under nitrogen. The resulting solution was stirred at room temperature for 12 hours tert-BuOOH (1 ml, 5-6M in decane, 5 mmol) was added to this mixture at $0^OC$and it was stirred to another 2 hours at 0 °C. This reaction was further stirred at room temperature another 1 hr. After aqueous workup, the residue was dried and dissolved in 30 mL ethanol, was added 0.5gm of 10% pd on carbon and stirred under hydrogen atmosphere more than 12 hrs. The catalyst was removed over celite and the residue was further purified with silica gel column chromatography eluting with chloroform:MeOH:Acetic acid / 98:2:1. 49% yield with 87% purity based on the ^{31}P NMR was obtained.; ^1H NMR, (400 MHz DMSO) d6; 1.15-1.20 (t, 3H); 4.10-4.32 (m, 6H); 4.87-4.89 (m, 1H), 5.66 (s, 1H), 7.33-7.91 (m, 8H, Aromatic), (100MHz, DMSO d6) ^{13}C NMR, 14.06, 46.58, 54.62, 60.97, 64.32, 66.02, 120.15, 125.32, 127.13, 127.69, 128.28; δ ^{31}P NMR (DMSO d6) δ 0.12 (s), δ ^{31}P NMR ($(CD3)_2CO+CD_3OD$) δ 0.66 (s) m/z (MALDI-TOF): observed m/z,

$M+K^+H^+$, M+2Na+, $M+Na^+K^+$, $M+3Na^+$ 475.01, 481.1, 497.2, 503.4 respectively; DESI-MS: M, $M+H^+$, $M+2H^+$, $M+3H^+$, 435.2, 436.12, 437.1 and 438.12 respectively.

6.10.4 Polymer preparation

Crushed monoliths: Imprinted polymers **P3** were prepared in the following manner. The bis-pentamethylpiperidine salt of Fmoc-pSer-OEt (template) (0.5 mmol), urea monomer (1 mmol), acrylamide (1mmol) and PETA (13.3 mmol) were dissolved in THF (5.6 mL). To the solution was added initiator ABDV (1% w/w of total monomers). The solution was transferred to a glass ampoule, cooled to 0^oC and purged with a flow of dry nitrogen for 10 minutes. The tubes were then flame-sealed while still under cooling and the polymerization initiated by placing the tubes in a thermostatted water bath pre-set at 50^oC. After 24 hour the tubes were broken and the polymers lightly crushed. They were thereafter washed 3 times with MeOH and extracted in a soxhlet-apparatus with methanol:0.1N HCl/50:50 for 24 hours. This was followed by further crushing and sieving, whereby the fraction from 36-50µm was used for packing the HPLC-columns to evaluate their binding properties. A non-imprinted polymer (**P_N2**) was prepared in the same way as described above, but with the omission of the template molecule from the pre-polymerization solution (Described in the previous chapters 4-5).

6.10.5 Solid phase extraction (SPE) of tripeptide

Solid-phase extraction cartridges (1mL), were packed with 20 mg of the pTyr imprinted (36-50 µm) P2, pSer imprinted (P3) and corresponding non-imprinted polymers (P_N2). The cartridges were equilibrated with 3 mL of loading solution and peptide stock solution (stock solution in water) was diluted with MeCN or buffer was percolated at a constant flow rate of 0.4 mL min^{-1} with the aid of a peristaltic pump. The cartridges were thereafter subjected to an elution step by percolating 300 µl of MeOH (2% TFA), diluted with 565 µl of water and were analyzed directly by reversed phase HPLC (The peptides were injected immediately after elution step because of stability reason). Quantification of reference was carried out by injecting 10 µl of stock solution after dilution with 300µl of MeOH and 555 µl of water. The cartridges were washed with MeOH (1% TFA) and re-equilibrated with 3 mL of loading buffer solution before reuse. In SPE experiments, loading solution and washing solution was not quantified with HPLC.

6.10.6 Reverse Phase HPLC method (tripeptides)

Chromatographic data was acquired with an HPLC 1100 system from Agilent Technologies that consisted of a quaternary pump, an autosampler and a diode array detector. Chromatographic separations of the peptides were performed using a Luna C18 (155 mm× 4.6mm I.D., 5µm) HPLC column protected by a C-18 guard column (4.0mm×3.0mm I.D., 5µm), both from Phenomenex (Torrance, CA, USA). The mobile phase composition resulting from combining solvent A (20:80 MeOH:Water (0.1% TFA)) and solvent B (80:20 Water:MeOH (0.1% TFA)) as 60:40 respectively. The flow rate was 1 mL/min and the column temperature was kept at room temperature 25°C. The injection volume was 100µl, and peptide VpYI, VYI, VpSI, VSI was eluted at retention time 6.6, 7.8, 6.3, 6.4 min respectively. The detector wavelength of diode array was set at 205nm for all the peptides.

6.10.7 Human cell lysate spiking offline SPE experiment

8 µl peptides (8 pmol) have spiked in (27,5 µg proteins digested by trypsin in 20 µl H_2O) cell lysate. This mixture was diluted up to 2 mL with organic solvent (1980 µl MeCN + 0.1% TFA) and further used for offline solid phase extraction (SPE). Approximately 1 mg of pTyr (P2) and pSer (P3) imprinted sorbent was packed into the micro column. The self-made micro column was prepared using pipette tip. The low end of the tip was packed with C18 plug prior to MIP Sorbent. In evaluation, sample loading and two elution steps were utilized to check efficiency of SPE method. Two elution steps of 100 µl of MeOH (0.1% TFA) were used. Eluted fractions was evaporated to dryness and re-dissolved in 10 µl of H_2O (0.1% TFA) and further masses of peptides were measured with MALDI-TOF/TOF-MS spectrophotometer.

6.10.8 MALDI-TOF/TOF-MS measurement

In order to identify the standard peptides, MALDI TOF/TOF instrument from Bruker Daltonics (MALDI Ultraflex II) was used to measure the masses. DHB Matrix preparation: 20 mg/ ml DHB was dissolved in MeCN:Water/50:50 (0,1% TFA) and 1% phosphoric acid. (2 µl) DHB matrix was mixed with 6µl of SPE fraction) would be spotted on the anchorchip target. These spots were evaporated to dryness and the masses were measured using MALDI-TOF/TOF-MS. Before measurement, the instrument was calibrated with calibration strategy of

"interactive",calibration standards Y, pY, 3Y and 3pY, mass tolerance 10 ppm. After calibration, samples could be measured by "peptide mass fingerprint method" using laser frequency of 50Hz, relative intensity 66%. Laser shot each sample 4 times to achieve 400 shots of spectra. Mass range of 600-2100 Da was chosen to detect all singly charged peptides. Detection was performed under "Delayed Extraction" adjustment.

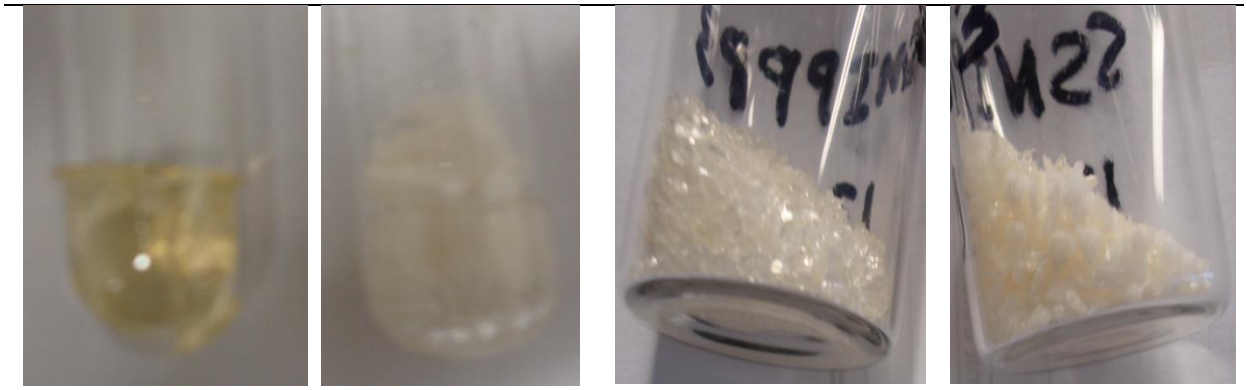

P3 (1) **P_N2 (1)** **P3 (2)** **P_N2 (2)**

Figure 6.15 The nature of imprinted and corresponding non-imprinted polymer before P3/P_N2 (1) and after extraction P3/P_N2 (2) of the Fmoc-pSer-OEt.

7 Outlook and Perspectives

In the present invention, MIPs was synthesized by using small amino acid templates and was used for selectively enriching phosphotyrosine, phosphoserine, and sulfotyrosine containing peptides from complex samples. These materials are under investigation for finding out unknown biomarkers from real samples in the collaborations with other research group. The present work can be extended in majorly two different directions 1) fundamental understanding of MIPs including synthesis in different formats and 2) applications.

MIPs prepared in this thesis have used for capturing short PTM peptide sequences but unable to capture bigger peptide sequences. This limitation can be overcome using an alternate synthetic template with larger size [165]. The synthetic templates can be designed to have PTM groups (mimicking side chains with phosphate and sulfate group etc.) and polymeric porogen. The presence of a PTM group of synthetic template can provide complementary recognition cavities in resultant material and polymeric porogen can be provide a pore volume within MIPs. The polymeric porogen can be chosen as linear or hyperbranched polymers which is comparable to the size and shape of the target peptides and proteins. This can be the general approach that larger peptide sequences and protein with these modifications can accessible to the imprinted sites of the MIP.

Further MIP material can be synthesized with enhanced mass transfer properties. This can be attempted via grafting of a thin film of the MIPs to the surface of porous silica particles [166, 167]. This approach can be useful to produce imprinted layer on various surfaces for ex. silica nanopartciles, magnetic beads or various sensing elements etc.

MIPs can be synthesized targeting for specific sequences flanking phosphorylation or sulfation site or sequence-generic phases for capturing phosphorylated and sulfated peptides from real samples. In future, this can be a cheaper alternative to as an antibody type enrichment material for early stage diagnosis of diseases like cancer, Parkinson etc.

If these recognized elements can be designed to bind specific proteins, a number of important applications in areas such as biotechnology (including downstream processing, sensors and diagnostics) can be foreseen.

8 Miscellaneous

8.1 Isothermal titration calriometery

Isothermal Titration Calorimetry (ITC) is a thermodynamic technique for monitoring any chemical reaction initiated by the addition of a binding component, and has become the method of choice for characterizing biomolecular interactions. When substances bind, heat is either generated or absorbed. Measurement of this heat allows accurate determination of binding constants (*K*), reaction stoichiometry (*n*), enthalpy (ΔH) and entropy (ΔS), thereby providing a complete thermodynamic profile of the molecular interaction in a single experiment [123, 168].

In ITC, a syringe containing a "ligand" solution is titrated into a cell containing a solution of the "macromolecule" at constant temperature. When ligand is injected into the cell, the two materials interact, and heat is released or absorbed in direct proportion to the amount of binding. As the macromolecule in the cell becomes saturated with ligand, the heat signal diminishes until the only background heat of dilution is observed.

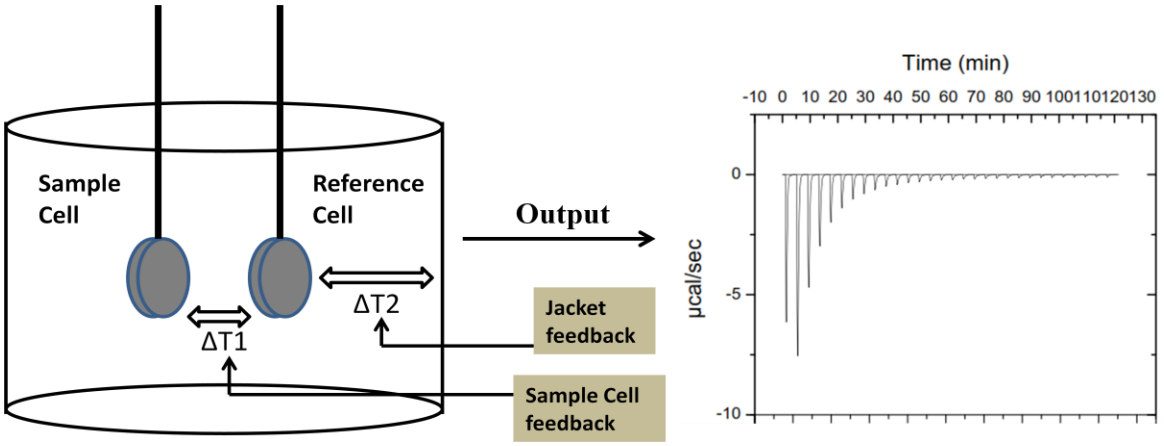

Figure 8.1 Representative diagram of ITC. (The power applied by the instrument to maintain constant temperature between the reference and sample cells is measured resulting in the instrument signal). Simulated ITC Raw Data showing the instrument response for a power compensation ITC instrument [168].

Typically, an ITC system a Cell Feedback Network (CFB) to differentially measure heat produced or absorbed between the sample and reference cell. Twin coin-shaped cells are

mounted in a cylindrical adiabatic environment, and connect to the outside through narrow access tubes.

A thermo-electric device measures the temperature difference between the two cells and a second device measures the temperature difference between the cells and the jacket. As chemical reactions occur in the sample cell, heat is generated or absorbed. The temperature difference between the sample and reference cells ($\Delta T1$) is kept at zero by the addition of heat to the sample or reference cell, as appropriate, using the CFB system. The raw signal in the power compensation calorimeter is the power (µcal/sec) applied to the control heater that is required to keep the calorimeter cell from changing temperature as a function of time. The heat change is then simply calculated by integrating the heater power over the time of the measurement.

8.2 ^{1}H-NMR titrations

The NMR characterization of functional monomer-guest molecule is the direct evidence for the formation of non-covalent interactions between the two entities [123]. Here, the ^{1}H-NMR titration was performed by following the Complexation Induced Shift (CIS) of the urea protons upon addition of increased concentrations of the guest molecule as followed: All ^{1}H-NMR titrations were performed in DMSO-d6. Association constants (K) for the interactions between hosts and guests were determined by titrating an increasing amount of guest (e.g. tetrabutylammonium benzoate) in a constant amount of functional monomer. The concentration of functional monomer was 1mM and the amounts of added guest were 0, 0.25, 0.5, 0.75, 1, 2, 4, 6 and 10 equivalents, respectively. The complexation induced shifts ($\Delta\partial$) of the host urea protons were followed and titration curves were then constructed of $\Delta\partial$ versus guest concentration. The raw titration data were fitted to a 1:1 binding isotherm, described in the equation below (Eq 1.1) by nonlinear regression using MicrocalTM Origin 6.0 from which the association constants could be calculated.

$$\Delta\partial = \frac{K_C.[M]}{1 + K_C[M]}.\Delta_{TM} \qquad \text{Eq.1 1}$$

Where $\Delta\partial$ is the CIS, [M] is the concentration of "free" monomer, Δ_{TM} is the CIS at 100% complexation between template and monomer, and K_C is the binding constant.

In order to determine the stoichiometry of a complex formed in solution, meaning the number of host and guest units taking part in a single complex molecule, or confirm an expected ratio of

host:guest, a Job plot needs to be prepared [123]. The experimental design will be explained through the study of the complex formed between urea-based monomer and TBA-PPA. Job plot was used to determine the complex stochiometry between host (FM) and guest (TBA salt of oxyanion) and graph is product of the mole fraction of functional monomer (f_M) and CIS of H from functional monomer versus f_M shown in Figure 8.2.

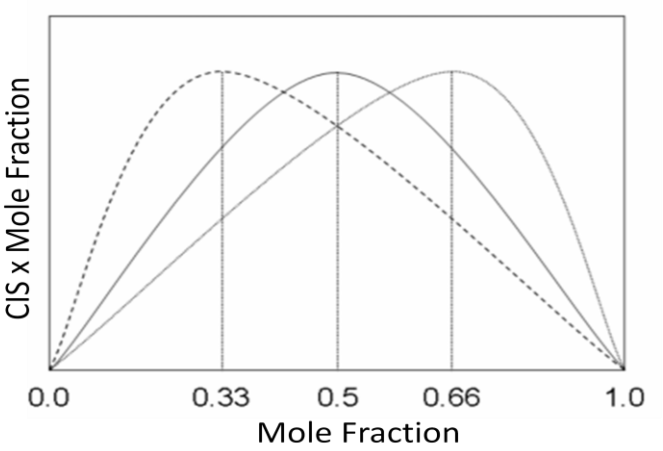

Figure 8.2 Schematic representation of Jobs plot for determining for complex stochiometry[123].

The samples are scanned and the mole fraction of the monomer is plotted against the CIS of a selected proton multiplied by the mole fraction of monomer expecting a bell-shaped curve. If the maximum of the curve is situated at X corresponding mole fraction (CIS × Xi=0.5, then a 1:1 complex is formed between the participating species. If the maximum is at 0.33 or 0.66, then a 1:2 or a 2:1 complex is formed respectively, and so on (Figure 8.2).

8.3 Elemental analysis

Analyses for carbon, hydrogen and nitrogen (CHN) were performed using a Heraeus Elemental Analyzer CHN-O-Rapid (Elemental-Analysis system, GmbH). About 10 mg of dried sample was submitted for elemental analysis. The experimental values obtained in this way were compared with the theoretical values calculated through Eq.1.3 given as follows:

$$\%X = M_{w(X)} \left(\frac{\sum_{j=1}^{k} N_{j,X} . n_j}{\sum_{j=1}^{k} n_j M_{w(j)}} \right) \times 100 \qquad \text{Eq.1 2}$$

where, *X* is the *C*, *H*, or *N* elements, $M_{w(X)}$ is the molecular weight of element *X*, n_j is the mole percentage of compound *j*, and $N_{j,X}$ and $M_{w(j)}$ are the number of *X* atoms and molecular weight of the compound *j*, respectively.

To calculate the percentage of each element in the polymer, we then need to consider all sources of each element.

$$\%X = \frac{(Number\ of\ element\ X\ in\ Monomer\ 1) \times (mole\ percent\ of\ Monomer\ 1) \times M_{w(element\ X)} + \ldots}{M_w} \times 100$$

or

$$\%X = \frac{M_{w(X)} \times \sum_{j=1}^{k} N_{j,X} . n_j}{M_w} \times 100 \qquad \text{Eq.1 3}$$

8.4 Imprinting properties

From the data collected, useful parameters such as retention, imprinting and separation factors are calculated and use to evaluate polymer affinity, cross reactivity and other features of the molecularly imprinted polymers.

In order to determine the imprinting factor (*IF*) the retention factor (*k*) of an analyte must be calculated for MIP and NIP

$$k = \frac{t_R - t_0}{t_0} \qquad \text{Eq.1 4}$$

Where t_R and t_0 are the retention time of the analyte and the void marker (acetone, unless otherwise mentioned), respectively. Thus,

$$IF = \frac{k_{MIP}}{k_{NIP}} \qquad \text{Eq.1 5}$$

The Specific Selectivity Factor (S), for two analytes *A* and *B* is defined by the ratio of their imprinting factor, IF_A and IF_B , respectively.

$$S = \frac{IF_A}{IF_B}$$ Eq.1 6

8.5 Binding Isotherms

Adsorption isotherms can yield important information concerning binding energies, modes of binding and site distributions in the interactions of small molecule ligands with receptors [169]. In the batch rebinding studies, a soluble ligand interacts with the binding sites in a solid adsorbent, i.e. the MIP or NIP. The adsorption isotherms are then simply plots of the equilibrium concentration of bound ligand versus the concentration of free ligand.

The isotherms can be fitted using various models depending on the range of concentrations investigated and the heterogeneity of the binding sites [170]. Due to the properties of the MIPs investigated in this work, and bi-Langmuir isotherm model has been used to fit the isotherms.

The mono-Langmuir equation have shown below

$$q^*(C) = \frac{a_1.C}{1 + b_1.C}$$ Eq.1 7

The bi-Langmuir isotherm equation have shown below.

$$q^*(C) = \frac{a_1.C}{1 + b_1.C} + \frac{a_2.C}{1 + b_2.C}$$ Eq.1 8

Where two distinct types of binding sites are considered to be present in the polymer, each with single binding constant, and their corresponding number given by the ratios a_1/b_1 and a_2/b_2.

8.6 Swelling tests

The Swelling properties of the polymers were studied as described in [171]. NMR tubes were filled during intermittent vibrations up to 1 cm (142 µl) with dry polymer particles and the solvent (1mL) added. The particles were allowed to equilibrate in the solvent for 24h, whereafter the volume of the swollen particles was measured. The volume swelling ration was calculated as:

$$Swelling\ ratio = \frac{bed\ volume\ swollen\ particle\ (V_s)}{bed\ volume\ dry\ particles\ (V_d)}$$ Eq.1 9

9 References

[1] P. D. Beer, P. A. Gale, *Angew. Chem. Int. Ed.Engl.* **2001**, *40*, 486.
[2] D. W. Christianson, W. N. Lipscomb, *Acc. Chem. Res.* **1989**, *22*, 62.
[3] A. Bianchi, K. Bowman-James, E. Garcia-Esapna, *Supramolecular Chemistry of Anions*, Wiley-VCH, New York, **1997**.
[4] A. E. Hargrove, S. Nieto, T. Zhang, J. L. Sessler, E. V. Anslyn, *Chem. Rev. 111*, 6603.
[5] J. W. Steed, J. L. Atwood, *Suparmolecular Chemistry*, Wiley, **2000**.
[6] J. M. Lehn, *Supramolecular Chemistry*, VCH, Weinheim, **1995**.
[7] R. Shannon, *Acta Crystallogr. Sect. A* **1976**, *32*, 751.
[8] E. A. Katayev, Y. A. Ustynyuk, J. L. Sessler, *Coord. Chem. Rev.* **2006**, *250*, 3004.
[9] M. D. Best, S. L. Tobey, E. V. Anslyn, *Coord. Chem. Rev.* **2003**, *240*, 3.
[10] A. Davis, I. Syed, K. McHugh, *Radiology Now* **2003**, *20*.
[11] J. L. Sessler, J. M. Davis, *Acc. Chem. Res.* **2001**, *34*, 989.
[12] J. L. Sessler, S. Camiolo, P. A. Gale, *Coord. Chem. Rev.* **2003**, *240*, 17.
[13] P. D. Beer, E. J. Hayes, *Coord. Chem. Rev.* **2003**, *240*, 167.
[14] D. M. Perreault, L. A. Cabell, E. V. Anslyn, *Bioorg. Medicinal. Chem.* **1997**, *5*, 1209.
[15] K. A. Schug, W. Lindner, *Chem. Rev.* **2004**, *105*, 67.
[16] P. Blondeau, M. Segura, R. Perez-Fernandez, J. de Mendoza, *Chem. Soc. Rev.* **2007**, *36*, 198.
[17] P. J. Smith, M. V. Reddington, C. S. Wilcox, *Tetrahedron Lett.* **1992**, *33*, 6085.
[18] E. Fan, S. A. Van Arman, S. Kincaid, A. D. Hamilton, *J. Am. Chem. Soc.* **1993**, *115*, 369.
[19] P. A. Gale, S. E. Garcia-Garrido, J. Garric, *Chem. Soc. Rev.* **2008**, *37*, 151.
[20] T. Gunnlaugsson, M. Glynn, G. M. Tocci, P. E. Kruger, F. M. Pfeffer, *Coord. Chem. Rev.* **2006**, *250*, 3094.
[21] V. Amendola, M. Bonizzoni, D. Esteban-GÃ³mez, L. Fabbrizzi, M. Licchelli, F. SancenÃ³n, A. Taglietti, *Coord. Chem. Rev.* **2006**, *250*, 1451.
[22] E. A. Katayev, Y. A. Ustynyuk, J. L. Sessler, *Coord. Chem. Rev.* **2006**, *250*, 3004.
[23] N. Busschaert, P. A. Gale, *Angew. Chem. Int. Ed.Engl.* **2013**, *52*, 1374.
[24] N. Busschaert, I. L. Kirby, S. Young, S. J. Coles, P. N. Horton, M. E. Light, P. A. Gale, *Angew. Chem. Int. Ed.Engl.* **2012**, *51*, 4426.
[25] L. Fabbrizzi, A. Poggi, *Chem. Soc. Rev.* **1995**, *24*, 197.
[26] D. A. Jose, D. K. Kumar, B. Ganguly, A. Das, *Tetrahedron Lett.* **2005**, *46*, 5343.
[27] T. R. Kelly, M. H. Kim, *J. Am. Chem. Soc.* **1994**, *116*, 7072.
[28] P. Bühlmann, S. Nishizawa, K. P. Xiao, Y. Umezawa, *Tetrahedron* **1997**, *53*, 1647.
[29] P. A. Gale, J. R. Hiscock, C. Z. Jie, M. B. Hursthouse, M. E. Light, *Chem. Sci.* **2010**, *1*, 215.
[30] C. Jia, B. Wu, S. Li, Z. Yang, Q. Zhao, J. Liang, Q.-S. Li, X.-J. Yang, *Chem. Commun.* **2010**, *46*, 5376.
[31] H. D. P. Ali, P. E. Kruger, T. Gunnlaugsson, *New J. Chem.* **2008**, *32*, 1153.
[32] M. Boiocchi, L. Del Boca, D. E. Gomez, L. Fabbrizzi, M. Licchelli, E. Monzani, *J. Am. Chem. Soc.* **2004**, *126*, 16507.
[33] V. Amendola, G. Bergamaschi, M. Boiocchi, L. Fabbrizzi, M. Milani, *Chem. Eur. J.* **2010**, *16*, 4368.
[34] R. Custelcean, P. Remy, P. V. Bonnesen, D.-e. Jiang, B. A. Moyer, *Angew. Chem. Int. Ed.Engl.* **2008**, *47*, 1866.

[35] S. K. Kim, N. J. Singh, S. J. Kim, H. G. Kim, J. K. Kim, J. W. Lee, K. S. Kim, J. Yoon, *Org. Lett.* **2003**, *5*, 2083.
[36] R. P. Dixon, S. J. Geib, A. D. Hamilton, *J. Am. Chem. Soc.* **1992**, *114*, 365.
[37] J. S. Mendy, M. L. Pilate, T. Horne, V. W. Day, M. A. Hossain, *Chem. Commun.* **2010**, *46*, 6084.
[38] W. P. Blackstock, M. P. Weir, *Trends. Biotechnol.* **1999**, *17*, 121.
[39] O. N. Jensen, *Nat. Rev. Mol. Cell. Biol.* **2006**, *7*, 391.
[40] E. S. Lander, *Science* **1996**, *274*, 536.
[41] M. W. H. Pinkse, P. M. Uitto, M. J. Hilhorst, B. Ooms, A. J. R. Heck, *Anal. Chem.* **2004**, *76*, 3935.
[42] C. Lohaus, A. Nolte, M. Blüggel, C. Scheer, J. Klose, J. Gobom, A. Schüler, T. Wiebringhaus, H. E. Meyer, K. Marcus, *J. Proteome Res.* **2006**, *6*, 105.
[43] S. Li, C. Dass, *Anal. Biochem.* **1999**, *270*, 9.
[44] T. E. Thingholm, T. J. D. Jorgensen, O. N. Jensen, M. R. Larsen, *Nat. Protocols* **2006**, *1*, 1929.
[45] T. E. Thingholm, O. N. Jensen, M. R. Larsen, *Proteomics* **2009**, *9*, 1451.
[46] P. Cohen, *Eur. J. Biol. Chem.* **2001**, *268*, 5001.
[47] C. Piggee, *Anal. Chem.* **2009**, *81*, 2418.
[48] G. Manning, D. B. Whyte, R. Martinez, T. Hunter, S. Sudarsanam, *Science* **2002**, *298*, 1912.
[49] P. T. W. Cohen, *J. Cell. Sci.* **2002**, *115*, 241.
[50] J. C. Venter, M. D. Adams, E. W. Myers, P. W. Li, R. J. Mural, G. G. Sutton, H. O. Smith, M. Yandell, C. A. Evans, R. A. Holt, J. D. Gocayne, P. Amanatides, R. M. Ballew, D. H. Huson, J. R. Wortman, Q. Zhang, C. D. Kodira, X. H. Zheng, L. Chen, M. Skupski, G. Subramanian, P. D. Thomas, J. Zhang, G. L. Gabor Miklos, C. Nelson, S. Broder, A. G. Clark, J. Nadeau, V. A. McKusick, N. Zinder, A. J. Levine, R. J. Roberts, M. Simon, C. Slayman, M. Hunkapiller, R. Bolanos, A. Delcher, I. Dew, D. Fasulo, M. Flanigan, L. Florea, A. Halpern, S. Hannenhalli, S. Kravitz, S. Levy, C. Mobarry, K. Reinert, K. Remington, J. Abu-Threideh, E. Beasley, K. Biddick, V. Bonazzi, R. Brandon, M. Cargill, I. Chandramouliswaran, R. Charlab, K. Chaturvedi, Z. Deng, V. D. Francesco, P. Dunn, K. Eilbeck, C. Evangelista, A. E. Gabrielian, W. Gan, W. Ge, F. Gong, Z. Gu, P. Guan, T. J. Heiman, M. E. Higgins, R.-R. Ji, Z. Ke, K. A. Ketchum, Z. Lai, Y. Lei, Z. Li, J. Li, Y. Liang, X. Lin, F. Lu, G. V. Merkulov, N. Milshina, H. M. Moore, A. K. Naik, V. A. Narayan, B. Neelam, D. Nusskern, D. B. Rusch, S. Salzberg, W. Shao, B. Shue, J. Sun, Z. Y. Wang, A. Wang, X. Wang, J. Wang, M.-H. Wei, R. Wides, C. Xiao, C. Yan, et al., *Science* **2001**, *291*, 1304.
[51] J. V. Olsen, B. Blagoev, F. Gnad, B. Macek, C. Kumar, P. Mortensen, M. Mann, *Cell* **2006**, *127*, 635.
[52] T. Hunter, B. M. Sefton, *Proc. Natl. Acad. Sci. USA.-Biologl. Sci.* **1980**, *77*, 1311.
[53] A. Ojida, Y. Mito-oka, M.-a. Inoue, I. Hamachi, *J. Am. Chem. Soc.* **2002**, *124*, 6256.
[54] A. Ojida, M.-a. Inoue, Y. Mito-oka, I. Hamachi, *J. Am. Chem. Soc.* **2003**, *125*, 10184.
[55] A. Grauer, A. Riechers, S. Ritter, B. König, *Chem. Eur. J.* **2008**, *14*, 8922.
[56] C. Schmuck, *Chem. Eur. J.* **2000**, *6*, 709.
[57] Y. Ishida, M.-a. Inoue, T. Inoue, A. Ojida, I. Hamachi, *Chem. Commun.* **2009**, *0*, 2848.
[58] S. Zhang, L. Han, C.-g. Li, J. Wang, W. Wang, Z. Yuan, X. Gao, *Tetrahedron* **2012**, *68*, 2357.

[59] S. Banerjee, B. König, *J. Am. Chem. Soc.* **2013**, *135*, 2967.
[60] S. Ewen, J. Steinke, R. Vilar, *Vol. 129*, Springer Berlin Heidelberg, **2008**, pp. 207.
[61] F. Monigatti, E. Gasteiger, A. Bairoch, E. Jung, *Bioinformatics* **2002**, *18*, 769.
[62] M. Farzan, T. Mirzabekov, P. Kolchinsky, R. Wyatt, M. Cayabyab, N. P. Gerard, C. Gerard, J. Sodroski, H. Choe, *Cell* **1999**, *96*, 667.
[63] J. W. Kehoe, C. R. Bertozzi, *Chem. Biol.* **2000**, *7*, R57.
[64] C. Seibert, T. P. Sakmar, *Pept. Sci.* **2008**, *90*, 459.
[65] H. Adam J, L. Julie A, M. Kevin L, Y. Yonghao, *Nat. Meth.* **2007**.
[66] M. Mann, S.-E. Ong, M. GrÃ¸nborg, H. Steen, O. N. Jensen, A. Pandey, *Trends. Biotechnol.* **2002**, *20*, 261.
[67] Y. Oda, T. Nagasu, B. T. Chait, *Nat Biotech* **2001**, *19*, 379.
[68] J. Rush, A. Moritz, K. A. Lee, A. Guo, V. L. Goss, E. J. Spek, H. Zhang, X. M. Zha, R. D. Polakiewicz, M. J. Comb, *Nat Biotechnol.* **2005**, *23*, 94.
[69] D. Balsved, J. R. Bundgaard, J. W. Sen, *Anal. Biochem.* **2007**, *363*, 70.
[70] Y. Yu, A. J. Hoffhines, K. L. Moore, J. A. Leary, *Nat. Meth.* **2007**, *4*, 583.
[71] A. Vaidya, B Lele, ,M. Kulkarni, R. Mashelkar, Council of Scientific and Industrial Research, US6420487B1, **2002**.
[72] B. Sellergren, *Molecular and Ionic Recognition with Imprinted Polymers, Vol. 703*, American Chemical Society, **1998**, pp. 49.
[73] B. Sellergren, *Techniques and Instrumentation in Analytical Chemistry, Vol. Volume 23*, Elsevier, **2000**, pp. 113.
[74] E. M. Yan and O. Ramström, (Ed.: M. Dekker), CRC, New York, **2005**.
[75] B. Sellergren, *Molecularly Imprinted Polymers: Man-Made Mimics of Antibodies and their Application in Analytical Chemistry, Vol. Volume 23*, Elsevier Science, Amstradam, **2000**.
[76] C. Alexander, H. S. Andersson, L. I. Andersson, R. J. Ansell, N. Kirsch, I. A. Nicholls, J. O'Mahony, M. J. Whitcombe, *J. Mol. Recogn.* **2006**, *19*, 106.
[77] A. Bossi, F. Bonini, A. P. F. Turner, S. A. Piletsky, *Biosensors. Bioelectron.* **2007**, *22*, 1131.
[78] V. Pichon, F. Chapuis-Hugon, *Anal. Chim. Acta* **2008**, *622*, 48.
[79] F. Puoci, G. Cirillo, M. Curcio, F. Iemma, U. G. Spizzirri, N. Picci, *Anal. Chim. Acta* **2007**, *593*, 164.
[80] P. Bures, Y. Huang, E. Oral, N. A. Peppas, *J. Control. Release* **2001**, *72*, 25.
[81] B. Sellergren, M. Lepistoe, K. Mosbach, *J. Am. Chem. Soc.* **1988**, *110*, 5853.
[82] Y. Shi, H. Lv, X. Lu, Y. Huang, Y. Zhang, W. Xue, *J. Mat. Chem.* **2012**, *22*, 3889.
[83] B. Sellergren, *Trends Anal. Chem.* **1999**, *18*, 164.
[84] A. Molinelli, J. O'Mahony, K. Nolan, M. R. Smyth, M. Jakusch, B. Mizaikoff, *Anal. Chem.* **2005**, *77*, 5196.
[85] F. Navarro-Villoslada, B. S. Vicente, M. C. Moreno-Bondi, *Anal. Chim. Acta* **2004**, *504*, 149.
[86] X. Shi, A. Wu, G. Qu, R. Li, D. Zhang, *Biomaterials* **2007**, *28*, 3741.
[87] P. A. G. Cormack, A. Z. Elorza, *J. Chromatogr. B* **2004**, *804*, 173.
[88] A. A. Vaidya, B. S. Lele, M. G. Kulkarni, R. A. Mashelkar, *J. Appl. Polym. Sci.* **2001**, *81*, 1075.
[89] N. W. Turner, C. W. Jeans, K. R. Brain, C. J. Allender, V. Hlady, D. W. Britt, *Biotechnol. Prog.* **2006**, *22*, 1474.

[90] A. Rachkov, N. Minoura, *Biochimica et Biophysica Acta (BBA) - Protein Structure and Molecular Enzymology* **2001**, *1544*, 255.
[91] A. Rachkov, M. Hu, E. Bulgarevich, T. Matsumoto, N. Minoura, *Anal. Chim. Acta* **2004**, *504*, 191.
[92] A. Rachkov, N. Minoura, *J. Chromatogr. A.* **2000**, *889*, 111.
[93] M. Quaglia, K. Chenon, A. J. Hall, E. De Lorenzi, B. Sellergren, *J. Am. Chem. Soc.* **2001**, *123*, 2146.
[94] A. J. Hall, L. Achilli, P. Manesiotis, M. Quaglia, E. De Lorenzi, B. Sellergren, *J. Org. Chem.* **2003**, *68*, 9132.
[95] A. J. Hall, M. Quaglia, P. Manesiotis, E. De Lorenzi, B. Sellergren, *Anal. Chem.* **2006**, *78*, 8362.
[96] M. M. Titirici, A. J. Hall, B. Sellergren, *Chem. Mater.* **2003**, *15*, 822.
[97] M. M. Titirici, B. Sellergren, *Anal. Bioanal. Chem.* **2004**, *378*, 1913.
[98] H. Nishino, C. S. Huang, K. J. Shea, *Angew. Chem. Int. Ed.Engl.* **2006**, *45*, 2392.
[99] Y. Hoshino, T. Kodama, Y. Okahata, K. J. Shea, *J. Am. Chem. Soc.* **2008**, *130*, 15242.
[100] Y. Hoshino, T. Urakami, T. Kodama, H. Koide, N. Oku, Y. Okahata, K. J. Shea, *Small* **2009**, *5*, 1562.
[101] Y. Hoshino, H. Koide, T. Urakami, H. Kanazawa, T. Kodama, N. Oku, K. J. Shea, *J. Am. Chem. Soc.* **2010**, *132*, 6644.
[102] G. Wulff, T. Gross, R. Schönfeld, *Angew. Chem. Int. Ed.Engl.* **1997**, *36*, 1962.
[103] A. G. Strikovsky, D. Kasper, M. Grün, B. S. Green, J. Hradil, G. Wulff, *J. Am. Chem. Soc.* **2000**, *122*, 6295.
[104] P. Manesiotis, Doctoral Thesis; Technical University Dortmund, **2005**.
[105] G. Wulff, K. Knorr, *Bioseparation* **2001**, *10*, 257.
[106] A. J. Hall, P. Manesiotis, M. Emgenbroich, M. Quaglia, E. De Lorenzi, B. Sellergren, *J. Org. Chem.* **2005**, *70*, 1732.
[107] U. Athikomrattanakul, C. Promptmas, M. Katterle, *Tetrahedron. Lett.* **2009**, *50*, 359.
[108] M. Emgenbroich, C. Borrelli, S. Shinde, I. Lazraq, F. Vilela, A. J. Hall, J. Oxelbark, E. De Lorenzi, J. Courtois, A. Simanova, J. Verhage, K. Irgum, K. Karim, B. Sellergren, *Chem. Eur. J.* **2008**, *14*, 9516.
[109] I. Lazraq, Doctoral Thesis;Technical university Dortmund, **2008**.
[110] R. Wagner, W. Wan, M. Biyikal, E. Benito-Pena, M. C. Moreno-Bondi, I. Lazraq, K. Rurack, B. Sellergren, *J. Org. Chem.* **2013**, *78*, 1377.
[111] Y. Zhang, D. Song, J. C. Brown, K. D. Shimizu, *Org. Biomol. Chem.* **2011**, *9*, 120.
[112] C. Lübke, M. Lübke, M. J. Whitcombe, E. N. Vulfson, *Macromolecules* **2000**, *33*, 5098.
[113] C. Gomy, A. R. Schmitzer, *J. Org. Chem.* **2006**, *71*, 3121.
[114] C. Gomy, A. R. Schmitzer, *Org. Lett.* **2007**, *9*, 3865.
[115] A. J. Hall, L. Achilli, P. Manesiotis, M. Quaglia, E. De Lorenzi, B. Sellergren, *J. Org. Chem.* **2003**, *68*, 9132.
[116] C. S. Wilcox, E. Kim, D. Romano, L. H. Kuo, L. B. Burt, D. P. Curran, *Tetrahedron* **1995**, *51*, 621.
[117] P. Manesiotis, A. J. Hall, M. Emgenbroich, M. Quaglia, E. D. Lorenzi, B. Sellergren, *Chem. Commun.* **2004**.
[118] J. L. Urraca, A. J. Hall, M. C. Moreno-Bondi, B. Sellergren, *Angew. Chem. Int. Ed.Engl.* **2006**, *118*, 5282.

[119] J. L. Urraca, M. a. C. Moreno-Bondi, A. J. Hall, B. Sellergren, *Anal. Chem.* **2006**, *79*, 695.
[120] S. Ewen, J. Steinke, R. Vilar, *Vol. 129*, Springer Berlin Heidelberg, **2008**, pp. 207.
[121] M. Kim, F. Sanda, T. Endo, *Macromolecules* **1999**, *32*, 8291.
[122] K. A. Connors, *Binding constants:the measurement of molecular complex stability*, Wiley, New York, **1987**.
[123] K. Hirose, *J. Inclusion Phenom. Macro.* **2001**, *39*, 193.
[124] V. Amendola, L. Fabbrizzi, L. Mosca, *Chem. Soc. Rev.* **2010**, *39*, 3889.
[125] C. Jin, M. Zhang, L. Wu, Y. Guan, Y. Pan, J. Jiang, C. Lin, L. Wang, *Chem. Commun.* **2013**, *49*, 2025.
[126] A. Pramanik, B. Thompson, T. Hayes, K. Tucker, D. R. Powell, P. V. Bonnesen, E. D. Ellis, K. S. Lee, H. Yu, M. A. Hossain, *Org. Biomol. Chem.* **2011**, *9*, 4444.
[127] D. Curiel, G. Sanchez, C. Ramirez de Arellano, A. Tarraga, P. Molina, *Org. Biomol. Chem.* **2012**, *10*, 1896.
[128] M. Kobaisi, M. Tate, C. Rix, T. Jakubov, D. Mainwaring, *Adsorption* **2007**, *13*, 315.
[129] J. J. Heymann, K. D. Weaver, T. A. Mietzner, A. L. Crumbliss, *J. Am. Chem. Soc.* **2007**, *129*, 9704.
[130] W. B. Huttner, K. M. Finn Wold, *Methods in Enzymol. Vol. Volume 107*, Academic Press, **1984**, pp. 200.
[131] B. Bodenmiller, L. N. Mueller, M. Mueller, B. Domon, R. Aebersold, *Nat. Meth.* **2006**, *4*, 231.
[132] C. Krog-Jensen, M. Christensen, M. Meldal, *Lett. Pept. Sci.* **1999**, *6*, 193.
[133] H.-G. Chao, M. S. Bernatowicz, P. D. Reiss, G. R. Matsueda, *J. Org. Chem.* **1994**, *59*, 6687.
[134] T. Tanaka, S. Tamatsukuri, M. Ikehara, *Tetrahedron Lett.* **1986**, *27*, 199.
[135] H.-G. Chao, M. S. Bernatowicz, C. E. Klimas, G. R. Matsueda, *Tetrahedron Lett.* **1993**, *34*, 3377.
[136] A. Ojida, Y. Mito-oka, K. Sada, I. Hamachi, *J. Am. Chem. Soc.* **2004**, *126*, 2454.
[137] S. Helling, S. Shinde, F. Brosseron, A. Schnabel, T. Müller, H. E. Meyer, K. Marcus, B. Sellergren, *Anal. Chem.* **2011**, *83*, 1862.
[138] J. G. Adamson, M. A. Blaskovich, H. Groenevelt, G. A. Lajoie, *J. Org. Chem.* **1991**, *56*, 3447.
[139] S. Han, C. M. Harris, T. M. Harris, H.-Y. H. Kim, S. J. Kim, *J. Org. Chem.* **1996**, *61*, 174.
[140] A. Alonso, J. Sasin, N. Bottini, I. Friedberg, A. Osterman, A. Godzik, T. Hunter, J. Dixon, T. Mustelin, *Cell* **2004**, *117*, 699.
[141] P. Onnerfjord, T. F. Heathfield, D. Heinegard, *J. Biol. chem* **2004**, *279*, 26.
[142] M. Salek, S. Costagliola, W. D. Lehmann, *Anal. Chem.* **2004**, *76*, 5136.
[143] K. F. Medzihradszky, Z. Darula, E. Perlson, M. Fainzilber, R. J. Chalkley, H. Ball, D. Greenbaum, M. Bogyo, D. R. Tyson, R. A. Bradshaw, A. L. Burlingame, *Mol. Cell. Proteomics* **2004**, *3*, 429.
[144] A. R. M. Bradbury, S. Sidhu, S. Dubel, J. McCafferty, *Nat. Biotech.* **2011**, *29*, 245.
[145] S. Futaki, T. Taike, T. Yagami, T. Ogawa, T. Akita, K. Kitagawa, *J. Chem. Soc.,Perkin Trans. 1* **1990**, 1739.
[146] Ueki M., Watanabe S., Yamanaka R., Ohta M., O. Okunaka., *Pept. Sci.* **2000**, *1999*, 117.
[147] M. Kempe, *Anal. Chem.* **1996**, *68*, 1948.

[148] X. Dong, H. Sun, X. Lu, H. Wang, S. Liu, N. Wang, *Analyst* **2002**, *127*, 1427.
[149] P. Manesiotis, C. Borrelli, C. S. A. Aureliano, C. Svensson, B. Sellergren, *J. Mat.Chem.* **2009**, *19*, 6185.
[150] P. Manesiotis, A. J. Hall, J. Courtois, K. Irgum, B. Sellergren, *Angew. Chem. Int. Ed.Engl.* **2005**, *117*, 3970.
[151] S. Shinde, A. Bunschoten, J. A. W. Kruijtzer, R. M. J. Liskamp, B. Sellergren, *Angew. Chem. Int. Ed.Engl.* **2012**, *51*, 8326.
[152] A. Bunschoten, J. A. W. Kruijtzer, J. H. Ippel, C. J. C. de Haas, J. A. G. van Strijp, J. Kemmink, R. M. J. Liskamp, *Chem. Commun.* **2009**, 2999.
[153] H. Choe, W. Li, P. L. Wright, N. Vasilieva, M. Venturi, C.-C. Huang, C. Grundner, T. Dorfman, M. B. Zwick, L. Wang, E. S. Rosenberg, P. D. Kwong, D. R. Burton, J. E. Robinson, J. G. Sodroski, M. Farzan, *Cell* **2003**, *114*, 161.
[154] M.Lederman, A. Penn-Nicholson, D.Mosier *JAMA* **2006**, *296*, 815.
[155] A. Bunschoten, Doctoral Thesis; Utrecht University, NL **2010**.
[156] E. G. Cormier, M. Persuh, D. A. D. Thompson, S. W. Lin, T. P. Sakmar, W. C. Olson, T. Dragic, *Proc. Natl. Acad. Sci. USA.* **2000**, *97*, 5762.
[157] J. H. Ippel, C. J. C. de Haas, A. Bunschoten, J. A. G. van Strijp, J. A. W. Kruijtzer, R. M. J. Liskamp, J. Kemmink, *J. Biol. Chem* **2009**, *284*, 12363.
[158] S. A. Johnson, T. Hunter, *Nat. Meth.* **2005**, *2*, 17.
[159] M. F. Byford, *Biochem J. 1991 Nov 15;280 (Pt 1):261-5.* **1991**, *280*, 261.
[160] D. T. McLachlin, B. T. Chait, *Anal. Chem.* **2003**, *75*, 6826.
[161] J. W. Perich, P. F. Alewood, R. B. Johns, *Phosphorus, Sulfur, and Silicon and the Related Elements* **1995**, *105*, 1.
[162] J. W. Perich, P. F. Alewood, R. B. Johns, *Aust. J. Chem.* **1991**, *44*, 233.
[163] M. Al-Bokari, D. Cherrak, G. Guiochon, *J. Chromatogr. A.* **2002**, *975*, 275.
[164] S. Z. Luo, Y. M. Li, Z. Z. Chen, H. Abe, L. P. Cui, H. Nakanishi, X. R. Qin, Y. F. Zhao, *Lett. Pept. Sci.* **2003**, *10*, 57.
[165] A. Hall, B. Sellergren, US2008/0064810 A1, **2008**.
[166] M. R. Halhalli, C. S. A. Aureliano, E. Schillinger, C. Sulitzky, M. M. Titirici, B. Sellergren, *Poly. Chem. 3*, 1033.
[167] M.-M. Titirici, B. Sellergren, *Chem. Mater.* **2006**, *18*, 1773.
[168] M. W. Freyer, E. A. Lewis, J. C. Dr. John, Dr. H. William Detrich, III, in *Methods in Cell Biology, Vol. Volume 84*, Academic Press, **2008**, pp. 79.
[169] K. A. Connors, *Binding Constants: The Measurement of Molecular Complex Stability*, Wiley, New York, **1987**.

CURRICULUM VITAE

Mr. Sudhirkumar Shinde
M.Sc. (Organic Chemistry)
INFU, Faculty of Chemistry,
Technical University of Dortmund,
Otto Hahn Strasse 6,
44221 Dortmund,Germany
Tel: +49-231-7556114
Mobile: +49-152-13036300
FAX: +49-231-7554234
Email: S.Shinde@infu.uni-dortmund.de
sudhirshinde1@gmail.com

Educational Qualification

Qualification	College/University/Board	Year
M.Sc. Organic Chemistry	Shivaji University, Kolhapur, India	2001-2003
B.Sc. Chemistry	Shivaji University, Kolhapur, India	1998-2001

Research Experience

1. **INFU, Faculty of Chemistry,Technical University of Dortmund, Germany**

   - PhD Thesis (Dec 2006- Jan 2012) "*Urea based hosts for oxyanions prepared by molecular imprinting. Applications in phospho- and sulfo- proteomics*" (funded by DFG).
   - Project: "Synthesis and characterization of phosphorylated peptides and polymeric protein surrogates "(January 2012 - present)
   - Co-supervised two master thesis and PhD thesis

2. **National Chemical Laboratory Pune, India**

   Worked as Senior Project Assistant on various projects

   - "Microcapsules for fabric Care" sponsored by Proctor & Gamble, USA (Aug 2005 to Dec 2006).

- Development of microencapsulated formulations of fungi and nematodes for "Integrated pest management" (IPM) of whitegrub sponsored by ICAR (Feb 2005 to Aug 2005).
- Development of microcapsules containing biocide for interior and exterior paint sponsored by Asian Paint India Ltd (May 2003 to Jan 2005).

PUBLICATIONS:

1. **S. Shinde**, A. Bunschoten, J A.W. Kruijtzer, R.M. J. Liskamp and B. Sellergren. *Imprinted polymers displaying high affinity for sulfated protein fragments*, ***Angew. Chem. Int. Ed.*** **2012 (**DOI: 10.1002/anie.201201314**).**
2. S. Ambrosini, **S. Shinde,** E. De Lorenzi, B. Sellergren. *Glucuronide directed molecularly imprinted solid-phase extraction: Isolation of testosterone glucuronide from its parent drug in urine*, ***Analyst,*** 137, 249-254, 2012. (DOI:10.1039/C1AN15606C)
3. S. Ambrosini, M. Serra, **S. Shinde**, B. Sellergren, E. De Lorenzi, *Synthesis and chromatographic evaluation of molecularly imprinted polymers prepared by the substructure approach for the class-selective recognition of glucuronides*, ***J. Chrom. A***, 1218, pp 6961-6969, **2011.** (DOI: 10.1016/j.chroma.2011.07.104).
4. S. Hellings, **S. Shinde**, F. Brosseron, A. Schnabel, T. Müller, H. Meyer, K. Marcus and B. Sellergren, *Ultractrace enrichment of tyrosine phosphorylated peptides on an imprinted polymer* ***Anal. Chem.***83 (5), pp 1862-1865, **2011.** (DOI: 10.1021/ac103086v)
5. M. Emgenbroich, C. Borrelli, **S. Shinde**, I. Lazraq, F. Vilela, A. Hall, J. Oxelbark, E. Lorenzi, J. Courtois, A. Simanova, J. Verhage, K. Irgum, K. Karim and B. Sellergren *A Phosphotyrosine-Imprinted polymer receptor for the recognition of Tyrosine phosphorylated peptides.*, ***Chemistry-A European Journal.***, Vol. 14, Issue 31, pp 9516-952**, 2008**. (DOI: 10.1002/chem.200801046)
6. V. Vinod, **S. Shinde**, P. Shukla, and M. Rao *Preparation and characterization of urea-formaldehyde-pepsin conjugate: A new biocatalyst system.* ***Biotechnology Progress***. Vol. 22, pp 1585-1590, **2006**. (DOI: 10.1021/bp0602247)

Manuscripts under preparations:

7. R. Sulc, **S. Shinde**, G. Szekely, B. Sellergren, *Molecularly imprinted polymers for selective extraction of phospholipids* (*Manuscript under preparation*)
8. **S. Shinde,** B. Sellergren, *The role of function monomers on the performance and morphology on oxyanion imprinted polymers* (*manuscript under preparation).*

9. **S. Shinde,** S. Sishodia, P. G. Shukla, *Microencapsulation of ibuprofen sodium in polyurethane through interfacial polymerization in non-aqueous medium*. (*manuscript under preparation for Journal of microencapsulation)*

10. **S. Shinde,** J. Chen, S. Helling, J. Urracca, K. Marcus**,** B. Sellergren *Imprinted polymers as artificial receptors for selective discrimination for phosphoryalted serine and tyrosine containing post- translationally modified amino acids and peptides (Manuscript under preparation for **Nature Method**).*

11. P. Kathirvel**,** M. Azenha, **S. Shinde**, P.Gomes, B. Sellergren and A. F. Silva; *Noval usage of ionic liquid functional monomer for the imprinting of anti-inflamatory drug Naproxen:Comparison of Acrylic and sol gel approaches* (communicated for publication).

CONFERENCES:

Oral Presentations:

1. R. Sulc, **S. Shinde**, G. Szekely, B. Sellergren, *MIPs for lipidomics*, ‘‘Selective recognition of Lipids`` **SLING** workshop, National University of Singapore (NUS), June 14-15, Singapore, **2012**.

2. **S. Shinde**, C. Esen, B. Sellergren, ‘‘*Imprinting via a placeholder approach for the recognition of larger phosphorylated protein fragments`` 7th International conference on Molecularly Imprinted Polymers* MIP2012, 27-30 August, Paris, France, **2012**.

3. **S. Shinde**, B. Sellergren, *MIPs targeting oxyanions: from fundamental to applications;* Tag der Chemie; Feb. 3rd, Dortmund, Germany, **2012**

4. P. Kathirvel,' M. Azenha, **S. Shinde**, P. Gomes, B. Sellergren and A. Silva *Different formats of molecularly imprinted gels for naproxen; Characterization by SPE and HPLC;* 7th National Meeting on Chromatography (9-11, Jan), Porto , Portugal**, 2012**

5. **S. Shinde**, C. Esen, B. Sellergren, *MIPs targeting oxyanions: from fundamental to applications* Graduate student symposium on Molecular Imprinting; Sept. 28-30, London, UK, **2011**

6. S. Ambrosini, M. Sera, **S. Shinde**, B. Sellergren and E. De Lorenzi, Synthesis, *chromatographic evaluation and application to solid-phase extraction of molecularly*

imprinted polymers for the class-selective recognition of glucuronides; Sept 28-30, London, UK, **2011**.

7. **S. Shinde**, C. Esen, S. Helling, K. Marcus, B. Sellergren. *Molecularly Imprinted Polymers (MIPs) targeting post-translationary modified protein fragments.* MIP2010, August 8th-12th 2010, New Orleans, USA **2010**.
8. P. Shukla., **S. Shinde**., S. Karndikar., A. Prabhune., *Preparation of polymer microspheres and their use in enzyme immobilization* XVII International Conference on Bioencapsulation, 24th -26th 2009, Groningen, Netherlands; **2009**.

Poster Presentations:

1. **S. Shinde**, C. Esen, B. Sellergren, *MIPs displaying pH dependent specific binding of sulphate or phosphate, 7th International conference on Molecularly Imprinted Polymers* MIP2012, 27-30 August, Paris, France, **2012.**

2. J. Chen**,** S. Helling**, S. Shinde**, B. Sellergren, K. Marcus; ''Selective enrichment of phosphotyrosine specific molecularly imprinted polymers'', *7th International conference on Molecularly Imprinted Polymers* MIP2012, 27-30 August, Paris, France, **2012.**

3. P. Kadhirvel, M. Azenha, **S. Shinde**, P. Gomes, B. Sellergren and A. Fernando, *Ionic Liquid based Functional Monomer Synthesis for the Imprinting of Anti- Inflammatory Drug Naproxen: Sol – Gel Approach,* Graduate student symposium on Molecular Imprinting; Sept. 28-30, London, UK, **2011** (**Best Poster Prize**).

4. S. Ambrosini, **S. Shinde,** M. Serra, B. Sellergren, E. De Lorenzi. *Development of molecularly imprinted polymers for the selective extraction of glucuronides in biological samples* "XX National Meeting on Medicinal Chemistry", Poster P91, page 189, Sept 2010, Abano Terme, Italy, **2010.**

5. **S. Shinde**, J. Urracca, A. Nematollahzadeh, S. Wei and B. Sellergren *The influence of functional monomer and template on the morphology and performance of oxyanion imprinted polymers.* MIP2010, August 8th-12th 2010, New Orleans **2010**.

6. **S. Shinde**, B. Sellergren. *Molecularly Imprinted Polymers (MIPs) targeting posttranslationally modified protein fragments and Peptides*. MACRO2010, Glasgow, UK, **2010**.

7. R. Wagner, I. Lazraq, J. Fernández Sánchez, A. Nematollahzadeh, J. Urraca, **S. Shinde**, E. Pena, M. Moreno-Bondi, G. Orellana, B. Sellergren. *Imprinted chromogenic and fluorogenic receptors for biological and environmental target analytes.* MIP2010, August 8th-12th 2010, New Orleans **2010**.

8. J. L. Urraca, C. S. A. Aureliano, A. Abdel Qader, **S. Shinde**, E. Schillinger, B. Sellergren *Imprinted polymers for affinity based extractions of biomarker and pathogenic peptides from blood plasma and other matrices.* MIP2010, August 8th-12th 2010, New Orleans **2010**.

9. R. Wagner, I. Lazraq, J. Fernández Sánchez, A. Nematollahzadeh, J. Urraca, **S. Shinde**, E. Pena, M. Moreno-Bondi, G. Orellana, B. Sellergren. *Imprinted chromogenic and fluorogenic receptors for biological and environmental target analytes.* EuCheMS Chemistry Congress Nürnberg **2010**

10. J. L. Urraca, C. S. A. Aureliano, A. Abdel Qader, **S. Shinde**, E. Schillinger, B Sellergren, *Imprinted polymers for affinity based extractions of biomarker and pathogenic peptides from blood plasma and other matrices.* EuCheMS Chemistry Congress Nürnberg **2010**.

11. S. Ambrosini, **S. Shinde**, M. Serra, B. Sellergren, E. De Lorenzi. *Imprinted polymeric receptors for the selective recognition of glucuronated drugs*. 35th International Symposium on High Performance Liquid Phase Separations and Related Techniques, Poster P-2066-W, page 128, Boston, USA, **2010.**
12. **S. Shinde**., B. Sellergren *Moleularly Imprinted polymers targeting post-translationally modified protein fragments and peptides***.**, Tag der Chemie, TU-Dortmund. Germany; **2009**.
13. **S. Shinde**., B. Sellergren, *Moleularly Imprinted polymers targeting post-translationally modified protein fragments.* MIP, Kobe, Japan. **2008**.

14. C. Borreli., **S. Shinde** et al. and B. Sellergren *Moleularly Imprinted polymers for selective recognition of phosphorylated amino acids and peptides.*, Tag der Chemie, TU-Dortmund. Germany; Feb. **2007**.
15. **S. Shinde**, S. Sisodia and P.G. Shukla**,** *Release of Ibuprofen-Na from Polyurethane microcapsules prepared with different diols***.** 33rd Annual Meeting & Exposition of the Controlled Release Society, 22-26th July, Vienna, Austria ; **2006**.

OTHER Experiences:

- Teaching experience in the course of separation science at Dortmund University of Technology.
- Research training to master students, DAAD exchange students, RISE students
- Experience in co-supervision for master and PhD Thesis.
- Referee of International Journal of Environmental Analytical Chemistry

IT Credentials

- MS Office (Word, Power Point and Excel), ISIS draw, Chem Office, MestReNova (Mnova), Origin, Sigma plot, TA universal analysis, PSS Porcheck.
- Literature search (SciFinder, Delphion, Scopus)

Awards

❖ DAAD matching fund scholarship (September 2012)

Personal Vitae

Name	Mr. Sudhirkumar Arjun Shinde
Date of Birth	9th May 1980
Marital Status	Single
Nationality	Indian
Languages known	English, Hindi, Marathi, German (Beginner)
Present Address	Adalbertstrasse, 149, 44149 Dortmund, Germany
Permanent Address	At: Post Padali, Tal: Tasgaon, Dist: Sangli 416314, State: Maharashtra, INDIA